Master Thesis

NTNU
Norwegian University of
Science and Technology
Faculty of Engineering
Department of Energy and Process Engineering

Student (Leon Henke)

Numerical simulation of an integrated CO2 heat pump/chiller and thermal storage system for a hotel in tropical weather conditions

Trondheim, 10 2022

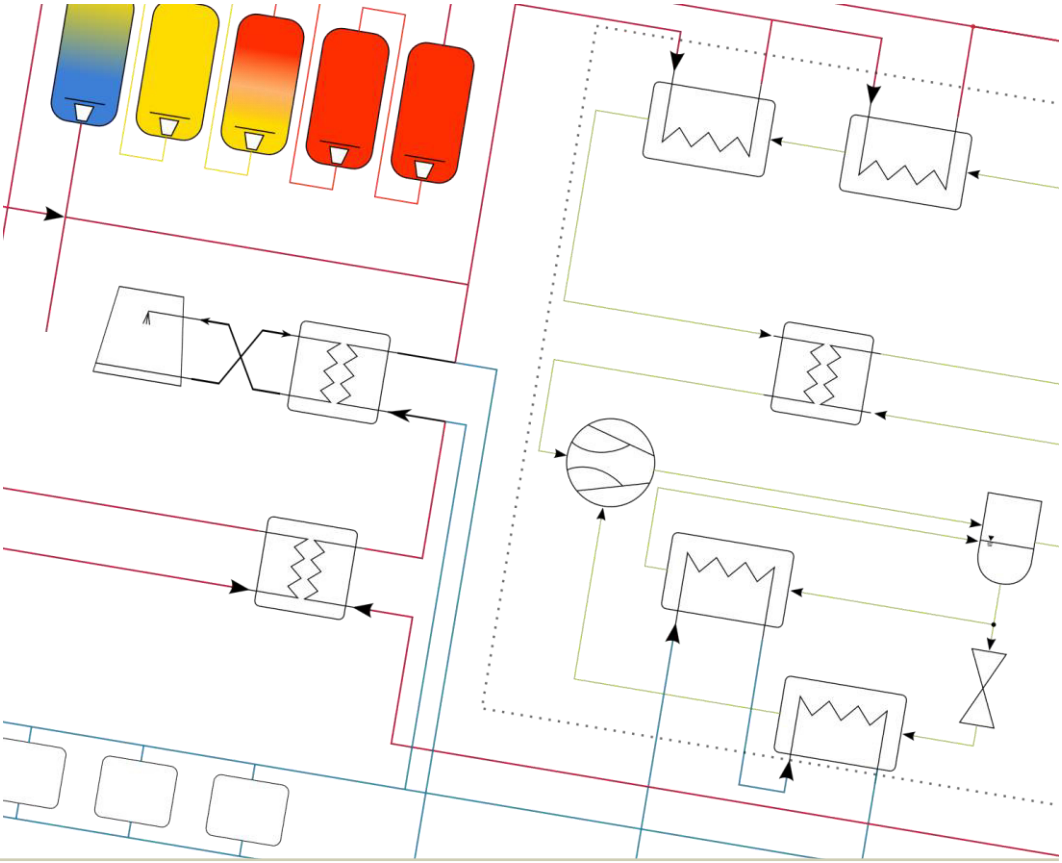

NTNU – Trondheim
Norwegian University of
Science and Technology

Norwegian University of Science and Technology

Faculty of Engineering
Department of Energy and Process Engineering

EPT-P-2022-XX

NTNU

Master Thesis

for

student Leon Henke

Autumn 2022

Numerical simulation of an integrated CO2/chiller and thermal storage system for a hotel in tropical weather conditions

Numerisk simulering av et integrert CO2/kjøler og termisk lagringssystem for et hotell i tropiske værforhold

Background and objective

Thermal systems i.e heating cooling and air conditioning counts for 40% from the total energy consumption in buildings. Meanwhile, the current status of CO_2 R744 systems proves the potential benefits of implementing integrated R744 in buildings with simultaneous cooling and large DHW demands, such as hotels.

Thermal energy storage combined with the single unit CO_2 heat pump/chiller enables higher operational flexibility and longer operational time for the heat pump/chiller unit. This is considered a competitive and efficient energy solution with high COP comparing to other conventional solutions. The unique design of the in-series stratification tanks assures a stability in hot water supply temperature and an optimum covering of the peak demands periods besides providing the hotel required cooling requirements.

The objective of the project is to analyze numerically the energy performance of a CO_2 heat pump/chiller system connected to thermal storage stratified tanks to provide for thermal needs of a luxury new hotel in India.

The following tasks are to be considered:

1. Literature review; CO_2 heat pump, thermal storage systems, DHW supply for hotel loads.
2. Overview of DHW demands of a new luxury hotel in India
3. Numerical development of the CO_2 heat pumps complete with thermal storage tank.
4. Economic and thermodynamical analysis of the results.
5. Summary report.
6. Proposals for further work.

-- “ --

The Master thesis comprises 30 ECTS credits.

The work shall be edited as a scientific report, including a table of contents, a summary in German, conclusion, an index of literature etc. When writing the report, the candidate must emphasise a clearly arranged and well-written text. To facilitate the reading of the report, it is important that references for corresponding text, tables and figures are clearly stated both places.
By the evaluation of the work the following will be greatly emphasised: The results should be thoroughly treated, presented in clearly arranged tables and/or graphics and discussed in detail.

Address
N-7034 Trondheim
Norway

Location
K. Hejes vei 1b

Tel. +47 73 59 38 60
Fax +47 73 59 35 80
Org. no. NO 974 767 880

The candidate is responsible for keeping contact with the subject teacher and teaching supervisors.

Risk assessment of the candidate's work shall be carried out according to the department's procedures. The risk assessment must be documented and included as part of the final report. Events related to the candidate's work adversely affecting the health, safety or security, must be documented and included as part of the final report. If the documentation on risk assessment represents a large number of pages, the full version is to be submitted electronically to the supervisor and an excerpt is included in the report.

According to "Utfyllende regler til studieforskriften for teknologistudiet/sivilingeniørstudiet ved NTNU" § 20, the Department of Energy and Process Engineering reserves all rights to use the results and data for lectures, research and future publications.

The report shall be submitted to the department via Blackboard.

Submission deadline:. 31st of October 2022

☒ Work to be done in lab
☐ Field work

Department for Energy and Process Engineering, 1st of May 2022

_____
Armin Hafner, Supervisor

Co-Supervisor(s): Hagar Elarga

Eidesstattliche Erklärung

Hiermit erkläre ich eidesstattlich, dass ich diese Arbeit eigenständig angefertigt und keine anderen als die angegebenen Hilfsmittel verwendet habe.

Braunschweig den 21. Oktober 2022

Zusammenfassung

In dieser Masterarbeit wird ein Simulationsmodell einer CO_2 -Wärmepumpe und des zugehörigen Energiesystems für ein Hotel in Chennai, Indien, erstellt und analysiert. Zunächst wird ein Überblick über den Stand der Technik von Wärmepumpen gegeben, mit einer Einführung in mögliche natürliche Kältemittel, sowie einer thermodynamischen Beschreibung der einzelnen Komponenten. Eine detailliertere Beschreibung von CO_2 -Wärmepumpen mit einer Vorstellung eines transkritischen Prozesses mit möglichen Verbesserungen, wie internen Wärmetauschern oder einem Ejektor, gibt einen umfassenden Überblick über das in dieser Arbeit beschriebene System. Darüber hinaus werden Möglichkeiten zur Optimierung der Sekundärseite, wie Kühltürme oder thermische Energiespeicher (TES), vorgestellt.

Als Grundlage für das Simulationsmodell muss zunächst das Energiesystem der Hotelanlage analysiert werden. Dieses befindet sich zum Zeitpunkt des Verfassen dieser Arbeit im Bau. Über das Energiesystem sollen der Warmwasserbedarf, der Klimatisierungsbedarf und ggf. der Raumwärmebedarf des Hotels gedeckt werden. Letztere sind jedoch aufgrund der heißen klimatischen Bedingungen in Chennai vernachlässigbar. Das System besteht aus einer CO_2 -Wärmepumpe mit internem Wärmeübertrager und Ejektor. Außerdem aus einem zweistufigen Verdampfer und einem zweistufigen Gaskühler. Diese beiden wurden jedoch im Simulationsmodell als einstufig betrachtet. Die Sekundärseite des Energiesystems ist in eine Warmwasser- und eine Kaltwasserseite unterteilt. Auf der Warmwasserseite ist ein Pufferspeicher in Form eines TES installiert. Des Weiteren ist ein Kühlturm zur Abführung überschüssiger Wärme implementiert. Für eine korrekte Dimensionierung wurde eine Abschätzung des Warmwasserbedarfs und des Klimatisierungsbedarfs vorgenommen. Da diese nicht permanent verfügbar sind, mussten verschiedene Betriebsmodi des Energiesystems erstellt werden. Dazu gehören ein Modus für gleichzeitigen Heiz- und Kühlbedarf, ein Modus für reinen Kühlbetrieb und ein Modus für reinen Heizbetrieb. Diese unterscheiden sich in den Wasserströmen sowie in den Wärmesenken und Wärmequellen. Für den Kühlmodus und den Heizmodus ist ein Kühlturm in das Energiesystem integriert.

Das Simulationsmodell wurde in Modelica erstellt, wobei verschiedene Komponenten von *Modelica Buildings Library*, *Modelica Standard Library* und *TIL Library* zum Einsatz kamen. Des Weiteren wurden einige Modelle selbst erstellt. Die Schwierigkeit bestand darin, einen Regelalgorithmus zu entwickeln, der zwischen den verschiedenen Betriebsmodi umschalten, den Heiz- und Kühlbedarf decken und die Simulation stabil laufen lassen kann. Daher wurde ein hierarchisches Regelsystem implementiert, das den Betriebsmodus auf der obersten Ebene steuert und die Steuervariablen in der mittleren Ebene anpasst, um die Sollwerte zu erreichen. Um festzustellen, ob der TES aufgeladen werden muss, wurde die Temperatur in der Mitte des TES gemessen. Sobald diese unter eine Schwellentemperatur von 65 °C fällt, wird nachgeheizt, bis die Rücklauftemperatur zur Wärmepumpe eine Temperatur von 35 °C überschreitet, was die Effizienz des Systems verringern würde.

Der Kühlbedarf wurde zur Vereinfachung der Simulation nicht quantitativ berücksichtigt, sondern nur als permanent vorhanden, um eine stabile Simulation zu gewährleisten. Um unterschiedliche Lastverhalten und thermische Anforderungen zu simulieren, wurde eine State Chart Regelung für eine Verdichtergruppe von zwei Verdichtern implementiert, die eine bessere Simulation von niedrigen thermischen Lasten ermöglicht.

Die Analyse der Ergebnisse hat gezeigt, dass auf der Basis von Vereinfachungen eine stabile und annähernd thermo- und fluiddynamisch korrekte Simulation des Energiesystems der Hotelanlage möglich ist. Darüber hinaus wurden die aus dem simulierten Energieverbrauch resultierenden Betriebskosten mit einem Referenzsystem verglichen, um Aussagen über die Wirtschaftlichkeit des Systems treffen zu können. Die wirtschaftlichen Einsparungen bei den Betriebskosten betragen bis zu $222.000 bei einem durchschnittlichen COP von 6 für einen Planungshorizont von zehn Jahren.

Abschließend wurden die Vereinfachungen und möglichen Änderungen des Simulationsmodells diskutiert. Insbesondere eine quantitative Betrachtung des Kühlbedarfs würde zu einem besserem Simulationsmodell führen. Dazu müssten jedoch empirische Daten über einen Referenzzeitraum erhoben werden, sobald das Energiesystem der Hotelanlage fertiggestellt ist. Darüber hinaus können Komponenten wie ein zweistufiger Verdampfer, ein zweistufiger Gaskühler oder Rohrelemente hinzugefügt werden, um den Wärmeübergang und die Verluste besser darzustellen.

Table of Contents

Table of Symbols

Abbreviation	Definition
CapEx	Capital Expenditures
CFD	Constant Frequency Drive
COP	Coefficient of Performance
deaBen	dead Band
DHW	Domestic Hot Water
D.O.E	U.S. Department of Energy
EER	Energy Efficiency Ratio
GWP	Global Warming Potential
HCFC	Hydrochlorofluorocarbon
HFC	Hydrofluorocarbon
HVAC	Heating, Ventilation and Air Conditioning
IHX	Internal Heat Exchanger
NTNU	Norwegian University of Science and Technology
ODP	Ozone Depletion Potential
OpEx	Operational Expenditures
VFD	Variable Frequency Drive

Symbol	Definition	Unit
A	Area	m^2
c	Velocity	m/s
CO_2	Carbon Dioxide	
c_p	Specific Heat Capacity	J/kgK
h	Enthalpy	J
k	Proportionality Contant	
k	Thermal Transmittance Coefficient	W/m^2K
$\dot{m}$	Mass flow	kg/s
Me	Merkel Number	
n	Amount	
p	Pressure	bar
$\dot{Q}$	Heat flow	W
R	Resistance	K/W
$\dot{S}$	Entropy flow	J/Ks
T	Temperature	°C

T'	Inlet Temperature	°C
T''	Outlet Temperature	°C
tau	Time Constant	s
V	Volume	m^3
$\dot{W}$	Work	W
z	Geodetic Height	m
α	Heat Transfer Coefficient	W/m^2K
δ	Thickness	m
Δ	Difference	
η	Efficiency	%
ρ	Density	kg/m^3

Indices	**Definition**
a	Air
c	Critical
com	Compressor
$cond$	Conductive
$conv$	Convective
$cool$	Cooling
dis	Discharge
$displ$	Displacement
dri	Driving
eff	Effective
eje	Ejector
el	Electric
eva	Evaporator
$evap$	Evaporation
fus	Fusion
$GasCoo$	Gascooler
$heat$	Heating
HP	Heat Pump
IHX	Internal Heat Exchanger
$isen$	Isotropic
lat	Latent
lay	Layer
M	Median
max	Maximum

Mea	Measure
prod	Production
sa	Saturated Air
sen	Sensible
set	Setpoint
suc	Suction
t	Technical
tan	Tank
th	Thermal
tot	Total
use	Usage
W	Water

List of Figures

List of Tables

1 Introduction

Due to increased concern for the sustainability of the energy industry and the rising cost of fossil fuels, the global energy market changed significantly in recent years [40]. Additionally, the pandemic and geopolitical events have put more strain on an already strained system/ caused further disruption in the fossil fuel trade. This leads to increasing pressure to develop renewable technologies in order to become less dependent on fossil energy sources. Renewable energy is mainly utilized as electricity, therefore, processes have to be electrified to utilize renewable energy sources instead of gas, coal and oil alongside the decarbonization of the energy mix [13].

In the European Union, approximately half of the total energy consumption is used for HVAC (heating, ventilation and air conditioning). In 2020, 23 % of that energy was obtained from renewable energy sources [16]. Norway, in particular, has great expertise in sustainable HVAC technologies. It has the most heat pumps per capita in Europe with one heat pump for every four Norwegens [24]. Heat pumps and chillers are power-to-heat systems that are particularly efficient for simultaneous heating and cooling. They combine energy efficiency and electrification of HVAC and are therefore a key technology for a more efficient and greener HVAC market. However, due to the dependence of heat pumps on ambient temperature, heat pump technology has long been efficient primarily in cold climates. There, the cold ambient temperatures can cool the refrigerant to colder temperatures in the evaporator leading to a more efficient operation and more possible refrigerants.

India, on the other hand, is the third largest energy consumer in the world behind China and the US [14]. Officially, 40 % of the energy is obtained from renewable energy sources [23]. The main consumption of energy in India is also the HVAC sector, which accounts for 40 % of the total consumption there [7]. However, this share will grow in coming years, as cooling energy demand alone is expected to grow by 220 % from 2018 to 2027 [15]. To reduce the accompanying increase in emissions, the *Energy Conservation Building Code* has been in effect since 2018, setting requirements for new residential units regarding HVAC energy consumption.

Innovation and research on heat pumps have improved their efficiency to the point where they are now an efficient alternative to conventional HVAC technologies, even in tropical climates [32]. Especially in view of the expected rise in India's energy consumption, widespread deployment of heat pumps has a great potential. As part of this development, the Norwegian Ministry of Foreign Affairs funds the exchange of knowledge between researchers at the Norwegian University of Science and Technology (NTNU) and project partners in India. These projects work with several hotel facilities, supermarkets and fishing boats in India. They are summarized under the umbrella projects called *Indee+*.

1.1 Indee+

The aim of Indee+ is to coordinate projects, provide training courses and create demonstration sites for knowledge transfer between different sectors in India [33]. For this purpose, the biggest regulatory hurdles are identified and research and development programs are planned. The latter will be used to investigate testbeds in the real, hot and humid environment of India. The implementation and installation of the HVAC systems will be done by local Indian companies in order to anchor the knowledge and processes locally. Through this knowledge transfer, the Indian refrigeration industry can directly utilize the latest refrigeration technology without going through a long, step-by-step development process as many Western countries have done in recent decades. Due to this leap forward of efficiency and sustainability, the huge projected growth of HVAC demands in India is more likely to be satisfied sustainably. Furthermore, this increase in knowledge will enable India to gain a stronger role in the global HVAC market by exporting the knowledge to markets other than its own [33].

1.2 Objectives

This master thesis is part of the Indee+ project and focuses on the energy system of a new hotel facility in Channai, India. There, a CO_2 heat pump/chiller system will be built to provide space heating, domestic hot water and air conditioning. In order to be able to investigate this system numerically, a simulation model will be developed that realistically represents the system behavior on the basis of local weather data. This thesis will describe the energy system and its components, as well as the creation and analysis of this simulation model.

State of the art heat pump technologies will be presented based on a literature review. This includes an overview of different refrigerants as well as the individual components and optimization of the heat pump/chiller cycle. Special attention will be given to CO_2 heat pump/chillers as well as thermal energy storage and cooling towers.

Initial estimates of the heating and cooling loads on the planned facility's HVAC system, will serve as the baseline of the simulation model. In addition, possible operation modes that improve the efficiency of the system will be considered and discussed.

The simulation model will be based on the Modelica programming language and will use different libraries for the individual components. The geometric as well as the thermodynamic and fluid dynamic properties of these components will be adapted in such a way, that the energy system can be represented dynamically by a custom control algorithm.

A final analysis and discussion of the results will provide information on compromises made for the numerical stability of the model and generates incentives for further work.

2 State of the Art

Heat pumps are very effective power-to-heat devices which use refrigerants as working fluids. Heat pumps are particularly efficient when heating and cooling demands occur simultaneously, since they are able to move heat from one place to another, even against thermal gradients, therefore utilizing waste heat. In this chapter, an overview of the the inner workings of state of the art heat pumps is presented, with special emphasis on natural refrigerants and efficiency-enhancing cycle components.

2.1 Compression Heat Pump Cycle

A schematic of a simple, closed cycle compression heat pump is pictured in Figure 2.1. The cold and low pressure refrigerant in the two phase area is heated in the evaporator, and is heated by the heat flow $\dot{Q}_{cool}$ ($4 \rightarrow 1$). During this process, the refrigerant is evaporated and afterwards pressurized in the compressor ($1 \rightarrow 2$). The compressor transfers the technical work $\dot{W}_t$ to the refrigerant dependent on the compressor efficiency η_{Com}. The high pressure and high temperature refrigerant is in the overheated gas phase. It is cooled in the condenser, releasing the heat flow $\dot{Q}_{heat}$ by a combination of sensible and latent heat ($2 \rightarrow 3$). After the condenser, the pressure is dropped in the expansion valve, depressurizing the refrigerant back into the two phase area ($3 \rightarrow 4$).

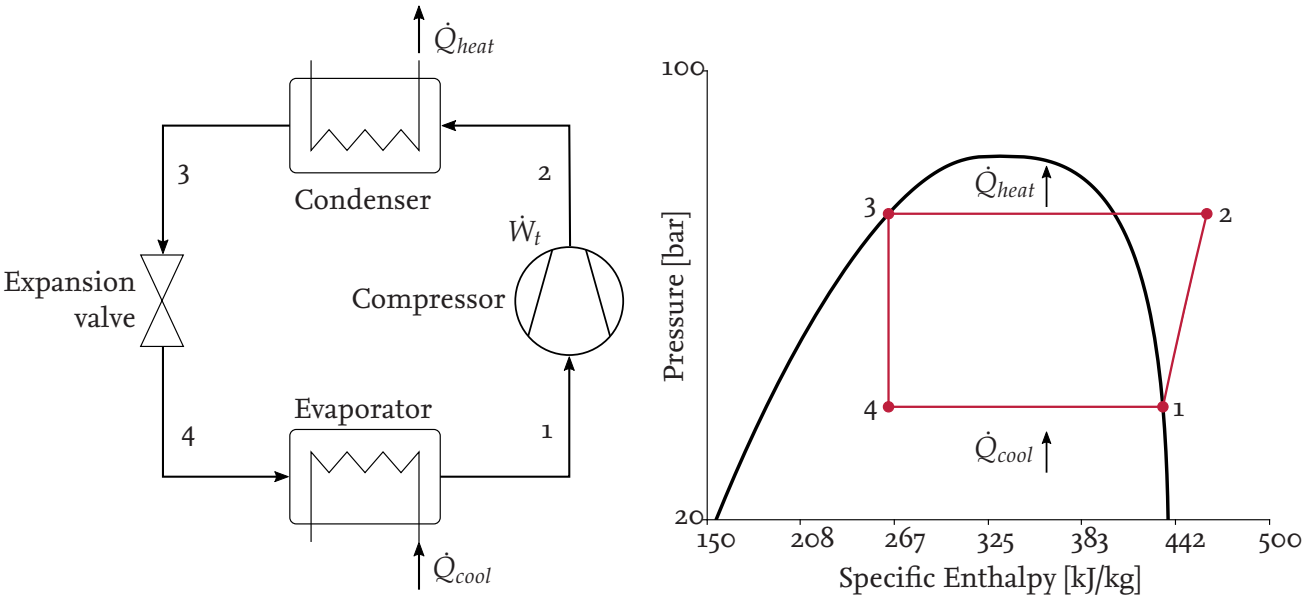

Figure 2.1: Flowchart and p-h-diagram of a simple compression heat pump cycle

This process provides the most usable energy when there are simultaneous heating and cooling demands. The cooling demands create the heat flow $\dot{Q}_{cool}$ and the heating demands consume the heat flow $\dot{Q}_{heat}$. The efficiency of a heat pump is measured with the Coefficient of Performance (COP). The COP is the quotient of the used energy and the applied electrical power. When neglecting other losses, the electrical work $\dot{W}_{el}$ can be expressed by the difference of the two heat flows $\dot{Q}_{cool}$ and $\dot{Q}_{heat}$. The following equations show the COP of a heat pump/chiller unit, with heating and cooling demands 2.2, for a heat pump used only for heating 2.3 and a chiller, used only for cooling 2.4. This differentiation is important, if the process is only for cooling, only for heating, or simultaneous heating and cooling.

$$COP = \frac{\dot{Q}_{use}}{\dot{W}_{el}} \tag{2.1}$$

$$COP_{HP/chiller} = \frac{\dot{Q}_{heat} + \dot{Q}_{cool}}{\dot{Q}_{heat} - \dot{Q}_{cool}} \tag{2.2}$$

$$COP_{HP} = \frac{\dot{Q}_{heat}}{\dot{Q}_{heat} - \dot{Q}_{cool}} \tag{2.3}$$

$$COP_{chiller} = \frac{\dot{Q}_{cool}}{\dot{Q}_{heat} - \dot{Q}_{cool}} \tag{2.4}$$

2.2 Refrigerants

According to DIN EN 378-1, a refrigerant is a fluid that absorbs heat at low pressure and low temperature and releases heat at higher pressure and higher temperature [1]. The selection of the refrigerant is very important when designing a heat pump. The refrigerants differ in their thermodynamic properties, availability and environmental impact, among other things. Some are presented in the following.

Due to rising awareness for sustainability, the difference between synthetic and natural refrigerants have become more important in recent years. Natural refrigerants also occur in nature and no unknown changes occur during the emission to the environment [9]. Those refrigerants include ammonia (R717), water (R718), hydrocarbons and carbon dioxide (CO_2 , R744). Since Lorentzen's research in the 1980s, CO2 in particular has been given the potential to be seen as the most promising alternative to the synthetic refrigerants HFC and HCFC which are commonly available on the market [31, 5]. These synthetic refrigerants contribute to the greenhouse effect, deplete the ozone layer and cause environmental damage. The different refrigerants can be compared by their impact on the environment, their safety classification and thermodynamic properties.

A refrigerant an impact the environment in several ways. It might be emitted to the atmosphere through leakages or wrong disposal of a heat pump. One measurement for the impact on the environment is the Global Warming Potential (GWP). The GWP describes the impact on the greenhouse effect of a fluid relative to the impact the equal mass of CO_2 . Therefore, CO_2 is referred to as the reference gas with a GWP of 1. Table 2.1 shows that the synthetic refrigerant R134a has a much high-

Refrigerant	Description	T_c [°C]	p_c [bar]	GWP [-]	Safety Group
R134a	1,1,1,2-Tetrafluoroethane	101.1	40.6	1300	A1
R718	Water	373.9	220.6	0	A1
R744	Carbon dioxide	30.98	73.75	1	A1
R717	Ammonia	132.3	113.3	0	B2L

Table 2.1: Properties of different natural refrigerants [2]. The relative price is compared to the price of the same mass of CO_2

er GWP (1300) than the listed natural refrigerants. This is one of the main reasons for the move towards natural refrigerants. Another indicator for the impact on the environment is the Ozone Depletion Potential (ODP). This describes the relative potential for the degradation of the ozone layer relative to the HCFC Trichlorofluoromethane. However, this is not considered in more detail as all refrigerants with an ODP higher than 0 are currently banned. Additionally, the natural refrigerants do not have to be produced specifically as refrigerants. The refrigerant CO_2 represents only a negligible fraction of total amount of the CO_2 emitted during industrial processes. It is obtained as a waste product from industrial processes and is therefore completely climate-neutral since it would have been emitted either way [9].

Some refrigerants come with safety concerns. Therefore, certain conditions for the installation of the heat pump are required. If the refrigerant is toxic or flammable, the place of installation should be well ventilated. Arpagaus et al [2] describes a safety classification shown in table 2.2, which differentiates between the toxicity and flammability of a refrigerant. Most of the described refrigerants are neither toxic nor flammable. Only ammonia requires special treatment in terms of safety.

Due to the usage of latent heat in heat pumps, the location and boundaries of the two phase area of the refrigerant have a significant influence on the area of application of the heat pump. Figure 2.2 shows the two phase areas of water, ammonia, CO_2 and R134a with their critical points. The curves of CO_2 and R134a look similar, with CO_2 having a higher critical pressure and R134a having a higher critical temperature. This shows, that the two refrigerants have similar thermodynamic properties when used in a heat pump, with R134a being able to reach higher temperatures in a basic compression cycle due to the higher critical temperature. In order to use CO_2 efficiently in higher-

Flammability	Toxicity: lower	Toxicity: higher
higher	A3	B3
lower	A2 / A2L	B2 / B2L
no flame propagation	A1	B1

Table 2.2: Safety group classifications for different natural refrigerants [2]

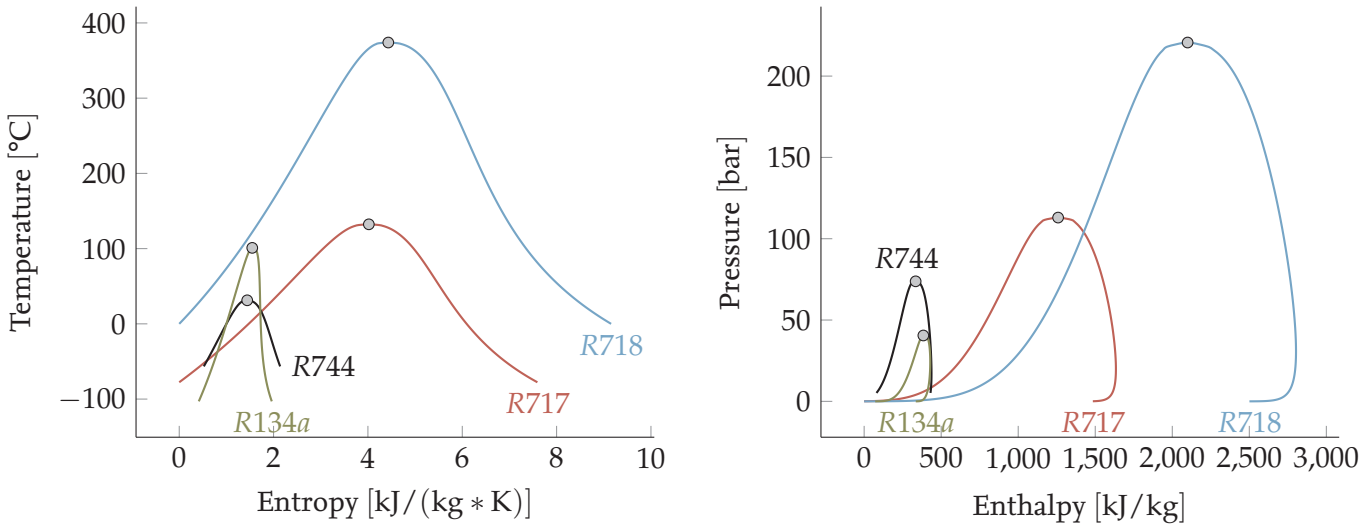

Figure 2.2: T-s and p-h diagrams with the two-phase region and critical point of different natural refrigerants and R134a

temperature heat pumps, it is necessary to optimize the basic compression cycle. This is described in more detail in the following part.

2.3 CO2 Heat Pumps

Due to the low critical temperature T_c of CO_2 , the refrigerant can not be used for moderate sink temperatures in a basic compression heat pump cycle. To counteract this problem, CO_2 can be warmed up above its critical point, resulting in a supercritical fluid. A supercritical fluid has no distinct border between a liquid and a gas phase and the properties differ from those of subcritical fluids. The p-h diagram of CO_2 in figure 2.3 shows, that an isobaric heat transfer of supercritical CO_2 is not isothermal.

2.3.1 Transcritical Heat Pump Cycle

A transcritical heat pump cycle (subcritical evaporation, supercritical heat emission) differs from the basic compression heat pump cycle. Since the refrigerant emits the heat supercritically, it is not condensed during that process. Therefore, the heat exchanger on the high pressure side of the heat pump is called *gascooler*, instead of condenser. Due to the temperature glide in the gascooler, which results from the isobaric heat emission above the critical point, supercritical CO_2 is good to heat District Heating Water (DHW) with a large temperature glide [9].

During each heat transfer, there is an irreversible entropy production. The amount of entropy depends on the temperature difference between the heat emitter and receiver. Stephan et al [39] describes it as follows:

$$\dot{S}_{prod} = \dot{Q} * \frac{T_1 - T_2}{T_1 * T_2}. \tag{2.5}$$

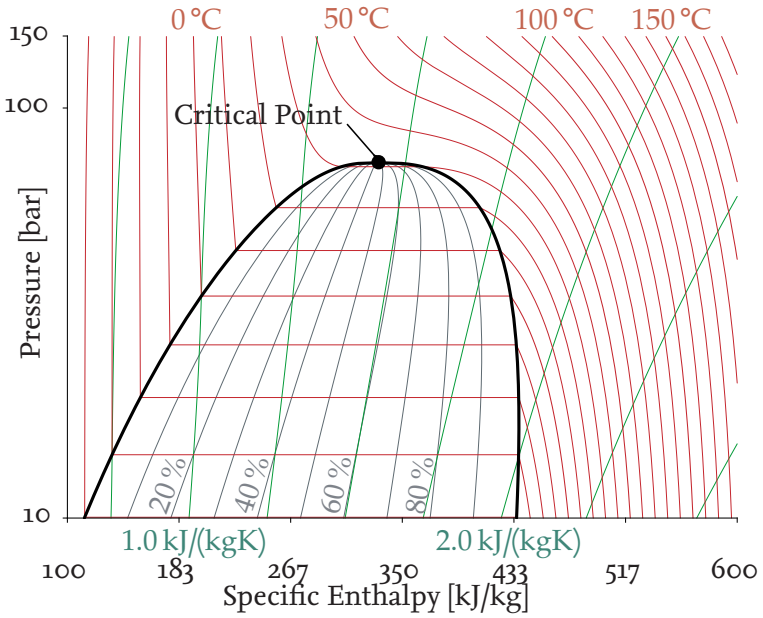

Figure 2.3: p-h diagram of CO_2

This means, for a more efficient heat transfer with less entropy production, the temperature difference has to be as small as possible. In a subcritical condenser, the temperature of the refrigerant is constant, as long as it is in the two phase area. However, the temperature of the fluid on the secondary side rises. This leads to a small temperature difference on the one end of the condenser, and a big temperature difference on the other end. For a supercritical heat transfer, the temperatures rise and fall simultaneously depending on the location inside the gascooler. This leads to an on average smaller temperature difference and lower entropy production. Figure 2.4 shows an example of this behavior for a desired secondary temperature glide from 30 °C to 70 °C. T' indicates the inlet, and T'' the outlet temperatures.

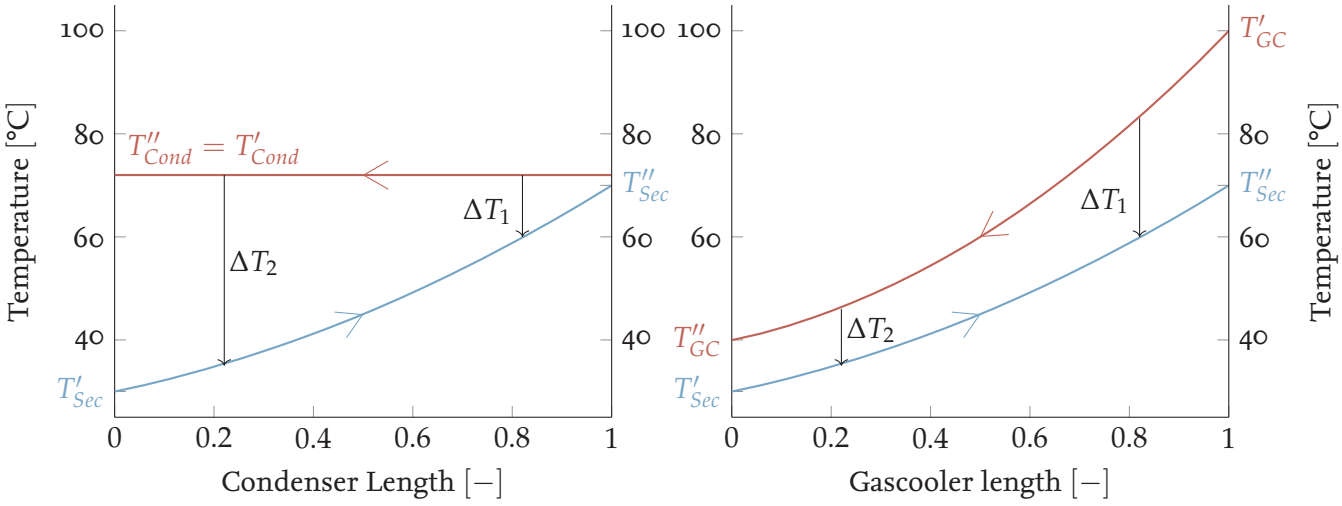

Figure 2.4: Temperature glides in a condenser and gascooler

The point with the smallest temperature difference between the hot and the cold fluid inside a heat exchanger is called *Pinch Point*. Ideally, the pinch point is at either end of the heat exchanger, however, it can also be inside the heat exchanger [25]. It is important to mention that the temperature of the secondary (cold) fluid can not be higher than the temperature of the refrigerant (hot fluid) at any specific point of the condenser/gascooler.

Due to the decoupling of isobars and isotherms above the critical point, the compressor capacity can be very decisive for the cooling capacity in a transcritical process [9]. Figure 2.5 shows three different processes with the same gas cooler outlet temperature of 40 °C and the same outlet point from the evaporator (4). However, the compressor capacity differs, leading to different high pressure temperature glides inside the gascooler. The cooling capacity depends on the difference between points 3 and 4.

$$\dot{Q}_{cool} = \dot{m} * (h_4 - h_3) \tag{2.6}$$

A slight increase in compressor capacity from 1 to 1' results in a greater temperature glide in the gascooler from 20 K to 40 K. Due to the small slope of the isotherm between pressure levels of 1 and 1', this results in a large increase of cooling capacity. Because of the location of the two phase area and the larger slope of the isotherm between 1' and 1", the compressor capacity has a less pronounced effect if further increased. Accordingly, for transcritical systems with CO_2 , it is important to note that especially at lower pressures above the critical point, there must be a low inlet temperature of the secondary fluid in the gascooler to obtain a reasonable cooling capacity [9]. In most cases, the minimum inlet temperature is defined by boundary conditions, so the necessary temperature glide comes from a corresponding increase in pressure. This leads to the fact that the discharge pressure in CO_2 systems is relatively high compared to other refrigerants, which has both advantages and disadvantages. On one hand, special high pressure equipment is required for a CO_2 heat pump leading to additional costs and research. On the other hand, the required displacement

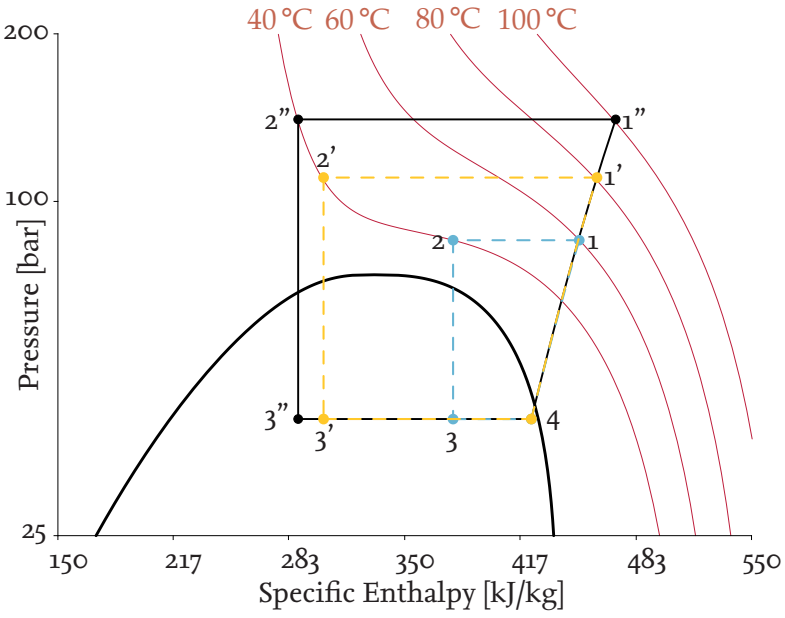

Figure 2.5: p-h diagram of CO_2

volume of the compressor is only 10 to 15 % of what other refrigerants require, which results in an overall smaller compressor [9].

Components of a transcritical Heat Pump Cycle

Compressor

A compressor is a working machine in which a fluid is compressed and brought to a higher pressure [45]. Technical work is used in the process. In real applications, however, the total technical work applied does not match the technical work done on to the fluid, as there are various losses within the compressor.

Figure 2.6 shows the derivation of the so-called *Isentropic Efficiency* η_{isen}. The two green lines are isentropic, where the entropy remains constant. An ideal process would run isentropically on such an isoline. A real, loss-making compression leads to an increase in entropy. Accordingly, the discharge enthalpy h_{dis} is higher than for the theoretical isentropic compression $h_{dis,isen}$. The efficiency can be determined from the ratio of the difference between the two enthalpies and the enthalpy at the starting point [45].

$$\eta_{isen} = \frac{h_{dis,isen} - h_{suc}}{h_{dis} - h_{suc}} \tag{2.7}$$

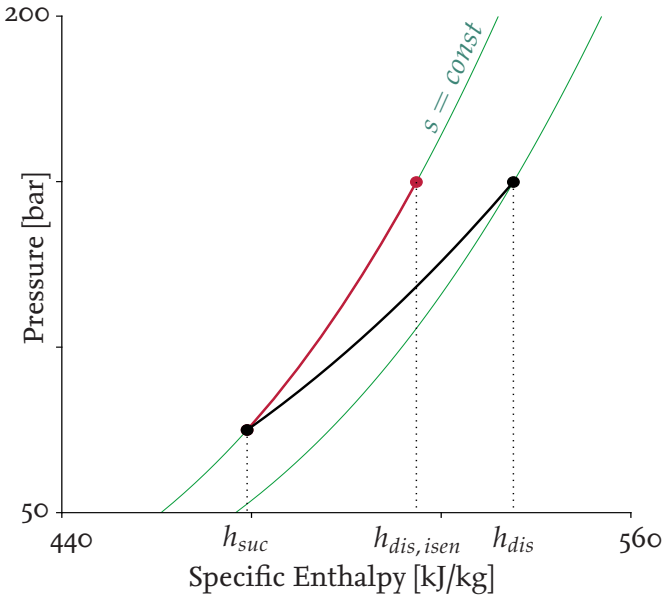

Figure 2.6: Derivation of the isentropic efficiency of a compressor [45]

In addition to the losses due to loss-making compression, which are represented in the isentropic efficiency, there are also losses due to volumetric inefficiencies, for example due to dead spaces in the compressor housing. These are taken into account in the so-called *Volumetric Efficiency* λ_{eff} , which describes the ratio between the theoretically possible mass flow and the actual mass flow [17].

$$\lambda_{eff} = \frac{\dot{m}}{V_{displ} * n * \rho_{suc}} \tag{2.8}$$

The efficiency, which describes the ratio between the work done on to the fluid and the shaft of the compressor, is called *Effective Isentropic Efficiency* $\eta_{effisen}$. This includes all but the electrical losses necessary to determine the required drive power of the compressor [17].

$$\eta_{effisen} = \frac{\dot{m} * (h_{dis,isen} - h_{suc})}{P_{shaft}} \tag{2.9}$$

Converted, the electrical drive power of the compressor $P_{el,com}$ with the electrical efficiency η_{el} of the motor is as follows [17]:

$$P_{el,com} = \frac{1}{\eta_{el}} * P_{shaft} = \frac{\dot{m} * (h_{dis,isen} - h_{suc})}{\eta_{effisen} * \eta_{el}}. \tag{2.10}$$

Heat Exchanger

The gas cooler and evaporator belong to the heat exchangers. In a heat exchanger, heat is transferred from a warmer to a colder fluid. This transferred heat flow depends, among other things, on the geometry and material of the heat exchanger, the two fluids and the flow properties [4]. There are multiple steps in the heat transfer. A convective heat exchange, which takes place from the warmer fluid to the pipe wall, heat conduction through the pipe wall, and a second convective part from the pipe wall to the colder fluid. A thermal resistance can be determined for each of the individual heat transfer components [4]. For the convective parts, this depends on the heat transfer area A and the heat transfer coefficient α. α can be determined as a function of the flow properties and geometries.

$$R_{th,conv} = \frac{1}{\alpha * A} \tag{2.11}$$

The thermal resistance resulting from the heat conduction through the wall depends on the thickness of the wall δ, the heat transfer area A and the thermal conductivity of the material of the wall λ.

$$R_{th,cond} = \frac{\delta}{\lambda * A} \tag{2.12}$$

In sum, the total resistance of the thermal resistors connected in series is calculated as follows:

$$R_{tot} = \sum R_{th,conv} + \sum R_{th,cond} \tag{2.13}$$

This is also the reciprocal of the so-called heat transfer capacity kA, from which the heat flow is calculated.

$$kA = \frac{1}{R_{tot}} \tag{2.14}$$

$$\dot{Q} = kA * \Delta T_M \tag{2.15}$$

Due to the temperature glides of the two fluids in the heat exchanger and the resulting variable temperature difference, the mean temperature difference is used to calculate the heat flow. It is calculated from the inlet and outlet temperatures of the two fluids [4].

$$\Delta T_M = \frac{\Delta T_1 - \Delta T_2}{ln(\frac{\Delta T_1}{\Delta T_2})} \tag{2.16}$$

Expansion Valve

The expansion valve is used to expand the fluid and reduce the pressure. The mass flow can be determined by the orifice equation depending on the pressure difference. The derivation based on Bernoulli's equation and the continuity equation can be traced in Bansal [3].

$$\dot{m} = A_{eff} * \sqrt{(p_{suc} - p_{dis}) * 2 * \rho_{suc}} \tag{2.17}$$

The effective flow area A_{eff} describes the smallest constriction of the valve.

2.3.2 Improvements of the transcritical CO_2 Heat Pump Cycle

As described in Figure 2.5, a low inlet temperature of the secondary fluid to the condenser/gascooler results in better cooling performance of the heat pump. This leads to heat pumps being more efficient in cold environments than in warm climates. For a long time, there was a so-called *Heat Pump Efficiency Equator* [32]. This metaphorically describes in which climatic zones the use of a heat pump at ambient temperature is efficient. Due to the use of CO_2 as refrigerant and the high compressor outlet temperature in the transcritical process, a reasonable temperature glide in the gascooler can be achieved even at a high ambient (sink-) temperature. This leads to an increase of cooling capacity. Much research is being done to further increase the efficiency [26]. Meanwhile, through research, the heat pump equator has disappeared, which means that the use of heat pumps around the world is efficient [32]. In the following, various efficiency-increasing modifications to the transcritical CO_2 heat pump cycle are presented.

Internal Heat Exchanger

One way to reduce the losses of a heat pump is to implement an internal heat exchanger (IHX). This reduces the losses during expansion by additionally cooling the supercritical fluid behind the gascooler [9]. The heat is transferred internally and being absorbed by the subcritical fluid behind the evaporator. Figure 2.7 shows a flowchart and p-h- diagram of a transcritical CO_2 heat pump cycle with IHX based on Wang et al [44]. The heat flow through the IHX $\dot{Q}_{IHX}$ depends on the difference between the enthalpy in points 3 and 4. The temperature in 4 cannot be smaller than the evaporator outlet temperature in 6. In addition, the IHX can prevent liquid slugging in the compressor, which is caused by incomplete evaporation in the evaporator. In the IHX, the subcritical gas is superheated to ensure that there is no liquid left that could damage the compressor. Without an IHX, this would have to happen in the evaporator. Since vapor bubble generation plays a major role in heat transfer in the evaporator, it is advantageous to operate it completely in the two-phase region [9]. If the superheating takes place outside the evaporator, this will be possible.

Using an IHX increases the cooling capacity of the heat pump to $\dot{Q}_{coolIHX}$. Compared to the cooling capacity of a heat pump without IHX $\dot{Q}_{cool}$, it looks the following:

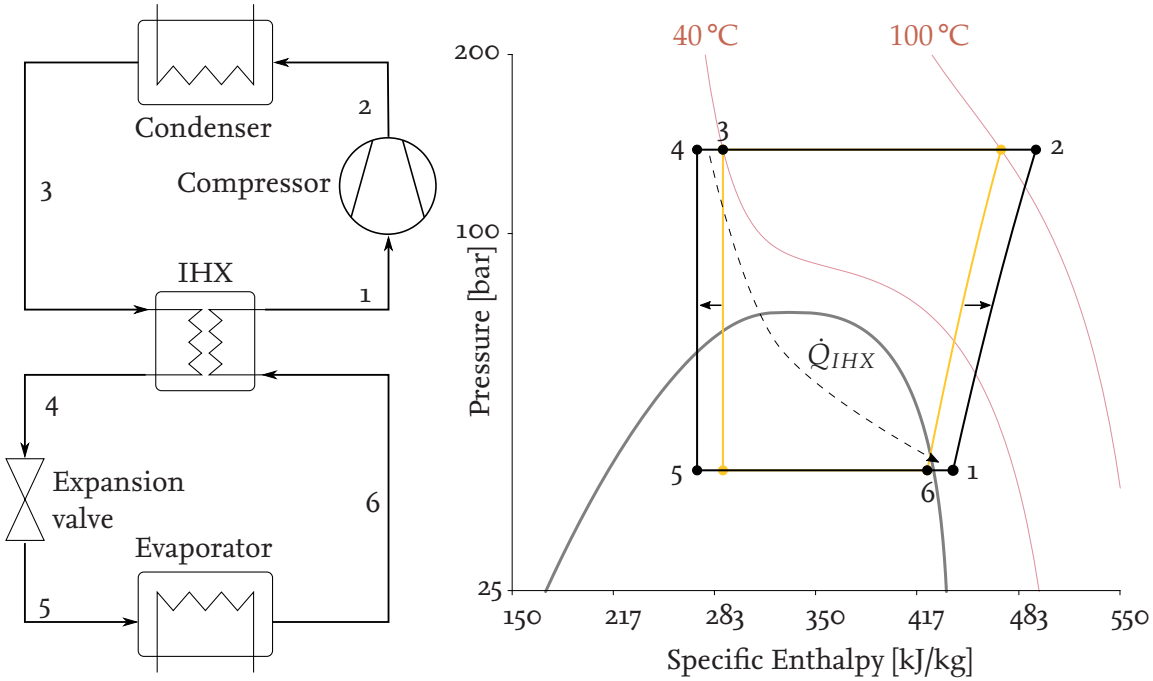

Figure 2.7: Flowchart and p-h-diagram of a transcritical CO_2 heat pump cycle with IHX

$$\dot{Q}_{cool\,IHX} = \dot{Q}_{cool} + \dot{Q}_{IHX} = h_6 - h_5. \tag{2.18}$$

However, if the cooling capacity does not need to be increased, the compressor discharge pressure can be reduced instead, which can reduce the necessary technical work [6].

Ejector

During the expansion in the expansion valve, a large part of the energy is lost in form of expansion losses [9]. Accordingly, there is great potential for increasing the efficiency of a heat pump if these losses are reduced or recovered. Next to the expansion valve, there are also other expanders. A turbine can be used for the expansion to recover expansion losses as mechanical work. This can be transmitted directly to the compressor via a shaft, replacing some of the compressor drive power. However, turbines are not yet mature due to the high cost and maintenance required for CO_2 systems [9].

Another way to recover expansion losses is to use an ejector. An ejector is a static component that is especially designed for high pressure differences [42]. Ejectors are widely used in CO_2 - refrigeration systems because they allow a significant increase in efficiency [30]. This depends on the geometry and application [42]. For CO_2 systems, this can mean an efficiency increase of up to 30 % compared to an expansion valve [19]. However, the efficiency of an ejector decreases sharply outside the design point, so an accurate design depending on the desired working conditions is important [42].

An exemplary ejector is shown in figure 2.8. The high pressure driving mass flow $\dot{m}_{dri}$ is entering the ejector in the nozzle. There, the mass flow is accelerated due to a decrease of the flow area.

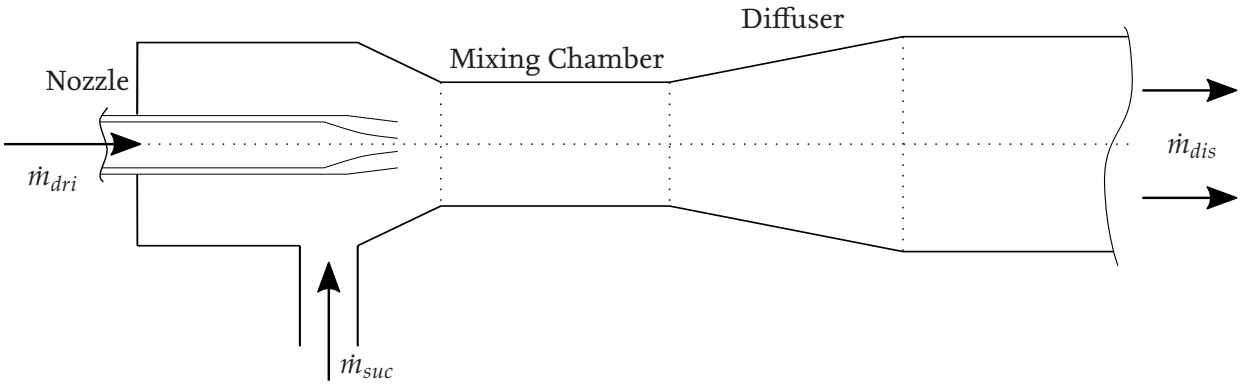

Figure 2.8: Sketch of an ejector [9]

$$\dot{m} = A * c = const \tag{2.19}$$

This increase of the velocity in the nozzle leads to an decrease of pressure, due to the Bernoulli equation 2.20. For 1 being the status of the fluid at the driving port, and 2 at the nozzle, the equation looks the following without including possible losses:

$$\frac{\rho}{2}c_1^2 + p_1 + \rho g z_1 = \frac{\rho}{2}c_2^2 + p_2 + \rho g z_2 \tag{2.20}$$

$$\frac{\rho}{2}c_1^2 + p_1 = \frac{\rho}{2}c_2^2 + p_2 \tag{2.21}$$

Since the nozzle and the driving port are on the same height, the potential energy term of the Bernoulli equation can be neglected. Equation 2.21 shows that an increase in velocity from 1 to 2 must result in a decrease in pressure so that the energy in the overall equation remains constant. The suction mass flow $\dot{m}_{suc}$ is sucked into the ejector through this negative pressure. Both mass flows, $\dot{m}_{dri}$ and $\dot{m}_{suc}$ are mixed into a homogeneous mass flow in the mixing chamber. The diffuser leads to a decrease of velocity and increase of pressure before being discharged from the ejector. Overall, this leads to a pre-compression of the fluid, since the pressure of the discharge mass flow is higher than at the respective expansion valve. For CO_2 systems, this increase of pressure is usually around 5 to 10 bar [9]. However, to use an ejector, a separator behind the ejector is mandatory, to split the gas and the liquid. The gas is being compressed and the liquid expanded and evaporated and afterwards used as $\dot{m}_{suc}$ [30]. $\dot{m}_{suc}$ depends on the ejector efficiency η_{eje} and is defined by Elbel and Hrnjak [12]. η_{eje} values differ between 0.2 and 0.3 for CO_2 systems [20].

$$\dot{m}_{suc} = \frac{\dot{m}_{dri} * \eta_{eje} * (h_{dri} - h_{dri,isen})}{h_{suc,isen} - h_{suc}} \tag{2.22}$$

The discharge mass flow is the sum of the driving and suction mass flow.

$$\dot{m}_{dis} = \dot{m}_{dri} + \dot{m}_{suc} \tag{2.23}$$

2.3.3 Improvements to of the Secondary Side

Not only the heat pump/chiller is influential for the efficiency of an entire energy system, but also the secondary side. In the following, components are presented that can increase the efficiency of the system by adapting the secondary side.

Cooling Tower

A cooling tower is a structure to remove heat from water. This is particularly useful if there are cooling demands, but there is no way to utilize or emit the heat on the high pressure side. A schematic illustration is shown in Figure 2.9. The fan on top of the tower creates negative pressure inside, to draw cold, dry air through vents into the tower. This air flow evaporates part of the hot water flow $\dot{m}_{hot}$, which is sprayed into the tower as droplets by spray nozzles to increase its surface area or heat transfer area. In order to evaporate the water, energy has to be added to the water to overcome the enthalpy of evaporation. This energy is provided by surrounding hot water droplets, which are cooled in the same process. The cold water $\dot{m}_{cold}$ is collected in a basin and can be drained for further use. The vaporized water $\dot{m}_{evap}$ is released into the ambient with a now warm and moist air flow [8]. To keep a constant water flow, the losses the in form of the evaporated water are compensated for with cold water from the grid.

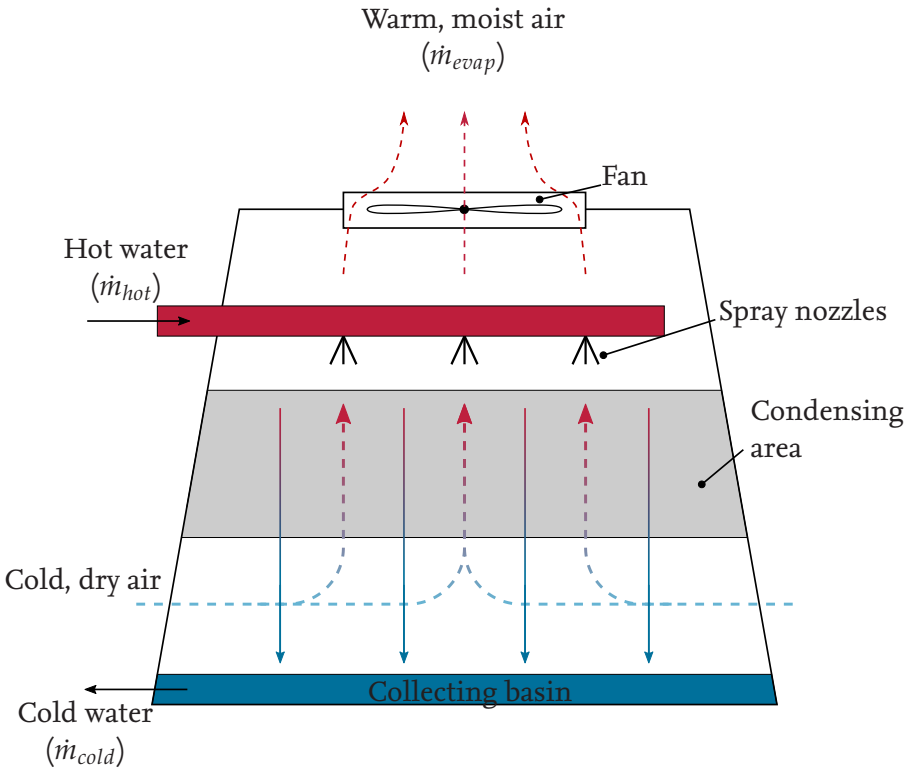

Figure 2.9: Sketch chart of a cooling tower [8]

A cooling tower can only reduce the temperature of the water depending on the ambient wet bulb temperature. This is the minimum temperature that can be achieved by evaporative cooling. For a cooling tower, the minimum temperature difference between the outlet temperature and the

wet bulb temperature is 2 K, meaning, the outlet water is 2 K warmer than the wet bulb temperature [38]. Numerically simplified, the cooling tower was depicted by Leopold Carl Friedrich Merkel in the 1920s. To characterize a cooling tower, he defined the so-called *Merkel number*, which establishes the relationship between the temperature difference of water and the enthalpy difference of air before and after the evaporation. The Merkel number *Me* is defined as follows [37]:

$$Me = \int_{T_{w,out}}^{T_{w,in}} \frac{c_{p,w}}{h_{sa} - h_a} dT_w \tag{2.24}$$

This is the integral of the heat capacity of water divided by the enthalpy difference between the saturated air at water temperature and the enthalpy of the air stream. The integral boundaries are the water inlet and outlet temperature. The Merkel number is usually known to the cooling tower manufacturer. Otherwise, it can only be obtained experimentally and correlated to air and water mass velocities or by back calculation [35, 28].

However, the Merkel number is also criticized because of the simplifications and assumptions that must be made. For example, it is assumed that the amount of water is constant or that the temperature dependence of the properties of air, water and the enthalpy of vaporization are neglected and also assumed to be constant [37].

Thermal Energy Storage

In order to switch a heat pump on and off as seldom as possible, Thermal Energy Storage (TES) can be implemented on the secondary side to store thermal energy even when there are no heating or cooling demands. TES can be used either as heat storage or as a cold storage system. The medium in the TES is heated or cooled in order to use this energy later for satisfying heating or cooling demands.

For TES, a distinction is made between sensible heat storage and latent heat storage. Sensitive TES stores heat by heating or cooling the storage medium. The corresponding amount of heat stored can be determined by equation 2.25.

$$Q_{sen} = m * c_p * \Delta T \tag{2.25}$$

Latent TES stores energy by changing the aggregate state of the storage medium. In the case of the phase transition from liquid to solid, the stored energy depends on the enthalpy of fusion of the medium. This is calculated as follows:

$$Q_{lat} = m * \Delta h_{fus}. \tag{2.26}$$

To store heat for a heating system with a TES, water is often used as the storage medium. Water has a high heat capacity, as well as low viscosity and toxicity. As long as temperatures do not exceed the boiling point of water at ambient pressure 100 °C, water can be used as a sensible heat storage medium [36].

A sensitive water TES for the storage of heating water can be used openly. This means that the water used to store the energy is also used for heating. This results in an exchange of water over

time. The TES can be operated either with a variable or constant level. If the level is constant, the amount of water taken from the TES must always be refilled. If, for example, there are demands for hot water, but no further water is heated via the heat pump. Cold water is usually refilled into the TES. This causes temperature differences in the tank. This temperature gradient leads to a stratification of the water in the tank into different temperature ranges. Since the density of warm water is lower than that of cold water, the warmest layer is at the top of the tank and the coldest at the bottom. For this reason, the warm water is taken and added from the top of the tank, and the cold water is added at the bottom.

If, due to turbulence or similar disturbances, the water in the TES is not stratified from warm to cold, buoyancy effects occur which lead to a physically correct stratification of the water. Numerically, it is assumed that a heat flow is exchanged between the individual layers. This is modeled according to [41] as followed:

$$\dot{Q} = k * \Delta T^2 \tag{2.27}$$

$$k = \frac{V * \rho * c_p}{tau * n_{lay}} \tag{2.28}$$

Here k is a proportionality constant, which depends on the volume, a time constant for mixing tau, the density, the heat capacity and the number of discretized layers n_{lay}. The temperature difference and the heat flow refer to the adjacent layers. This results in the stratification in the tank always going from warm to cold in steady state. In addition, the stratification allows several tanks to be connected in sequence. The temperature gradient is then not only over one tank, but over several tanks. Hereby, the lowest layer in the first tank is the coldest, and the top layer in the last tank is the warmest.

An advantage of the TES is that the capacity of the heat pump can be reduced. In turn, it runs longer in its design point. The TES is therefore slowly filled up, and then quickly discharged if necessary. Therefore, a careful dimensioning of the volume of the TES is required. In the following, an exemplary dimensioning is presented.

Simplified, it is assumed that the tank is filled with a constant mass flow of $0.2\,\mathrm{kg\,s^{-1}}$ water if the heat pump is running. At a density of $997\,\mathrm{kg\,m^{-3}}$, this corresponds to a volume flow of approximately $0.72\,\mathrm{m^3\,h^{-1}}$. Figure 2.10 shows the volumes of exemplary hot water demand taken from the tank and hot water supply added to the tank accumulated over one day.

The demand may not exceed the supply at any time. Otherwise, the demand cannot be satisfied. The difference between the two curves is the current fill level of the TES, which is $0\,\mathrm{m^3}$ when both curves are equal. The maximum difference ΔV_{max} is accordingly the minimum required volume of the TES to satisfy all hot water demands over one day. The difference between the two curves at the end of one day is the difference at the beginning of the next day. What figure 2.10 also shows is the effect of the TES on the on and off cycles of the heat pump. It is best for a heat pump to operate as continuously as possible. By using a TES in this example, the heat pump operating time was increased from 11 h to 20 h per day. Additionally, when operating with a TES, the heat pump is also

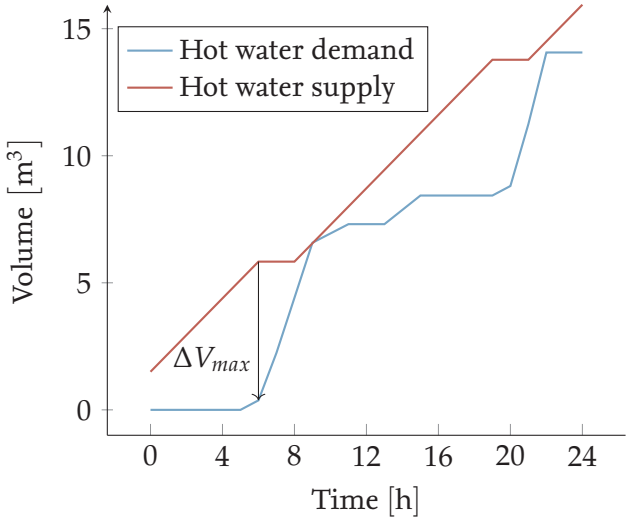

Figure 2.10: Exemplary determination of the minimum TES volume based on Elarga [10]

operated at a constant heating capcacity. This increases the efficiency of the heat pump, as it can be operated continuously at the design point if designed accordingly.

In summary, however, a good design of the TES is only possible if there is a good knowledge of the hot water demands.

3 Energy System of the Hotel

The Norwegian University of Science and Technology (NTNU) administers the project *Indee+*, funded by the Norwegian Ministry of Foreign Affairs, to reduce the CO_2 equivalent emissions of the heating, ventilation and air conditioning (HVAC) sector in India. The umbrella project Indee+ includes several individual projects. Norway has a lot of know-how in the refrigeration field with natural refrigerants, as this field has been promoted by the Norwegian government for decades. The improvements to the CO_2 cycle described in chapter 2 allow the heat pump/chiller to be used in warmer climates. Therefore, NTNU and the Norwegian Ministry of Foreign Affairs are supporting the development of the sustainable HVAC sector in India with their refrigeration know-how [33].

One of these projects is the installation of a CO_2 heat pump/chiller system in a hotel in Chennai, India. In the luxury hotel, a heat pump/chiller unit is to be integrated to satisfy the space heating, air conditioning and domestic heating water demands. The energy system built for this purpose is described in this chapter.

3.1 Overview of the Energy System

The energy system of the hotel is shown in figure 3.1. It can be divided into a heat pump/chiller unit (green) and a heating- (red) and chilled water (blue) section. The heat pump/chiller operates according to the transcritical CO_2 heat pump cycle described in chapter 2.3. Special features are the two gascoolers and the two evaporators. These lead to smaller temperature glides per heat exchanger and thus, according to equation 2.5, to a more efficient heat transfer.

The heating water section consists of five stratified tanks, which together represent the thermal energy storage (TES). These are charged with thermal energy from hot water heated by the heat pump/chiller unit. The TES is discharged when DHW is needed for the hotel building. In the chilled water section the water is used for air conditioning of the individual rooms. The return flow is then cooled by the heat pump/chiller unit.

In addition, there is a cooling tower in case heat that can not be utilized for heating has to be removed from the system . A circulation loop ensures that all rooms continuously have hot water available, even if no DHW demands are present. A detailed description of the energy system can be found in chapters 3.2 and 4.1.

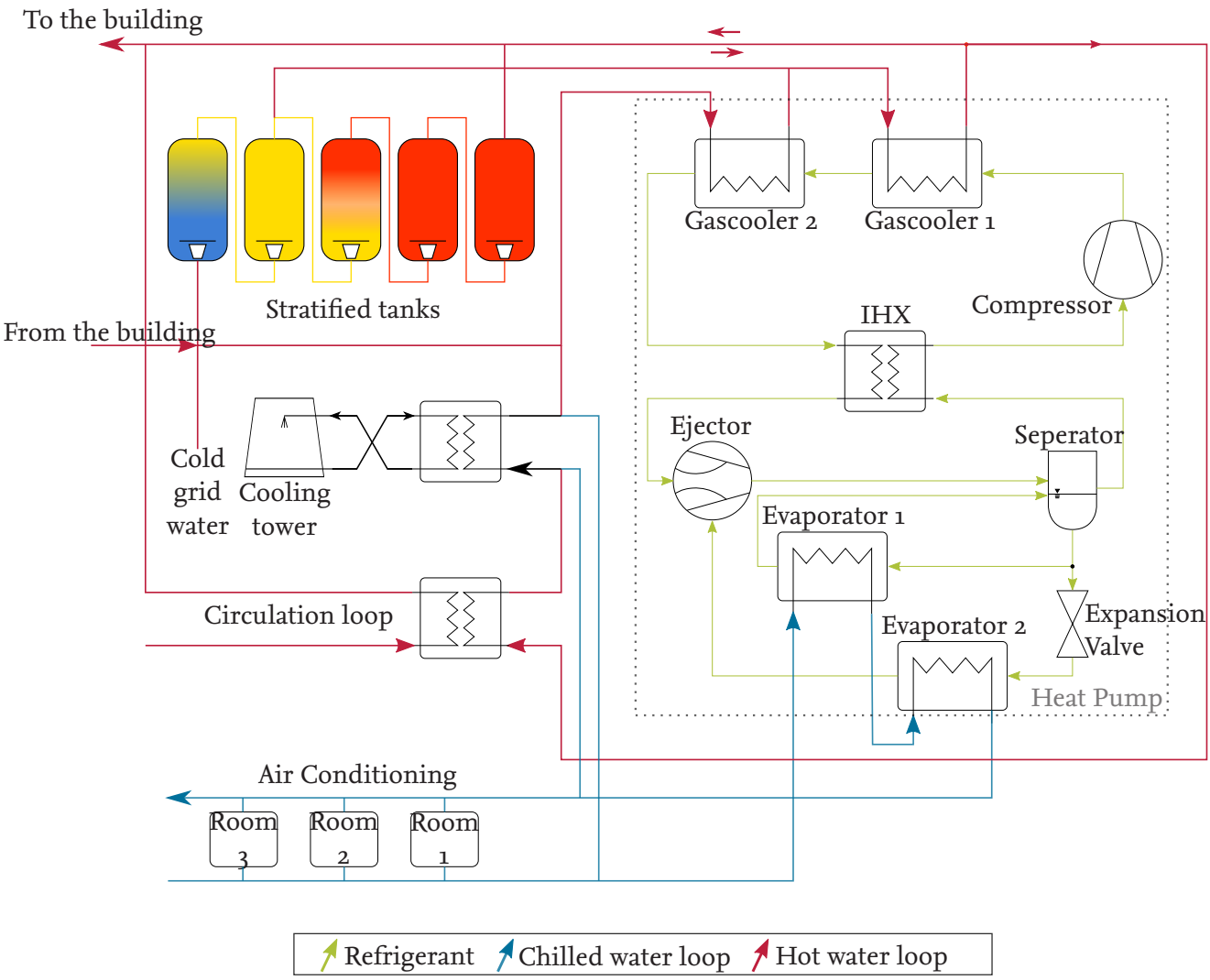

Figure 3.1: Flowchart of the energy system with the heat pump/chiller unit for the hotel in Chennai

Energy systems for hotels with CO_2 heat pump/chiller units in tropical ambient conditions have also been analyzed by Lemke [29]. There, a two-stage heat pump/chiller process is analyzed and numerically simulated to increase the efficiency when using CO_2 as a refrigerant. Such a process can better compete with the efficiencies of conventional synthetic refrigerants, especially in warm and tropical ambient temperatures, than a single stage CO_2 process [29]. However, due to the in chapter 2 explained improvements to the CO_2 heat pump/chiller process, a two-stage operation is not further considered in this thesis.

3.2 Operating Modes of the Energy System

Due to a heat pump/chiller's ability to utilize waste heat effectively, it works most efficiently when there are simultaneous heating and cooling demands. However, as will be explained in chapter 3.3, the different energy demands vary over the course of the day. During periods, when there is the need for DHW but no air conditioning, the water supply system has to operate differently compared to

scenarios with air conditioning but no DHW. To satisfy all demands, there have to be three different operating modes of the system: a mode for the simultaneous heating of water for DHW and the production of chilled water for air conditioning, a cooling mode, when the TES does not have to be charged and a heating mode, for no need for air conditioning but heating demands to charge the TES. The following section describes the different modes in detail.

3.2.1 Mode for Simultaneous Heating and Cooling

Each of the modes require specific conditions to be activated. The mode for simultaneous heating and cooling is active when there are cooling demands while the TES has to be charged. Ideally, the heat pump is designed, to satisfy the heating demand using only the waste heat from the cooling process. This leads to a good heat recovery and an efficient operation of the heat pump. In case, the heat recovery does not satisfy the heating demand, the high pressure of the heat pump can be increased to receive a higher temperature glide in the gascooler and thereby the heating capacity is increased. It is possible to operate the heat pump/chiller transcritically for higher temperatures, with a subcritical refrigerant in the gascooler. With an flexible operation like this, different heating

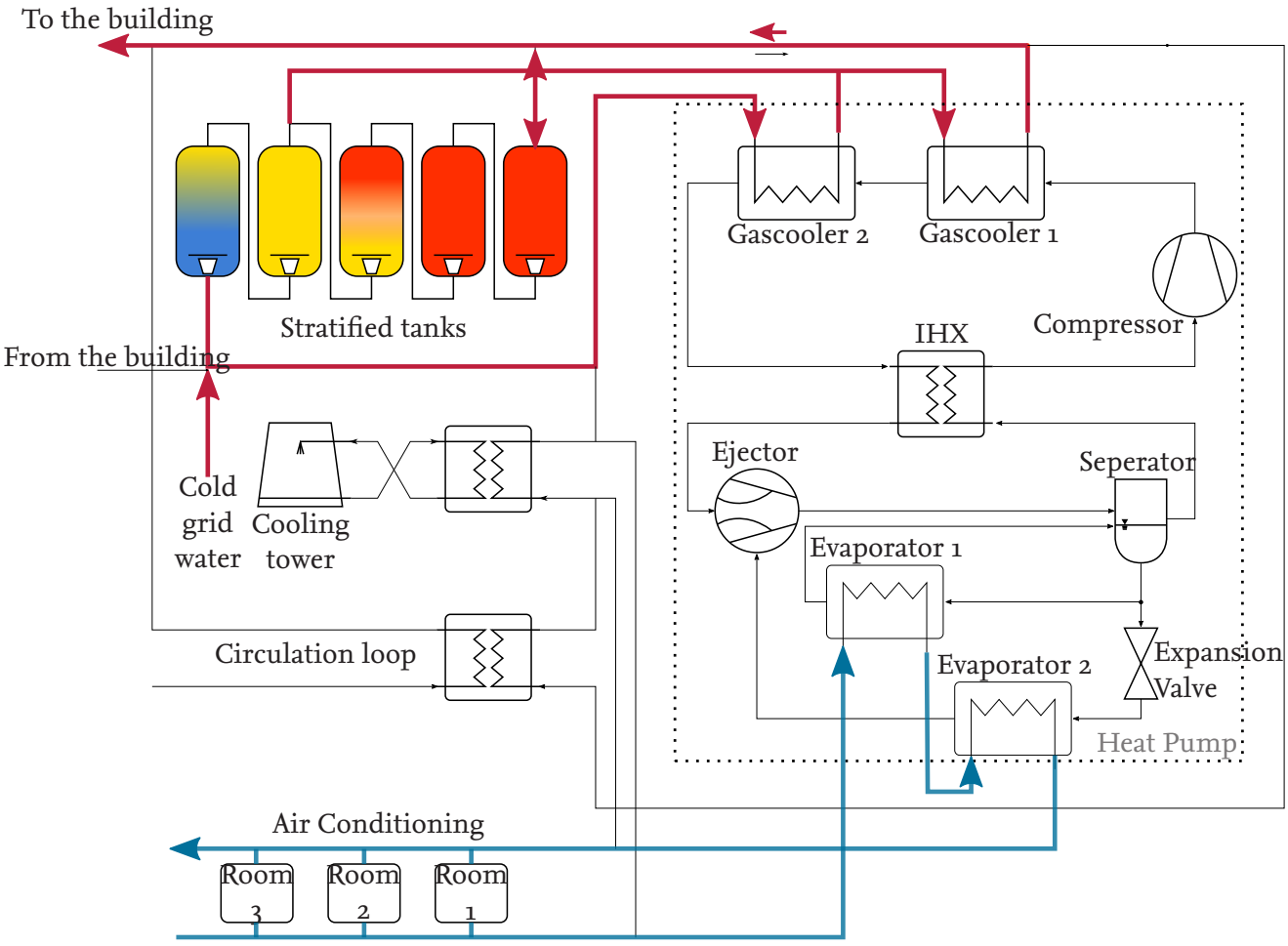

Figure 3.2: Flowchart of the mode for simultaneous heating and cooling

and cooling demands can be satisfied by the same heat pump/chiller.

For the heat pump/chiller to work, there has to be a heat sink and a heat source. The heat sink is the heating water loop, depicted in red. It is heated in the gascooler for DHW and space heating demands. The heat source is a chilled water loop, cooled in the evaporator for air conditioning. The heating water is sourced from the city's water grid with a water inlet temperature of 30 °C. It is then heated in the gascooler to 70 °C. The heated water is used to fill the TES until it is at full capacity. To satisfy the DHW and space heating demands, the water is taken from the TES. The return water in the chilled water loop (12 °C) is cooled to 7 °C in the evaporators, and thereby serves as the heat source. It is then used as chilled water again.

3.2.2 Cooling Mode

In a scenario, where the TES is completely charged but chilled water is needed, the cooling mode is activated. Due to the lack of heating demands, there is no efficient way to use the waste heat from the cooling process. However, to operate the heat pump, the energy still has to be transferred to a

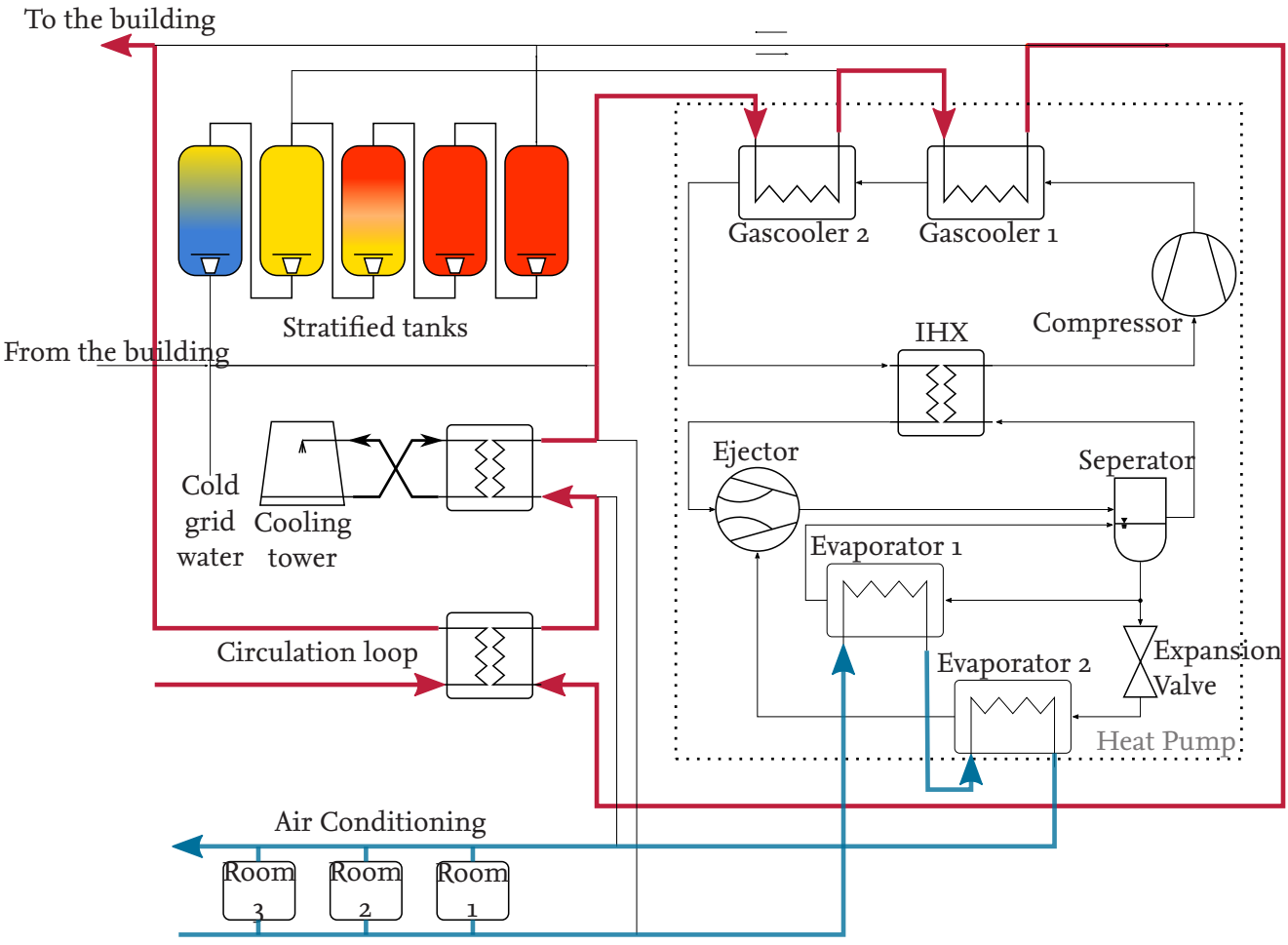

Figure 3.3: Flowchart of the cooling mode

heat sink, which in this case is a cooling tower. This process works best in hot, dry climates and is therefore well suited for the hotel site in India.

Since there is no need to heat water to a specific temperature, the high pressure of the heat pump only has to be high enough, to allow a sufficient heat transfer in the evaporator.

In the cooling mode, the water cooled by the cooling tower to around (30 °C) is heated in the gascooler to transfer the heat away from the refrigerant of the heat pump/chiller. The heated water is then directed through a heat exchanger, transferring part of the received thermal energy to a circulation water loop. The circulation water loop satisfies minor short term DHW demands for all rooms, As it provides hot water immediately while the DHW from the TES is pumped on demand with lag. The circulation water loop and the heat exchanger has to be designed to provide hot water immediately at a specific temperature to the room furthest from the heating system. The circulation loop is a way to recover heat from the process, however, the heat transferred to the circulation loop is only a portion of all the thermal energy, which has to be emitted by the heat pump. To emit the rest of the heat, the water is directed to the cooling tower. As mentioned, the use of a cooing tower is the main heat sink of the system in cooling mode. Due to the hot, moist climate in the cooling tower, the water inside is prone to bacteria contamination and should not be consumed [8]. That is why the heated water is cooled indirectly in a heat exchanger by the cooling tower, instead of directly by spraying the heated water into the tower. After transferring the heat to the cooling tower, the water then proceeds in its loop by being heated in the gascooler again. The chilled water loop is the same as in the dual mode. The returning chilled water (12 °C) is cooled in the evaporator to 7 °C to be used for cooling again.

3.2.3 Heating Mode

When TES has to be charged without the need for any chilled water, the heat system operates in the heating mode. This is often the case for facilities in cold climates. However, at the hotel site in India, this is only rarely the case due to warm climate demanding air conditioning almost all year long. Nevertheless, for these occasions it is important to implement a heating mode to the system, especially because it requires only little extra equipment. Different from the cooling mode, the heating mode is missing a heat source instead of a heat sink. This role is fulfilled by the same cooling tower used in the cooling mode by reversing its function. By spraying cold water from the chilled water side into the cooling tower, it can be heated up to a maximum temperature of the wet bulb temperature of the ambient.

In the heating mode, the heating water loop is very straightforward. The water from the grid (30 °C) is heated in the gascooler to 70 °C before it is pumped into the TES to be used as DHW. However, the chilled water loop is more complicated. After emitting heat in the evaporator, the chilled water (7 °C) needs to be heated to 12 °C in order to remain being able to evaporate the refrigerant in the evaporator. This is done in the heat exchanger connected to the cooling tower. The temperature of the cooling tower is above 12 °C, so it is possible to use part of the thermal energy in the cooling tower to heat the chilled water to its desired temperature. Afterwards, the chilled water is used again to evaporate the refrigerant.

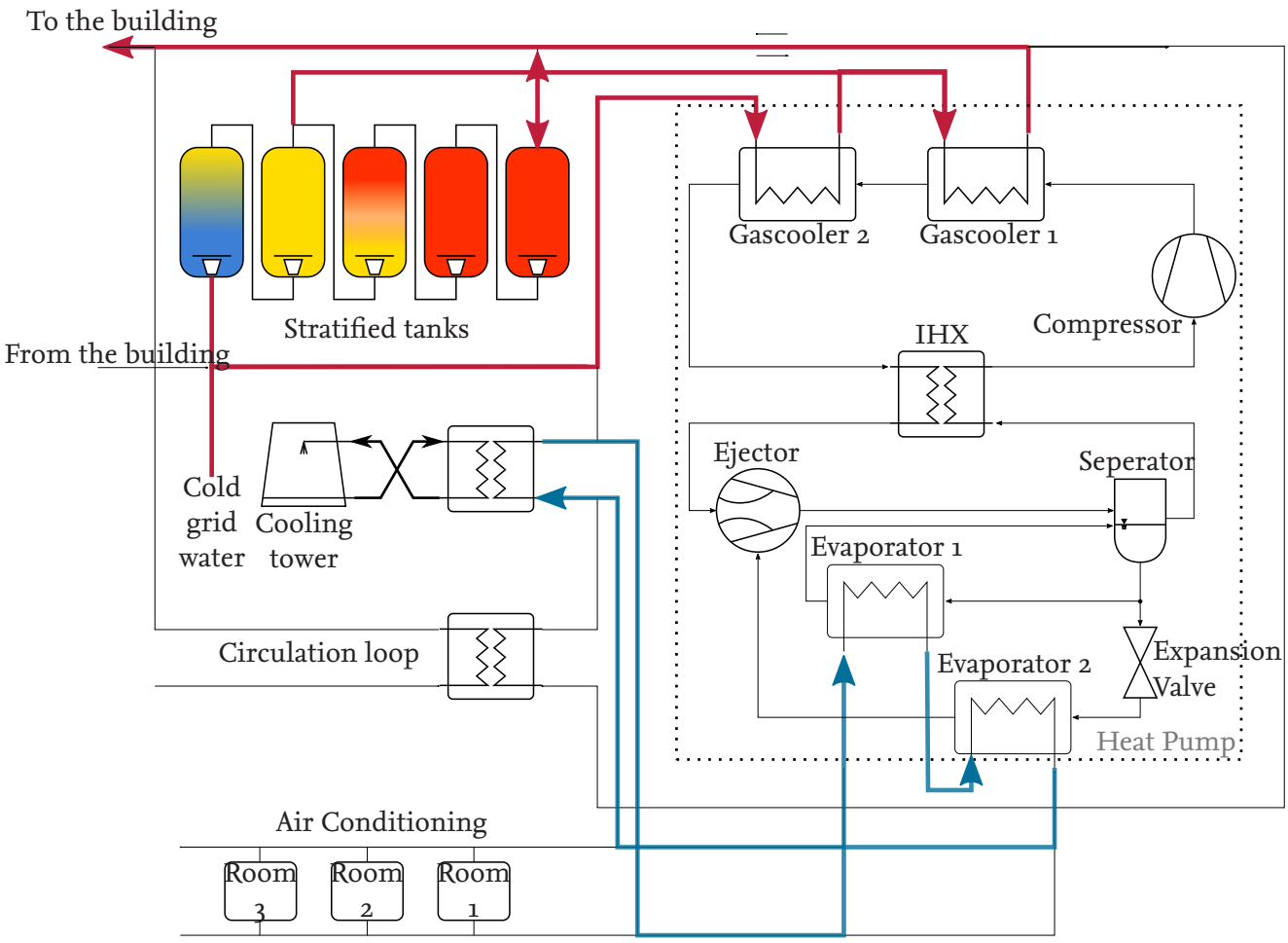

Figure 3.4: Flowchart of the heating mode

3.3 Energy Demands of the Hotel

To distinguish between the different operating modes and also to decide on the capacities of the heat pump/chiller, the heating and cooling demands of the hotel must be known. Since the hotel is new, no exact measurement data of the hotel is available. Accordingly, the heating and cooling demands have to be estimated by comparisons and approximations.

There are different approaches to determine the cooling demands. One is to look at the ambient temperature. This can be measured either as dry bulb temperature or as wet bulb temperature. The dry bulb temperature is the temperature that can be measured independently of the humidity. The wet bulb temperature is the minimum temperature that can be achieved by direct evaporative cooling. The dry bulb temperature can be used to estimate whether cooling demands are present or not. In the figure 3.5 a) one can see that in the coldest week of the year, from January 10 to January 17, the dry bulb temperature does not fall below 17.5 °C. This low temperature is reached only briefly. In addition, one can also see relatively weak fluctuations between day and night. That means that not even at night the temperature drops so far that there are no air conditioning demands for a

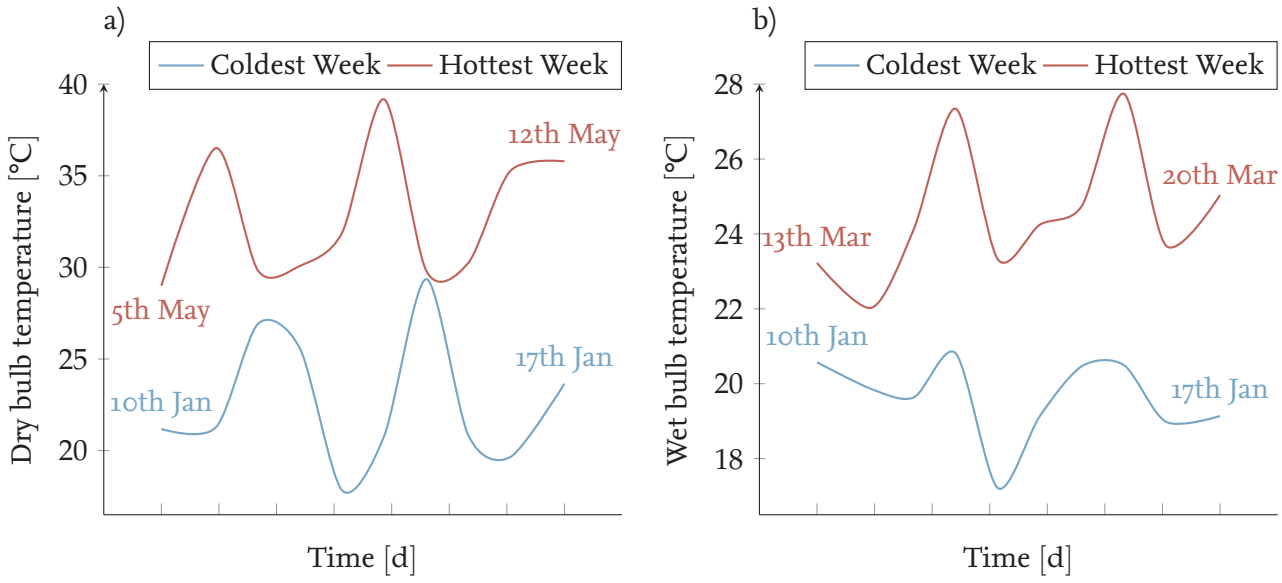

Figure 3.5: Week with the hottest and coldest a) dry bulb temperature and b) wet bulb temperature from the weather data in Chennai

longer time. Accordingly, it can be assumed that due to the location of the hotel in Chennai, India, there are continuous cooling demands. The maximum cooling demands are reached in the week from May 5 to 12. There, the dry bulb temperature reaches values of up to almost 40 °C.

The wet bulb temperature is important for the use of the cooling tower. Since it cools the water by evaporation, the temperature in the cooling tower cannot be reduced below the wet bulb temperature or, if reversed, cannot be raised above the wet bulb temperature. Figure 3.5 b) shows that the warmest week in terms of wet bulb temperature, from May 13 to 20, reaches a maximum of 28 °C. Since the heat pump/chiller is designed for a heat transfer from 30 °C to 70 °C, the water gascooler inlet temperature should not exceed 30 °C to 35 °C. Due to the maximum wet bulb temperature of 28 °C, the desired gascooler inlet temperature is always achievable by using the cooling tower. The same applies to the use in heating mode, where the cooling tower is used to heat the water to 12 °C. The wet bulb temperature does not fall below 17 °C even in the coldest week, which gives the possibility to heat the water to the evaporator inlet design temperature of 12 °C in the cooling tower all year round.

However, this comparison can only determine whether cooling demands are present and whether they can be met via the cooling tower. It is not possible to determine the extent of cooling demands, since factors such as the insulation of the rooms, the behavior of the guests, the usage of the kitchen, etc. would have to be taken into account. It is difficult to make assumptions about these and other variables.

In his work, Lemke [29] presents a standardized method for determining the cooling demands of a hotel under tropical conditions as a function of the ambient temperature. However, this leads to very high cooling demands in relation to the existing, estimable heating demands. In the reference case he investigated, the difference is so large that it has to be satisfied by different heat pump/chiller units. A two-stage chiller unit with a large capacity for the cooling demands and a

single-stage heat pump with small capacity for the heating demands [29]. By using a TES on the hot water side, it is possible to satisfy these large differences between heating and cooling demands also with one heat pump/chiller unit. However, once the TES is fully charged, a lot of heat from the heat pump/chiller unit has to be wasted to the ambient. This thesis does not focus on the scenario of extreme differences between heating and cooling demands. Therefore, the approach presented in Lemke [29] to estimate the cooling demands is not further elaborated.

Another possibility to estimate the cooling demands of the hotel is the comparison with other hotels of similar size and under similar climatic conditions. For this purpose, the U.S. Department of Energy (D.O.E) has published a *Commercial Reference Buildings Library* that shows the heating and cooling demands of various commercial buildings such as retail stores, schools, hospitals and also hotels in the different climatic zones of the USA over one year [34]. A large hotel in the most tropical conditions available is selected for comparison with the hotel in Chennai. In the library, these are available for Miami, Florida.

From the demands of the large hotel in Florida, the ratios are taken and adjusted for the hotel in India. In the file from D.O.E. a maximum cooling load of 90 kW is assumed. However, the maximum cooling load on the heat pump/chiller unit of the hotel in Chennai is only 35 kW. Accordingly, the cooling demands from the library are adjusted by multiplying them by $\frac{35}{90}$. Thus, the maximum cooling load of the hotel in Chennai is not exceeded, but the ratios over the year remain the same. The week with the largest cooling demands from November 19 to 26 is shown in figure 3.6. There is large variability between day and night. Cooling demands are present continuously, although only to a small degree at night.

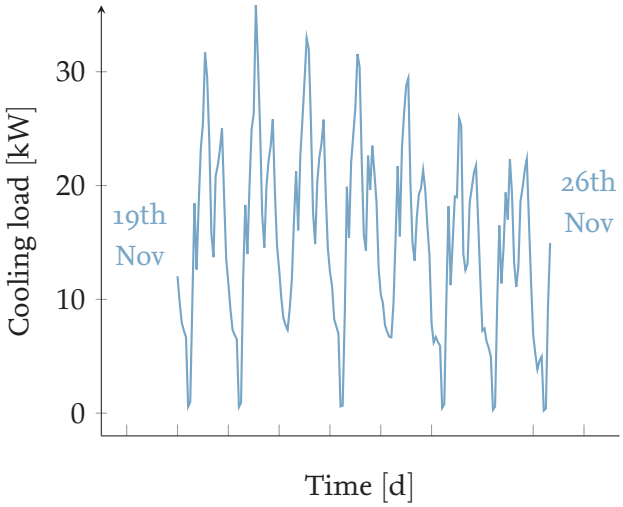

Figure 3.6: Week with the highest cooling load for the hotel in Channai, bases on the loads of the large hotel in Miami, Florida, by the *Commercial Reference Buildings Library* from the U.S. Department of Energy

Determining DHW and space heating demands is easier than cooling demands. As shown in figure 3.5 a) there are continuous cooling demands due to the temperatures in Chennai. Accordingly, the heating demands are negligible. Therefore, the DHW demands largely determine the heating

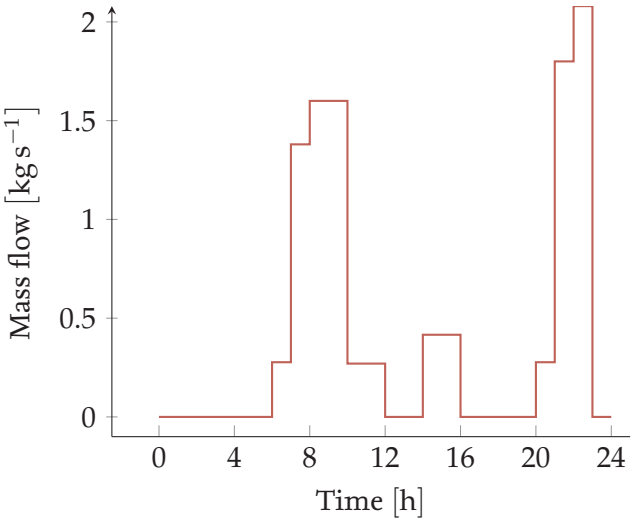

Figure 3.7: DHW demands at 45 °C for one day

demands. Compared to the cooling demands, these are less dependent on the location of the hotel. Showers, kitchen and sanitary facilities are used irrespectively of the temperature and climatic conditions, which means that hotels of the same size have similar water demands. The Indee+ project also retrofitted a heat pump/chiller unit in Goa, India. The hotel is of similar size, accordingly it can be assumed that the DHW demands of the two hotel facilities overlap. The DHW demands at 45 °C hot water are shown over one day in figure 3.7. It is easy to see that around 7AM DHW demands increase as guests wake up, shower, and the kitchen starts working. Throughout the day, demands decrease before increasing again and reaching their maximum of 2.08 kg s^{-1} in the evening between 8PM and 11PM. There, hotel guests prepare for bed. It is assumed that DHW demands repeat every day.

4 Simulation of the System

The simulation model is created in Dymola based on the Modelica programming language. Modelica is an object-oriented language for which there are several different libraries. For this work, the open source libraries *Modelica Standard Library* and *Modelica Buildings Library*, as well as the commercial *TIL Library* were used. The creation and description of the simulation model and the presentation of the simulation results are described in this chapter.

4.1 Simulation Model

The simulation model is based on the flow chart of the energy system shown in figure 3.1. It consists of a combination of blocks from the above mentioned libraries, and custom blocks. Figure 4.1 shows a simplified flowchart of the simulation model in Dymola. The figure shows the refrigerant and water mass flows. The control of the system is presented separately in chapter 4.2 for a better and clearer visualization of the system.

The flows of the VLE fluid respectively the refrigerant are shown in green. The individual green blocks and connections thus represent the heat pump/chiller. This consists of two parallel compressors, which are up- and downstaged as required. Both compressors have a volumetric, isentropic and effective isentropic efficiency of 0.95. The displacement volume of the two compressors differs based on criteria stated in chapter 4.2.

The high pressure, high temperature fluid transfers its heat to the gas cooler to the secondary side, the heating water. The gascooler is a tube and tube heat exchanger and its geometry is designed so that a heat flow of 50 kW heats the heating water from 30 °C to 70 °C. A constant αA value of 400 kW K^{-1} and a pressure loss free flow are assumed. Similar to the gas cooler, the internal heat exchanger is also of type tube and tube with constant αA and zero pressure drop.

Based on Gullo [20], the ejector efficiency is 0.25 and the effective flow area A_{eff} is controlled by the *Ejector Control*. The ejector control is also responsible for opening and closing the expansion valve to expand the liquid refrigerant, which is separated from the gas phase in the separator. The corresponding separator has a volume of 60 L.

Finally, the evaporator is also of the tube and tube type and is defined by its geometry, the constant αA value of 1000 kW K^{-1} and the zero pressure drop to absorb a heat flow of 35 kW from the chilled water on the secondary side. Ideally, the refrigerant should have a vapor fraction of approximately 0.9 behind the evaporator. For a more stable simulation, only one gascooler and evaporator are used in the simulation.

While the operation of the heat pump during simulation differs mainly in the temperatures and pressures to be reached, the secondary side changes not only temperatures, but also mass flows and flow directions. As described in chapter 3.1, the flow directions of the chilled and hot waters change

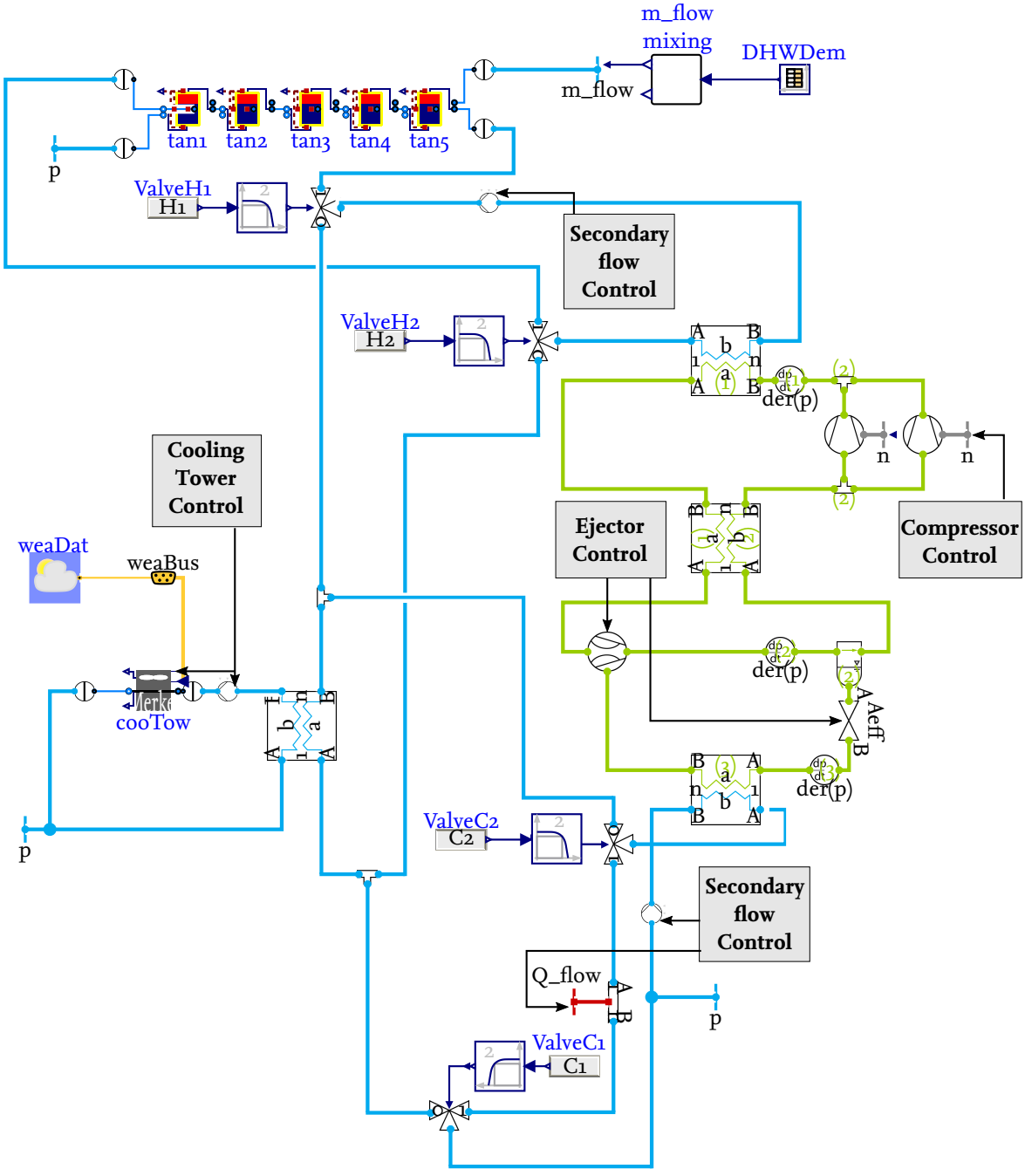

Figure 4.1: Dymola flow chart of the simulation model

depending on the operating mode. This is controlled by the four three-way valves H1, H2, C1 and C2. Each valve can direct the water from the inlet port completely or proportionally to one or the other outlet port via a value between 0 and 1. To which number the values must be set depending on the operating mode is listed in table 4.1.

This way, in the presence of heating demands (heating mode and simultaneous mode) the heating water is directed to and from the TES, and in the presence of cooling demands (cooling mode and simultaneous mode) the chilled water is used as air conditioning. In the other cases, the water is

Mode	H1	H2	C1	C2
Heating	1	1	0	0
Cooling	0	0	1	1
Simultaneous	1	1	1	1

Table 4.1: Values for the three way valves depending on the operating mode

passed via the cooling tower to cool it down in the case of cooling mode or to heat it up in the case of heating mode.

In each operating mode, the heating water is delivered by a pump after it was heated in the gas cooler. The temperature and mass flow of the water depend on the operating mode and are controlled in the Secondary Flow Control. In case of existing heating demands, a water temperature of 70 °C is aimed for, and then the water is transferred to the last TES element tan5 via the three-way valve H1. The five stratified tanks constitute the TES, each having a volume of 6 m^3. While the top volume element should have a temperature of 70 °C, the bottom volume element of tan1 should have a temperature between 30 °C and 35 °C. In between, the temperature is stratified over the five tanks. The water from the lowest volume element of tan1 is then used as water via the three-way valve H2 as inlet for the gas cooler. If the temperature of the water exceeds 35 °C, the efficiency of the heat pump would decrease significantly, because the heat which can be emitted from the heat pump/chiller is being reduced.

The warm water from the TES is used to meet DHW demands of the hotel facility. These are specified in the *DHWDem* block based on known measurements and experience data from a similar hotel in Goa, India. The DHW demand curve at 45 °C over one day is shown in figure 3.7.

Since the temperature differs between the DHW demands and the top section of tan5 where the warm water is taken, the warm water must be mixed with tap water. Tap water in India has an approximate temperature of 30 °C. The required mixing ratio between warm and tap water to obtain the DHW at the desired temperature is calculated in the block *m_flow mixing*. When mixing two water mass flows, *Richmann's law of mixtures* can be applied, determining the required mixing ratio. The law of mixtures is shown in equation 4.1 with the ideal mixing ratio in equation 4.2.

$$\dot{m}_{hot} T_{hot} + \dot{m}_{cold} T_{cold} = (\dot{m}_{hot} + \dot{m}_{cold}) T_{DHW} \tag{4.1}$$

$$x_{mix} = \frac{\dot{m}_{hot}}{\dot{m}_{cold}} = \frac{T_{DHW} - T_{cold}}{T_{hot} - T_{DHW}} \tag{4.2}$$

The calculation of the warm and tap water mass flows is shown in the schematic diagram in figure 4.2. Here, the two equations 4.3 and 4.4 determine the ideal mass flow of the warm water to equation 4.5.

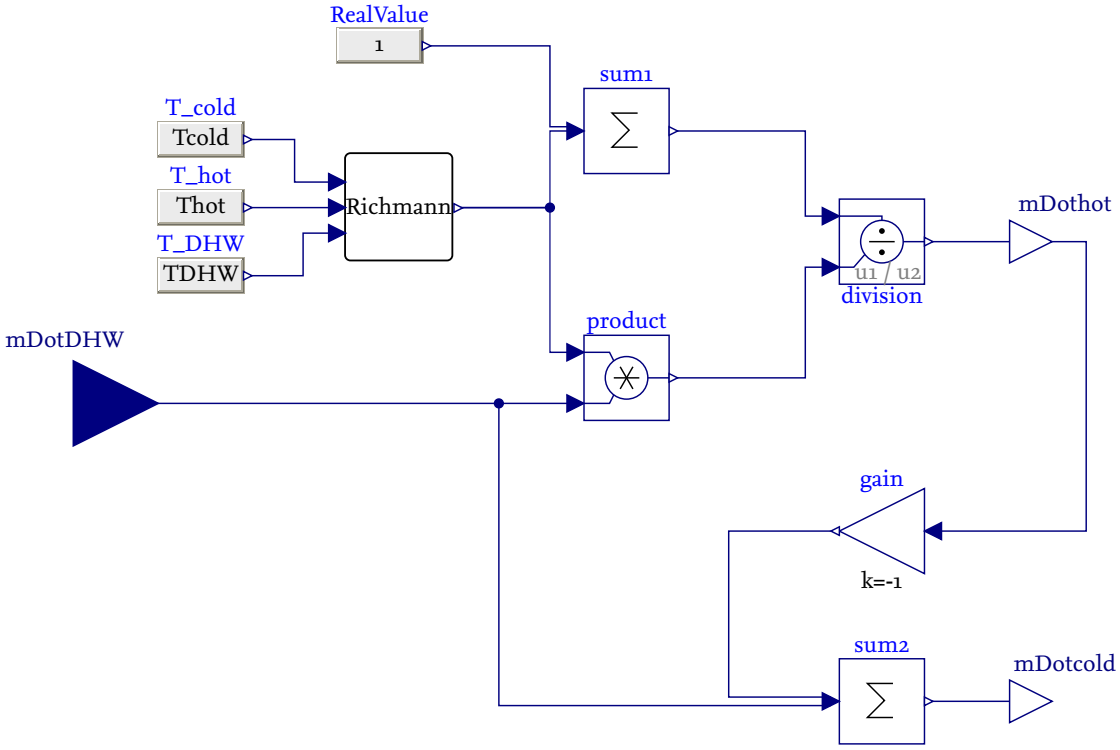

Figure 4.2: Ideal mixing mass flows of hot and tap water

$$\dot{m}_{cold} = \dot{m}_{DHW} - \dot{m}_{hot} \tag{4.3}$$

$$\dot{m}_{cold} = x_{mix} * \dot{m}_{hot} \tag{4.4}$$

$$\dot{m}_{hot} = \frac{\dot{m}_{DHW}}{x_{mix} + 1} \tag{4.5}$$

Subsequently, by inserting $\dot{m}_{hot}$ back into equation 4.3, the mass flow $\dot{m}_{cold}$ can be calculated.

Whenever more hot water is taken from tan5 for the DHW than is added via water heated in the gascooler, the difference is added as tap water with 30 °C in the lowest volume element in tan1. In this way, there is a constant amount of water in the system.

With existing cooling demands the chilled water side is simpler than the hot water side due to the lack of a TES. The three-way valves C1 and C2 are in cooling mode and simultaneous mode on 1, which leads to a simple water circuit with a pressure boundary condition. The water enters the evaporator with a temperature of 12 °C and is cooled down to 7 °C. As a simplified simulation of the air conditioning cooling demands, a corresponding heat flow is added to the water via a tube element, and heats it to 12 °C.

The simulation of the hot water side in cooling mode and the chilled water side in heating mode is more complex. In cooling mode, both three-way valves H1 and H2 are set to 0, so that the heating water is directed via the cooling tower. There, the water is cooled in a tube and tube heat exchanger. This has a constant αA value of 100 kW K^{-1}. The cooling tower itself is of type *Merkel* and has a

nominal pressure difference of 6000 Pa. The fan reaches a maximum power of 4.8 kW with a mass flow at design conditions of 3.5 $kg\,s^{-1}$. Since the cooling tower can only cool depending on the ambient wet bulb temperature, a weather file with the weather data from Chennai, India is inserted via the block *weaDat*. In heating mode, both valves C1 and C2 are set to 0, and the chilled water is passed through the heat exchanger at the cooling tower to heat up.

The circulation loop shown in figure 3.1, which is responsible for the permanent supply of hot water to the hotel visitors, is not considered in the simulation model because of the unpredictable, but also quite low usage.

4.2 Control System

The control system of the simulation model is based on a hierarchical control system. A hierarchical control system is a system in which there are multiple layers, some of which override or monitor the actions of the others [46]. This way, the functions of each controller are simpler and less extensive. A hierarchical control system consists of several layers of controllers, which intervene with increasing frequency within the system [46]. This so-called *Multilayer System* for the simulation model is shown in figure 4.3.

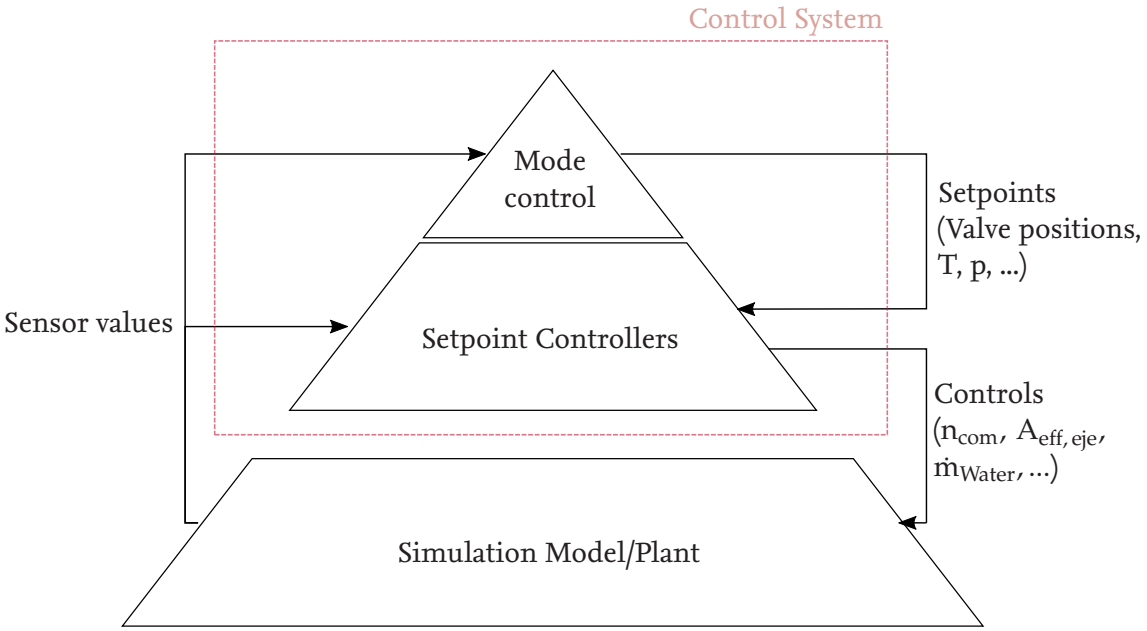

Figure 4.3: Scheme of a hierarchical control system

The top layer controls the different modes of the system. These include heating mode, cooling mode and mode for simultaneous heating and cooling. The top layer controller uses sensor inputs to switch between the modes and set the target values for temperatures, pressures and flow directions based on the active mode.

The mid layer controllers are given the setpoints by the top layer controller as an input, and set the control variables accordingly so that the setpoints are reached. These are then passed on to the

simulation model. These include, for example, the frequency of the compressor or the effective flow area of the ejector.

Since the model is dynamic, this feedback loop happens permanently. The top layer controller changes the mode and thus the setpoints only occasionally. The different control layers are described in more detail below.

4.2.1 Top Layer Controller

The purpose of the top layer controller is to determine the mode in which the system is to be operated on the basis of temperature values. For this purpose, it must be determined whether heating and/or cooling demands exist. Table 4.2 shows which mode should be active based on which existing demands.

Demands		Cooling	
		True	False
Heating	True	Simultaneous	Heating
	False	Cooling	off

Table 4.2: Conditions for the different modes

Figure 4.4 shows the algorithm for switching modes. Whether heating and cooling demands are present is determined by a boolean input, which is true if there is a corresponding demand. Heating demands are present when the temperature in the middle of tan3 falls below 65 °C while the temperature at the bottom of tan1 is less than 35 °C. Due to the high temperatures in Chennai, cooling demands are assumed to be present throughout. A true-signal is then converted into a real value. This value is 1 if the heating demands are there, and 2 if the cooling demands are there. These are then added. This way it can be clearly determined which mode has to be active. The sum can take on four different values. A 0 indicates that there is neither a heating nor a cooling demand and that the system should be off. A 1 indicates the heating mode, since only heating demands are present. A 2 indicates the cooling mode, and a 3 indicates simultaneous heating and cooling. This result is processed in the CombiTable shown in table 4.3.

Sum	y[1]	y[2]	y[3]
0	0	0	0
1	0	0	1
2	0	1	0
3	1	0	0

Table 4.3: CombiTable for the switching of modes

The first column shows the four possible results of the sum. This is used to select which row of the table is active. For example, if the sum is 2, the corresponding row with 2 as the sum defines the values that will be read for y[i]. Here, y[1] stands for simultaneous mode, y[2] for cooling mode and y[3] for heating mode. Afterwards, it will be converted to a true signal for each column y[i], if it

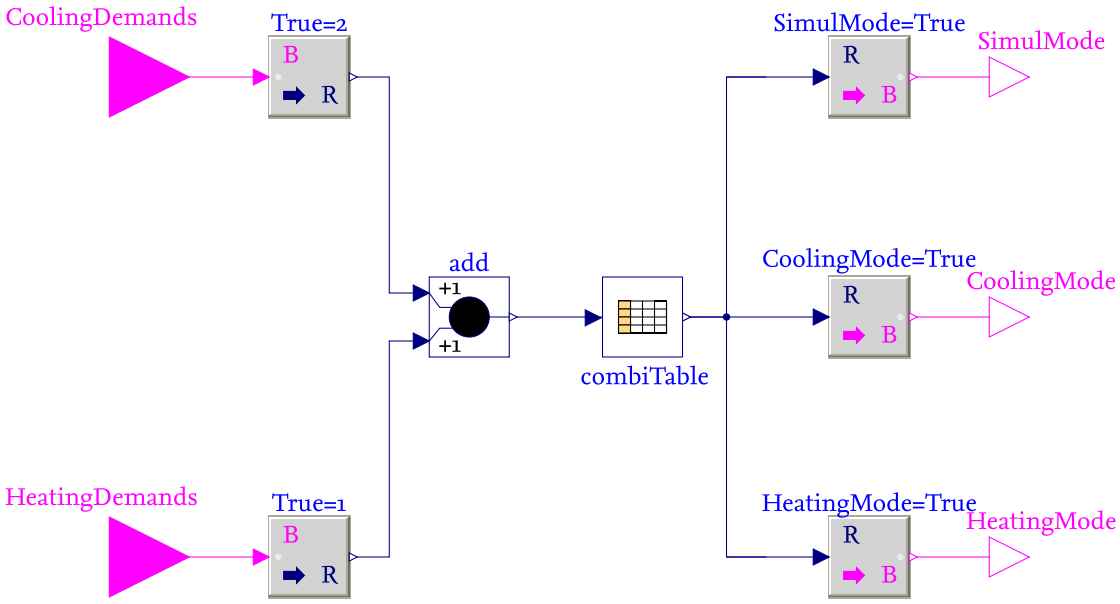

Figure 4.4: Top layer controller for the switching of modes

is equal to 1. Otherwise the signal is false. In this way, the top layer controller can determine the active mode of the system from the information from two different boolean inputs, whether heating and/or cooling demands are existent.

4.2.2 Mid Layer Controller

The mid layer controllers are given the different setpoints by the top layer controller. The aim of the mid layer controller is to intervene in the system in such a way that these setpoints are reached. Many interventions in the system influence each other, therefore it must be decided which setpoint should be controlled by which variable. However, by using PI controllers for different setpoints, these influences on other variables can be compensated over time. For example, the low pressure is controlled by the compressor speed and the high pressure by the variable cross-section of the ejector. In the following the different control-schemes are presented.

Compressor Control

A compressor has a constant displacement volume, but can be operated with a variable frequency drive. However, this frequency is not freely variable, but must lie between a maximum and a minimum value. For this model, the frequency is between 30 Hz and 70 Hz. However, this means that the compressor cannot reach a low enough speed for low cooling and heating loads, especially under part-load conditions, and thus short cycling occurs. In this case, the compressor is repeatedly switched on and off, since the optimum speed would be between 0 Hz and the minimum 30 Hz. 30 Hz are needed to allow continuous oil return in the compressor. To prevent this, or at least mitigate it, a group of compressors can be used. This consists of two or more compressors, one of which is operated with a variable frequency drive (VFD), and the others with a constant frequency drive

(CFD). The control of the constant frequency compressors works by switching the compressors on and off. This model uses a frequency for the CFD of 50 Hz.

To ensure that the part-load behavior can be controlled properly by a group of compressors, it is important to design the displacement volume of the compressors correctly. The the displacement flow rate of the VFD compressor at maximum load (70 Hz) should larger than the sum of the displacement volumes of the VFD compressor at minimum load (30 Hz) and the CFD at 50 Hz. This behavior is also shown qualitatively in figure 4.5. This ensures that the transition from one-compressor operation to two-compressor operation does not result in an operating range that could not be satisfied by the compressor group. In this simulation model, the variable frequency compressor has a displacement volume of 0.0285 l and the fixed frequency compressor of 0.02 l.

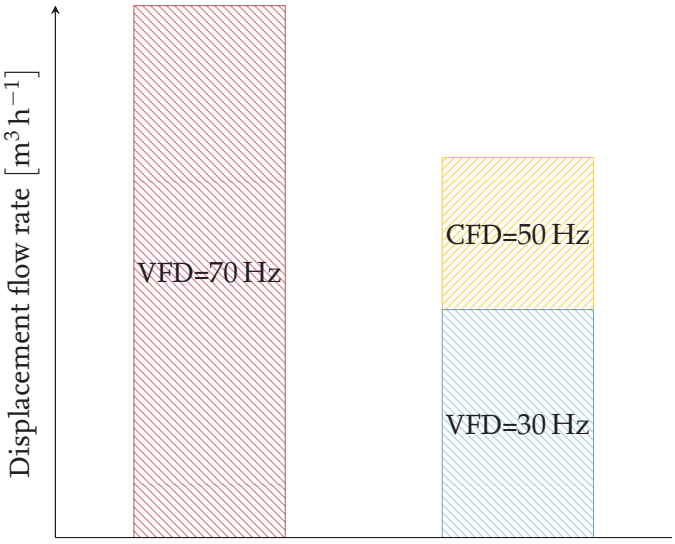

Figure 4.5: Displacement flow rate of different frequency combinations of the compressor group based on [10]

Simulating and controlling this so-called *Up- and Down Staging* of compressors is much more complex than doing the entire control via one compressor. In addition, there are the different operating modes of the system and thus different setpoints of the top layer controller, so the control must also be divided between them. The mid layer controller of the compressor is shown in figure 4.6.

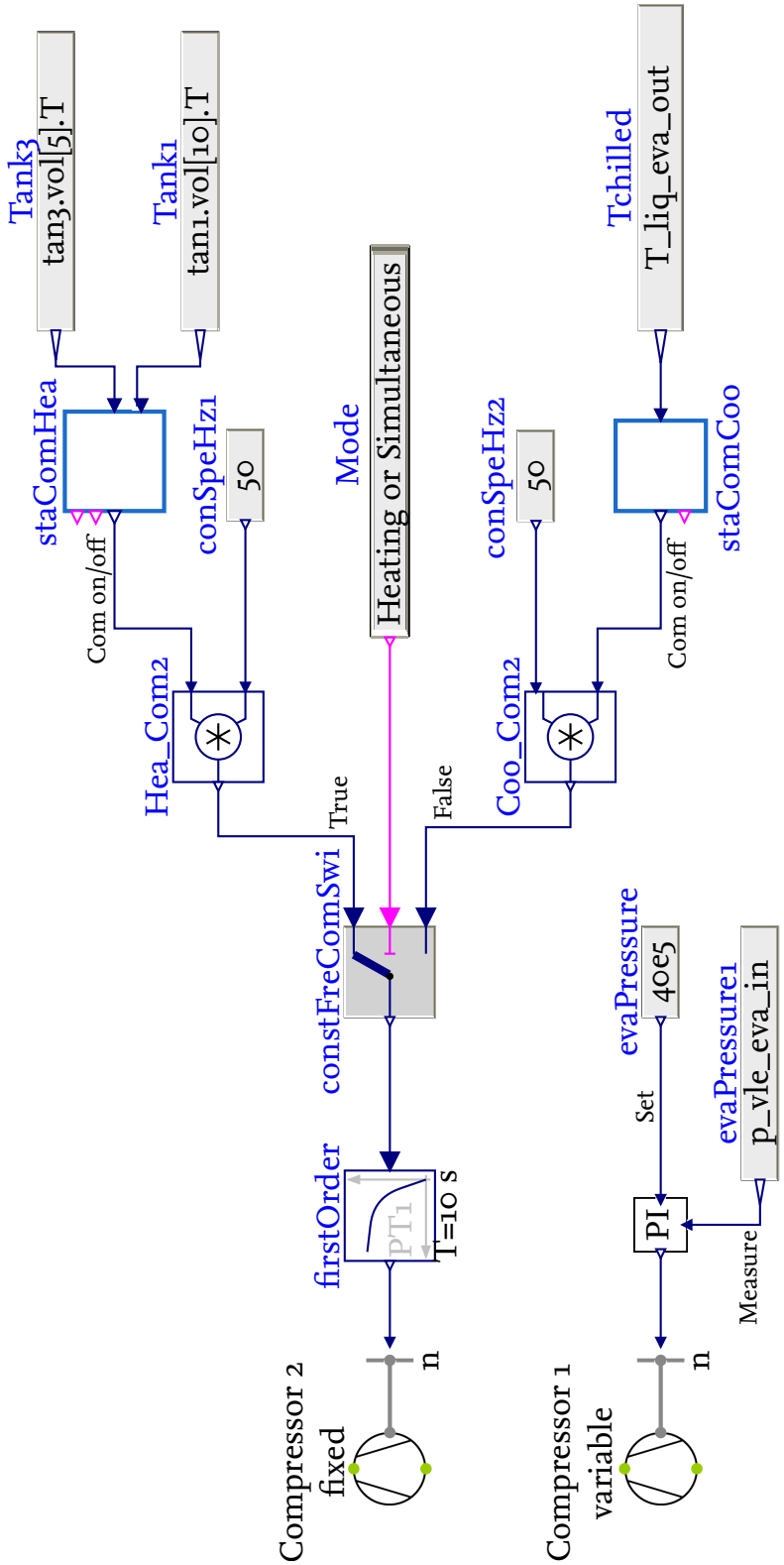

Figure 4.6: Mid layer controller for the compressor group

The two compressors are regulated differently from each other. The variable frequency compressor ensures that the pressure of the refrigerant in the evaporator is maintained at 40 bar. The higher

the frequency, the lower the pressure. The evaporation temperature of CO_2 at 40 bar is 5.3 °C. This ensures that the desired water outlet temperature from the evaporator can theoretically reach 7 °C.

The constant speed compressor can run either at 50 Hz or at 0 Hz. Values in between are not possible. Depending on the presence of heating demands, it is checked whether the fixed frequency compressor is running. In the two blocks staComHea, if heating demands are present, and staComCoo, if heating demands are missing, it is checked if the second compressor should be switched on. In figure 4.7 the procedure is explained by using a state control chart. Additionally, staComHea is also able to indicate the presence of heating demands.

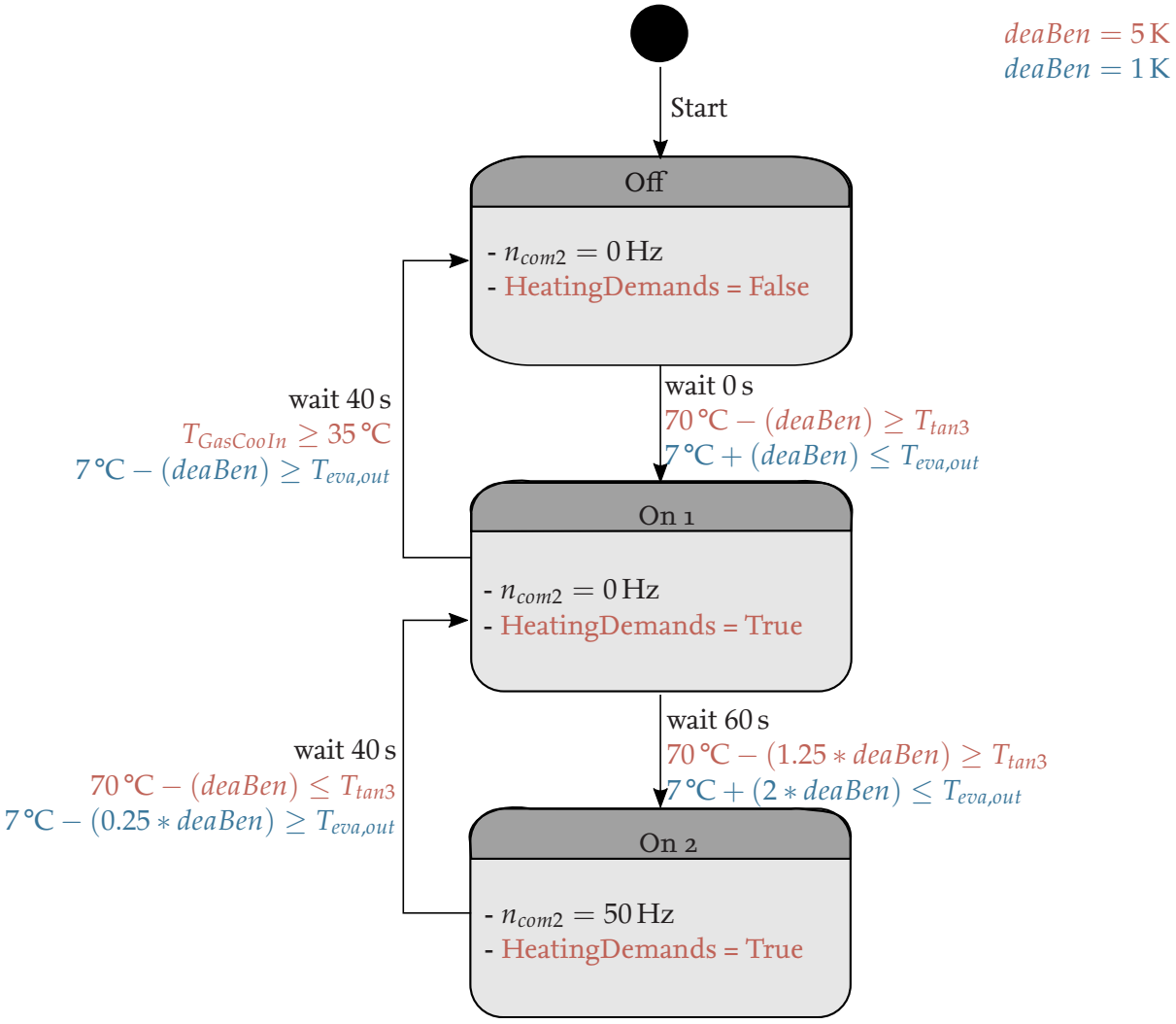

Figure 4.7: State control chart of the controller to determine the on and off compressors in the different modes. Blue is staComCoo exclusively, red is staComHea exclusively

Blue indicates staComCoo exclusive and red staComHea exclusive contents. At the start the fixed frequency compressor is off and staComHea does not detect heating demands. It is then checked whether the condition to go to the next state *On 1* is met. This condition differs depending on staComHea and staComCoo. The setpoint temperature is 70 °C for the temperature in the middle of the third tank or 7 °C for the water outlet temperature of the evaporator. T_{Mea} is the corresponding

measured temperature. In order to prevent the states from changing continuously, two mechanisms are installed. A waiting time and a dead band. By dead bands a hysteresis is integrated in the system, allowing more flexibility. In other words, the setpoint temperature is manipulated by a dead band, adjusting the setpoint by multiplying the dead band (5 K for staComHea and 1 K for staComCoo) with a factor preventing constant switching between states.

As soon as state *On 1* is reached, staComHea outputs a True boolean for the heating demands. Since both staCom state charts are running permanently, staComHea also outputs a True signal for the heating demands in state *On 1* if the cooling mode is currently active. After further waiting time it is then examined whether the signal goes either to the state *On 2*, back to the state *Off* or if it remains at state *On 1*. If it reaches *On 2*, the staCom blocks give an output of 50 Hz for the fixed frequency compressor, turning it on.

In staComCoo in cooling mode there is no difference between the two modes *On 1* and *Off*, because they give the same output. However, if the VFD compressor is also to be included in the up- and downstaging, it is good to have this intermediate state in which the VFD compressor is on, but the CFD compressor is not. The same applies to heating and simultaneous mode with staComHea.

A special aspect is the transition from *On 1* to *Off* at staComHea. To maintain the efficiency and cooling capacity of the heat pump, there must be a suitable water inlet temperature in the gas cooler which is taken from the bottom of the first tank. As soon as this temperature exceeds 35 °C or 308.15 K, the efficiency of the heat pump drops significantly. Therefore, in the staComHea all compressors are switched off and the state switches to *Off* as soon as the temperature exceeds this value.

The absence of a finish block in the state control chart indicates that the state control first ends when the whole system finishes simulating.

Afterwards, it is decided whether the result of staComHea in heating or simultaneous mode, or the result of staComCoo from cooling mode is taken. Finally the output signal goes through a first order transition, which has a transition time of 10 s from one to the other value in case of abrupt changes of values (like changing the mode).

In summary, the compressors control the thermal load in the heat exchangers. This thermal load depends on the outlet temperature of the chilled water in staComCoo or the tank temperature in staComHea, and the refrigerant pressure in the evaporator. As long as the frequency of the VFD compressor does not reach the limits of 30 Hz and 70 Hz with a constant low pressure of 40 bar and a desired outlet water temperature, the required thermal load in the heat exchanger can be met. However, when the outlet water temperature does not reach its setpoint, the thermal load has to be adjusted by turning the CFD compressor on. As a result, the VFD compressor decreases its frequency. This way, the desired thermal loads of the evaporator and gascooler can be met by controlling two different variables.

Ejector Control

The effective flow area of the ejector controls how much refrigerant can flow through the ejector and be pre-compressed. This controls the high pressure. The high pressure setpoints is variable, as it depends more on the temperatures and temperature differences that prevail in the heat exchangers. Nevertheless, to control the high pressure, a value p_{Mea} and a value p_{Set} must be given to the PI controller. Accordingly, in order for the high pressure to be properly controlled, the temperature to be reached must be converted into a pressure. For this the two ReSet blocks hPResetCoo and hPResetHea in figure 4.8 are there. How a temperature signal is converted into a pressure signal in these is shown in generalized form in figure 4.9.

The two axes x and y represent the two units that are to be converted to each other. In this case, a measured temperature (x) is given and converted into a pressure (y). It is simplified assumed that there is a linear relationship between the two units. The higher the measured temperature, the

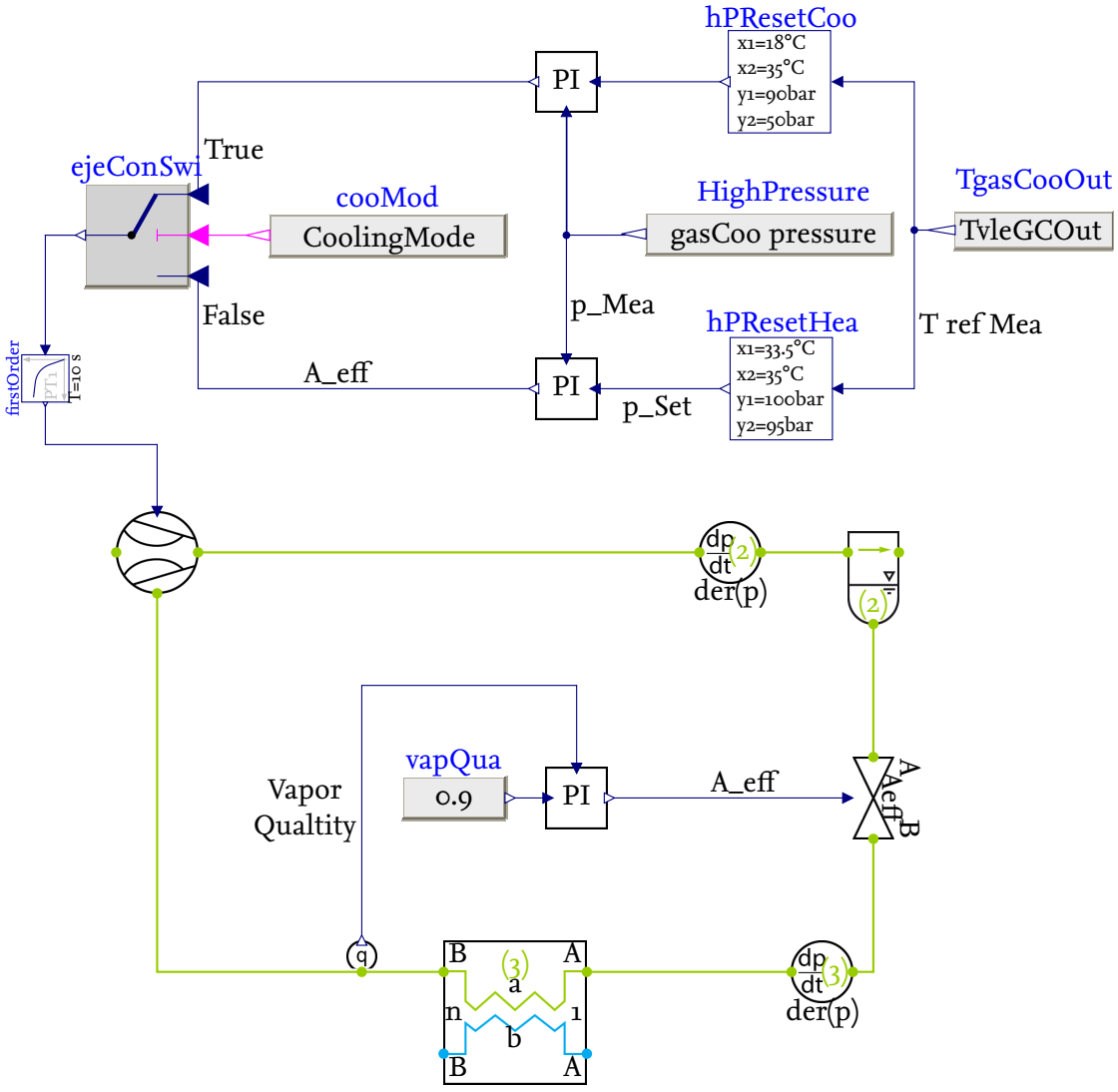

Figure 4.8: Mid layer controller for the effective ejector flow area and vapor quality

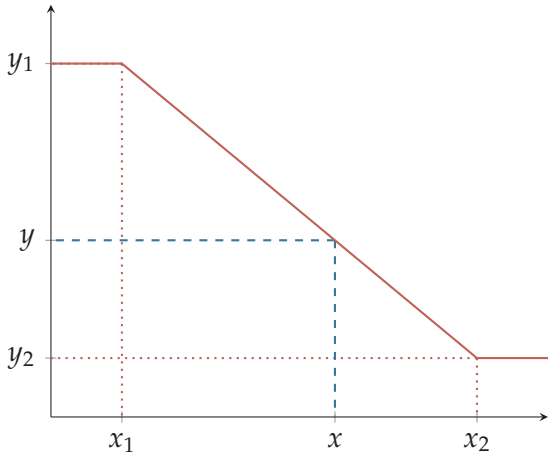

Figure 4.9: Graph and function of the ReSet blocks

lower the pressure. The conversion function is given by fixed input values x_1, x_2, y_1 and y_2. The fixed input values are given in figure 4.8. If now a measured value T_{Mea} is passed to the ReSet, the corresponding y-value of the function is passed to the output. If the measured value is above or below the limits, a constant progression of the ReSet function is assumed, so that the minimum and maximum y values are not undershot or overshot.

For the cooling mode, it is not important to achieve a high temperature in the gas cooler. The gascooler must only emit enough heat from the refrigerant so that the cooling capacity of the heat pump is sufficient to satisfy the cooling demands. Accordingly, the limits of the ReSet function are in a wider range. Thus, depending on the cooling demands, the high pressure can be turned up and down. In heating mode and simultaneous mode, where heating demands are present, it is important to maintain an appropriate temperature in the gascooler so that the water on the secondary side can be heated sufficiently. Therefore, the limits for the hPResSetHea are narrower for a higher pressure to ensure that a sufficient heating capacity is available.

The output signal from the ReSet blocks is passed as p_{Set} to PI controllers, which determine the effective flow area of the ejector based on the measured high pressure. The switch at the end of the control changes between the control in cooling mode and the control in heating and simultaneous mode depending on existing heating demands.

Cooling Tower Control

The cooling tower control consists of two components. One is the control of the water mass flow that goes through the cooling tower and the other is the control of the power used by the fan when drawing the air into the cooling tower. Both the mass flow and the fan power are controlled using the same setpoints and measurements. Furthermore, a distinction is made between the cooling mode, and heating and simultaneous mode. However, since the wet bulb temperature from the weaDat in Chennai, India, never drops to an ambient temperature without the need for air condi-

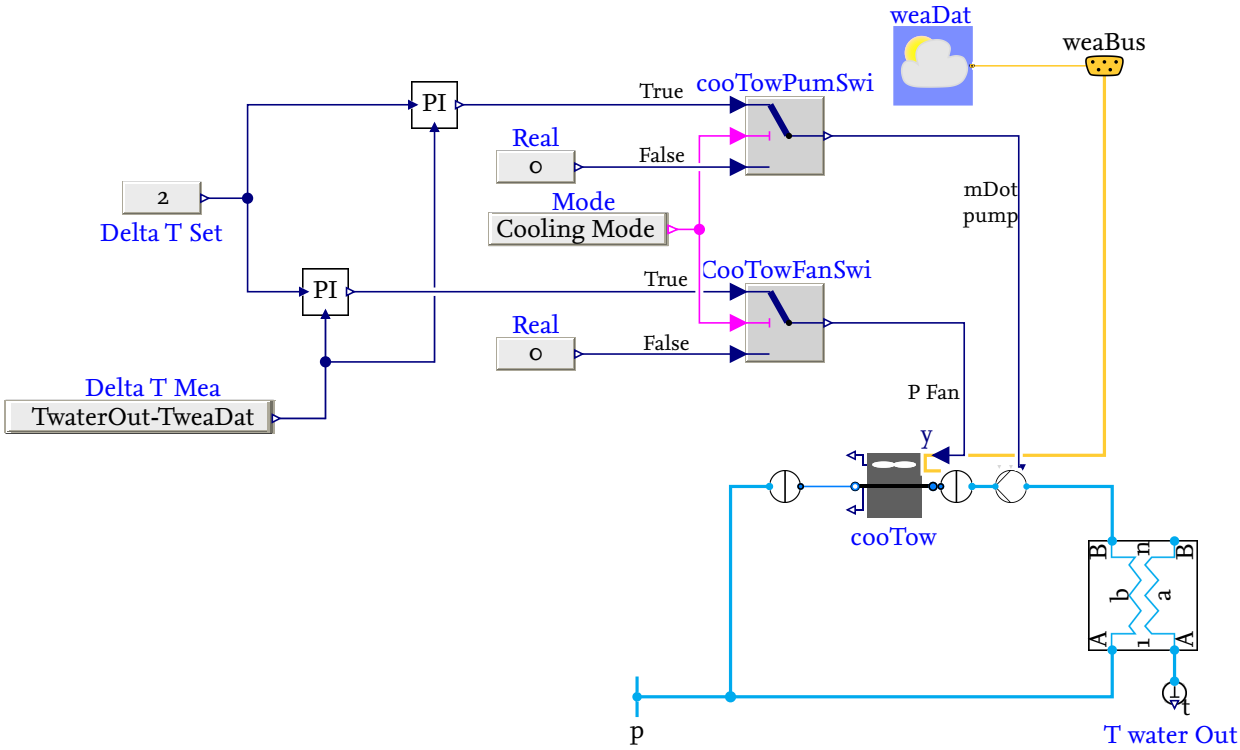

Figure 4.10: Mid layer controller for the cooling tower

tioning leading to permanent cooling demands, the mid-layer controller of the cooling tower only includes the cooling mode. While simultaneous heating and cooling demands, the cooling tower is not in use anyway, and heating only mode never occurs in the underlying ambient conditions.

If the cooling mode is inactive, both the water mass flow and the fan power are regulated to zero. In cooling mode, however, both control variables are regulated by the temperature difference between the water outlet temperature of the secondary side and the wet bulb temperature from the weather file in Chennai. The cooling tower and the pump should cool the water on the secondary side until a ΔT of 2 °C is reached. A switch for each of the control variables is used to switch between the output of the PI-controller in cooling mode and zero.

The signal that is passed to the cooling tower fans is a value between 0 and 1. This is a factor by which the maximum fan power is multiplied. According to [22], the required fan power for a maximum cooling capacity of 50 kW is 2.2 kW for each fan, for a total of 4.4 kW with two required fans.

Secondary Side Controller

The control of the water on the secondary side is divided into the hot water side (top) and the chilled water side (bottom). In both cases, the setpoints are reached by controlling the water mass flow and the compressor group (see above). The control in Dymola is shown in figure 4.11.

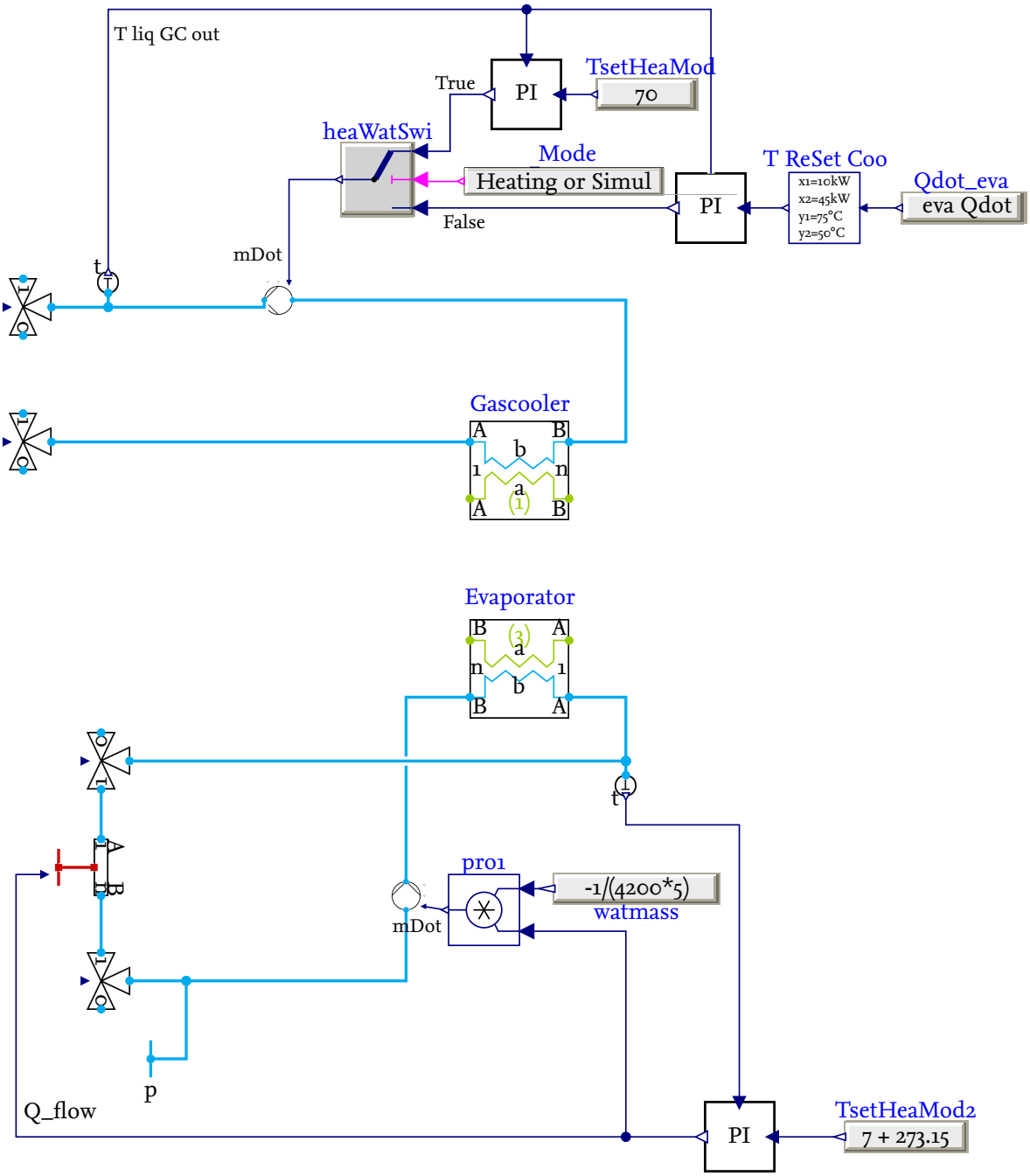

Figure 4.11: Mid layer controller for the secondary side

In the hot water control, the water outlet temperature from the gas cooler is controlled. The setpoints differ depending on the operating mode. When there are heating demands, in heating and simultaneous mode, the temperature is to be controlled to 70 °C. For the heat transfer to the water the following relation is given as a function of the heating capacity in the gascooler $\dot{Q}_{heat}$:

$$\dot{Q}_{heat} = \dot{m} * c_p * \Delta T \tag{4.6}$$

As a consequence, a higher outlet temperature (at constant inlet temperature) can be achieved when the mass flow rate decreases. Since there are no heating demands in cooling mode, and therefore no required outlet temperature of the water from the gascooler, the setpoint temperature is set depending on the transferred heat flow in the evaporator. Accordingly, the heat pump/chiller unit should heat the water only so far that the cooling demands in the evaporator can be satisfied. Therefore the cooling capacity of the evaporator is smoothed by a ReSet, which gets a heat flow as x-value and outputs the setpoint temperature as y-value.

Since there is no thermal energy storage for the chilled water, the chilled water side must be permanently adjusted to the operating conditions. The control has two control variables. First, the water mass flow, and then a heat flow that is added to the water mass flow via a tube element. Both are controlled so that the outlet temperature of the water mass flow from the evaporator is 7 °C. The PI controller outputs a heat flow that is added to the water via the tube. This simulates the air conditioning of the individual rooms, with the heat flow as the combined required cooling capacity. The water mass flow is adjusted by the equation 4.6 so that the same heat flow can be removed from the water with a temperature difference of 5 °C in the secondary side of the evaporator.

For a better visualization, heating mode control is not implemented because cooling demands are always present. However, it is similar to the described control, but the inlet temperature in the evaporator comes from the cooling tower instead of the tube. In that case, the outlet temperature is controlled by the water mass flow.

4.3 Analysis of the Results of the Simulation

In order to analyze the simulation results, a simulation period must first be determined. This period is one day and is the day with the highest ambient wet bulb temperature (March 18). Since the initial period of the simulation is very dependent on the initial values, two weeks are simulated, of which only the second to last day is analyzed. This ensures that the initial values have little to no influence on the simulation results to be analyzed. This can be seen directly from figure 4.12. There, the layering of the five tanks is shown with the temperatures at the bottom, middle and top of the tanks over the second simulated week. First, it is evident that there is approximately a periodic temperature behavior in the tanks. This suggests that the influence of the initial values is negligible. If this were not the case, the extrema of the temperatures of the respective stratifications would not be approximately constant. As a consequence, the total simulation period of two weeks can be reduced, since the influence of the initial values is already negligible after the first week.

Furthermore, it can be concluded from figure 4.12 that the simulation model can simulate longer periods of time without developing instabilities. Additionally, the figure shows the perfect stratification from cold to warm without the need to simulate the buoyancy effects originating from falsely layered temperatures.

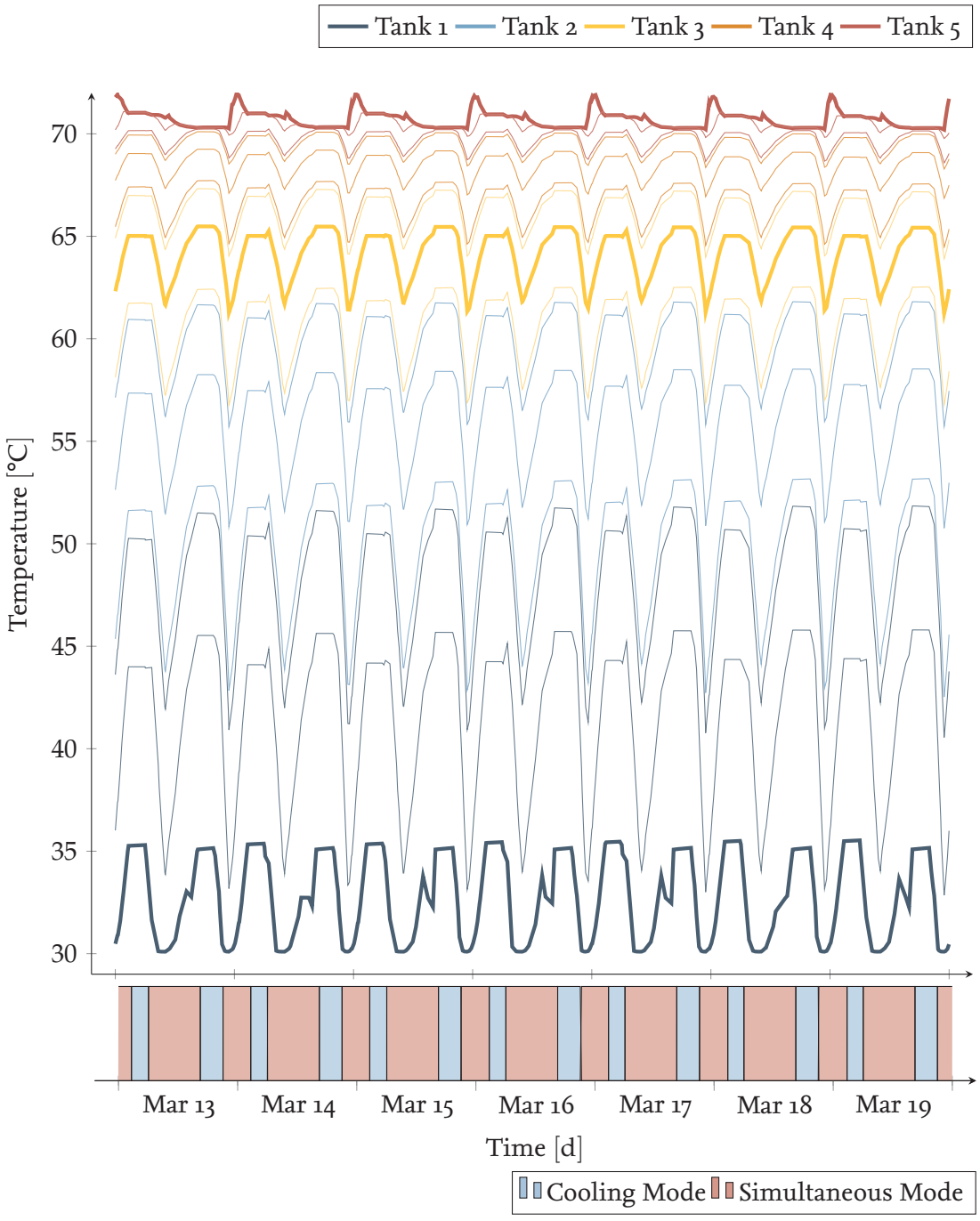

Figure 4.12: Stratification of tanks 1 to 5 with the top, middle and bottom temperatures and the resulting operating mode

With the help of the charts at the bottom of figure 4.12 the functionality of the top layer controller can be understood. Under the assumption made in chapter 4.1 that cooling demands are present over the entire simulation period, a differentiation can be made between the cooling mode and the simultaneous mode depending on the heating demands. Heating demands are present when the temperature in the middle of tank 3 falls below 65 °C. This is the highlighted thick yellow graph in figure 4.12. However, once the highlighted thick black temperature at the bottom of tank 1 exceeds 35 °C, heating demands are no longer present and the system is operated in cooling mode.

Furthermore, it can be observed that the temperature at the top of tank 5 does not fall below 70 °C. Accordingly, there is always enough hot water to be taken from the TES.

Figure 4.13 is a detailed view of the three temperatures important for the top layer controller. It shows the top temperature in tank 5, the middle temperature in tank 3 and the bottom temperature in tank 1 over the warmest day of the year, March 18. In addition, the times during which the system is operated in cooling mode are highlighted in blue. The setpoint temperatures of 35 °C and 65 °C, which are important for the control, are also highlighted so that the control algorithm can be easily understood.

By highlighting the cooling mode it is also shown whether heating demands are present. This is always the case when the system is operated in simultaneous mode, whenever the cooling mode is not active. In figure 4.13 it can be seen that as soon as the system reaches a temperature of 35 °C at the bottom of tank 1, there are no more heating demands. Furthermore, it can be seen that as soon as the temperature in the middle of tank 3 drops below 65 °C, heating demands arise again and the system switches to simultaneous mode.

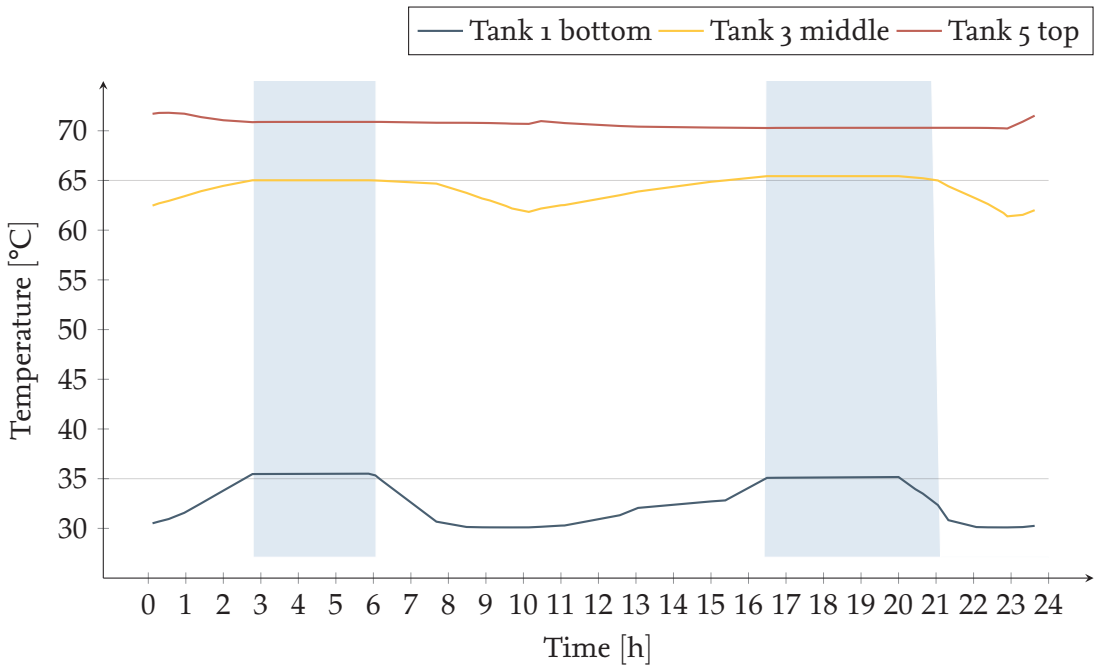

Figure 4.13: Tank temperatures and setpoints for the control

At first glance, it seems counter intuitive that the temperature at the bottom of tank 1 and middle of tank 3 decrease at approximately 6 h as soon as heating demands occur. This is because at that time both hot water is added to the tank, but DHW demands are also present. Thus, more hot water is removed from the TES than added, which is compensated for by cold water in tank 1.

Furthermore, it can be seen that the temperature in the middle of tank 3 only slightly exceeds the setpoint temperature of 65 °C, below which heating demands are present, before the temperature at the bottom of tank 1 reaches 35 °C. Due to the approximately periodic behavior of the temperatures in the tanks. This is the case for each reheating period. This ensures that, taking into account the COP of the heat pump/chiller unit, as much heat as possible is stored in the TES without having to waste it to the environment via the cooling tower. If a volume element other than the center of tank 3 is to be used for control, the setpoint temperature of 65 °C must also be adjusted. For colder volume elements the temperature must be reduced, otherwise it will never be reached, so heating demands will always be present as soon as the temperature at the bottom of tank 1 drops below 35 °C. For a warmer volume element, the setpoint temperature should be increased, otherwise usable heat will be released to the environment via the cooling tower.

The water outlet temperature of the heat exchanger and the CO_2 high and low pressure for one day are shown in figure 4.14. One can see a correlation between the pressure and the water outlet temperature in the evaporator as well as in the gascooler. This is not surprising, since especially in the evaporator pressure and temperature are constant and coupled due to the state of the refrigerant within the wet steam area. Since the water outlet temperature depends primarily on the temperature of the refrigerant, the water temperature is also dependent on the pressure. The phenomenon is also observed in the gascooler, even though the refrigerant there is supercritical in heating and

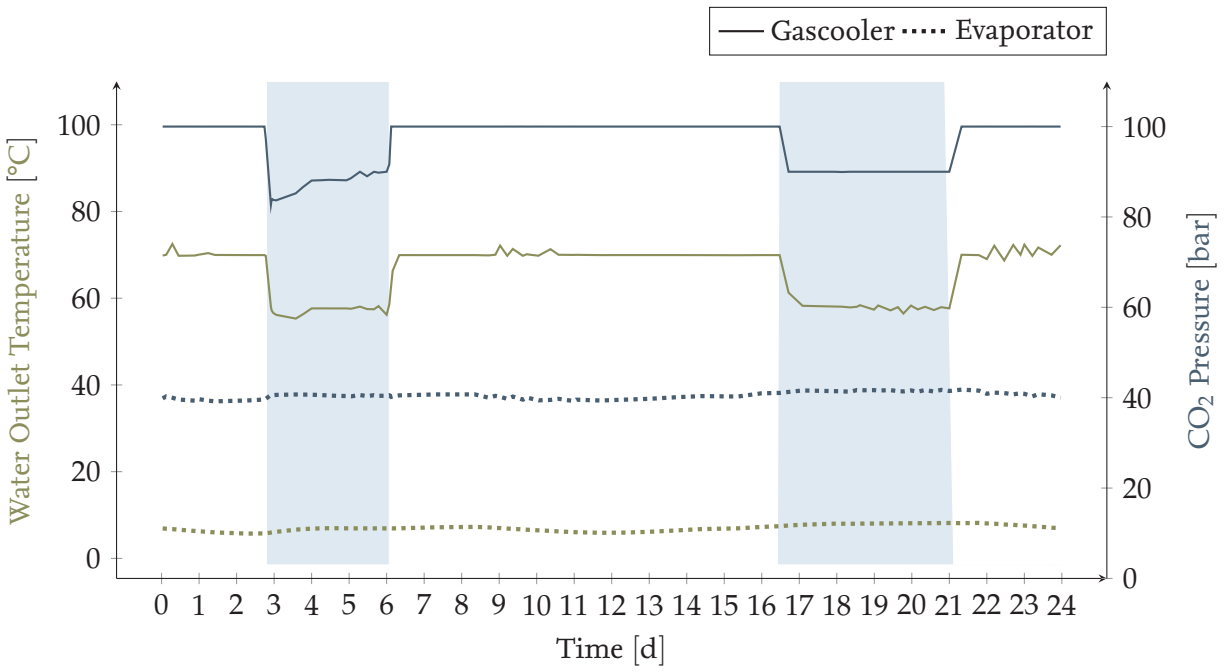

Figure 4.14: High and low pressure of the heat pump compared to the heating and chilled water temperatures

simultaneous mode. Nevertheless, it is the case for CO_2 , that as the pressure increases, the temperature also increases, even in the supercritical state. This leads good correlation of refrigerant pressure and water outlet temperature in the evaporator and the gascooler.

Furthermore, from figure 4.14 the influence of the top layer controller and thus the active operating mode on the hot water outlet temperature can be seen. Since in cooling mode the hot water is not used for DHW, it does not have to be heated to a minimum defined temperature. To save energy, the water is not heated to 70 °C or any specific temperature. The only condition is to have a heat sink that the heat pump/chiller can operate efficiently to satisfy the cooling demands in the evaporator. Accordingly, the refrigerant is not compressed to 100 bar in cooling mode, but to lower pressures between 80 bar and 90 bar. Since the temperature of the refrigerant also depends on its pressure, this leads to a lower CO_2 temperature and thus also to a lower heating load in the gascooler. The water is not heated as much, and only reaches temperatures of 55 °C to 60 °C. This reduces the required compressor power in cooling mode.

The frequencies of the two compressors over one day are shown in figure 4.15. As described in chapter 4.2.2, the thermal load of the heat exchanger is controlled via the frequencies. The VFD compressor keeps the pressure in the evaporator at 40 bar. The speed varies between 30 Hz and 70 Hz. The fluctuations are delayed by appropriate PI control parameters so that the control response is not too fast and a low frequency change takes place. This allows to compensate the small variations of the pressure in the evaporator, which can be seen in figure 4.14.

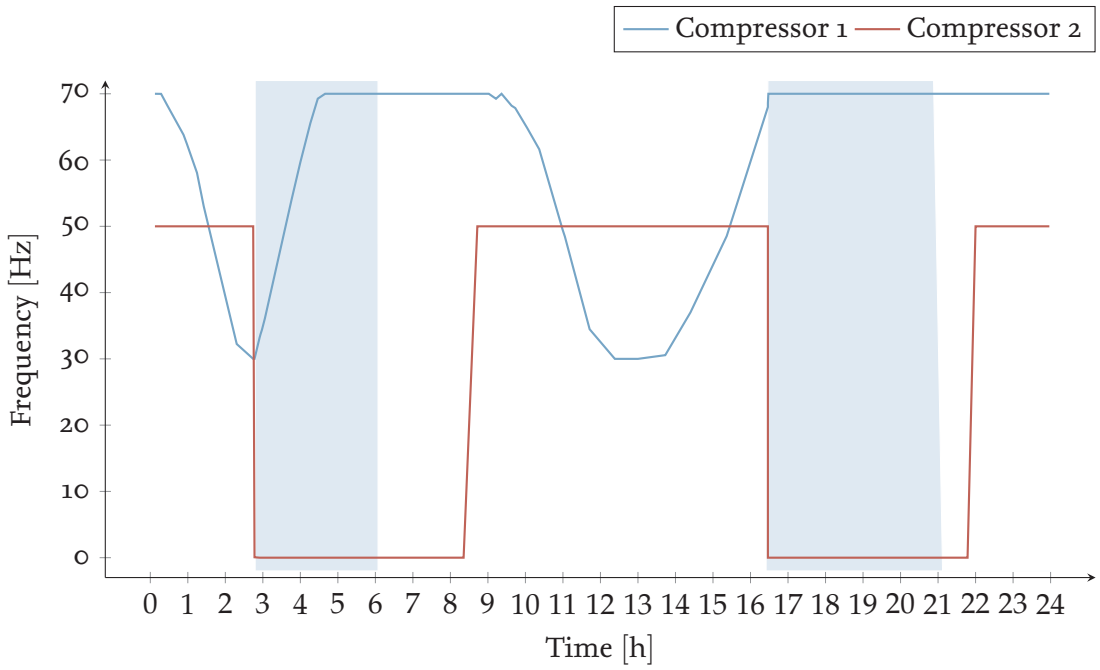

Figure 4.15: Frequencies of the VFD (Compressor 1) and CFD (Compressor 2) compressors

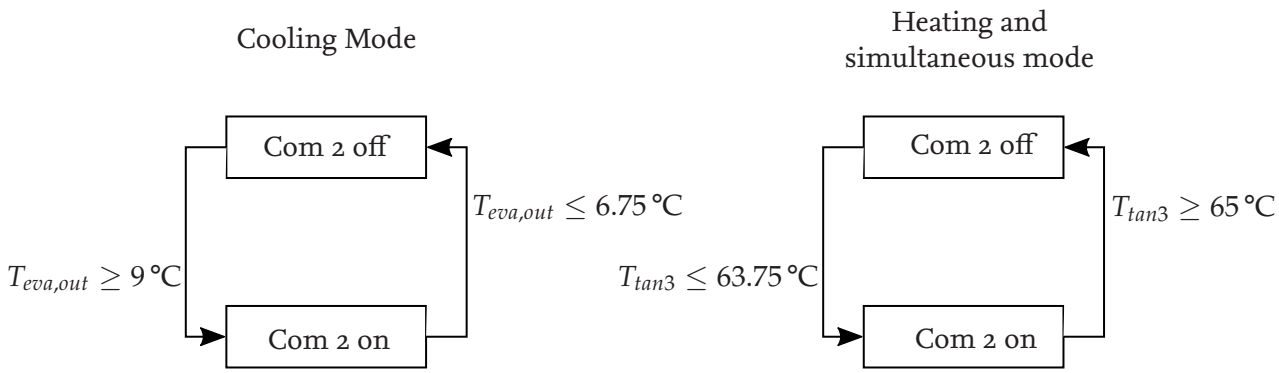

Figure 4.16: Simplified illustration of the CFD compressor control

The CFD (Com 2) compressor is controlled by the state chart control described in chapter 4.2.2, which switches between different modes to ramp up and down the compressor. In simplified form this control of the Com 2 compressor is shown in figure 4.16.

The two state controls for the cooling mode and the heating and simultaneous mode run simultaneously. In the initial state, Com 2 is off. Over the entire course of the simulation, the water outlet temperature from the evaporator does not reach 9 °C so that Com 2 could be switched on. Accordingly, this compressor is always off when cooling mode is active.

In heating and simultaneous mode it is not the outlet temperature at the gascooler, but the control temperature in the middle of tank 3 that is decisive. Com 2 is ramped up when the temperature in the center of tank 3 falls below 63.75 °C and ramped down when a temperature of 65 °C is reached. The temperature in the middle of tank 3 is shown in figure 4.13.

When Com 2 is ramped up, the control of VFD compressor (Com 1) reacts by reducing the frequency and vice versa. Since the displacement volume of Com 2 is smaller than that of Com 1 (see chapter 4.2.2), a wider load range can be achieved compared to a single compressor.

Ideally, the up and down ramping of Com 2 happens without delay. However, it is visible that the step response is slightly delayed, especially during the ramp-up. This is due to the numerical discretization during the simulation, where the states are determined at individual times and interpolated in between. In the case of the ramp-up, the time points before and after switching on Com 2 are so far apart that the ramp-up is slightly delayed.

The pressures in the evaporator and in the gas cooler are shown again in figure 4.17, together with the intermediate pressure level that results from the recovery of the expansion losses in the ejector. The ejector has a constant efficiency of 0.25 as described, which means that the ratio between the compression power and the expansion work is 25 %. Accordingly, the discharge mass flow has a higher enthalpy level than without the recovery.

This can also be seen in figure 4.17. The discharge pressure, neglecting the numerical inaccuracies caused by the discretization, is always between the suction pressure, in the evaporator, and the driving pressure from the gascooler. Due to the assumed constant efficiency, in cooling mode, when the driving pressure decreases, a decrease of the absolute difference between the suction and

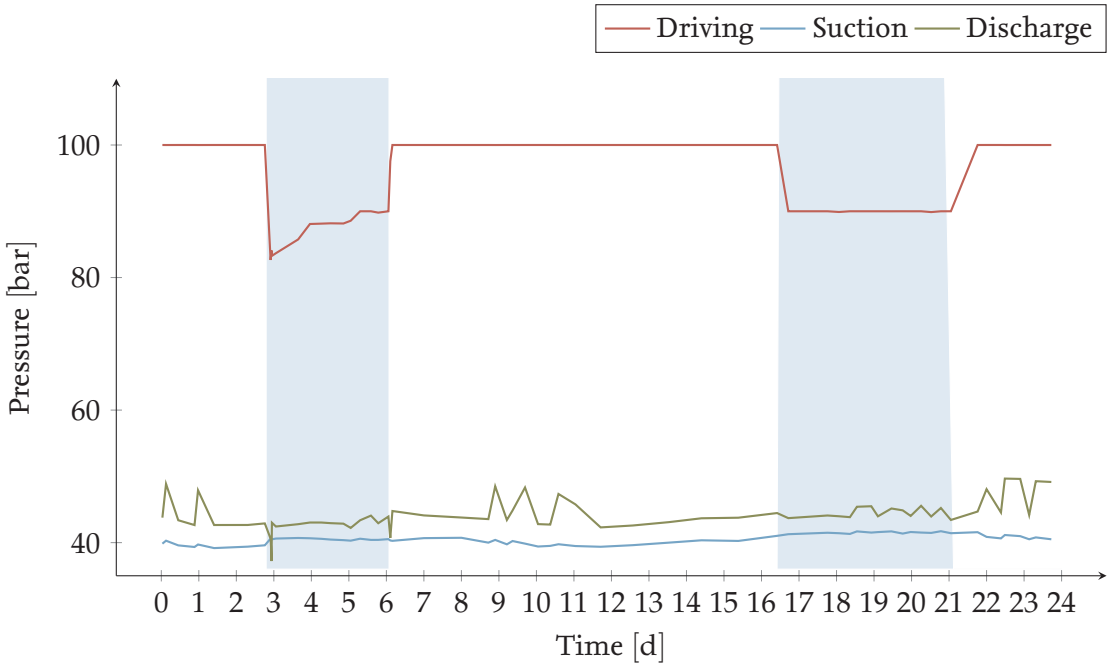

Figure 4.17: Driving, suction and discharge pressure of the ejector

the discharge pressure can be seen. This is the case because the losses during the expansion from a lower high pressure to the same low pressure are smaller than at a higher high pressure. This reduces the pressure difference to be achieved and the expansion losses. Since the recovery of expansion losses is defined by the constant relative factor of 0.25, the absolute recovery of expansion losses decreases accordingly.

The fluctuations of the discharge pressure are mainly related to a fluctuating mass flow. This depends to a large extent on the compressors. It can be seen in comparison to figure 4.15 that the fluctuations mainly occur when the CFD compressor is ramped up. When this is the case, it takes some time until the fluctuations of the mass flow and thus the discharge pressure will stop again.

The water mass flows are important for the heat transfer in the gascooler and evaporator. These are shown in figure 4.18. The chilled water mass flow shown in blue is relatively smooth. This is because of the simplification of the control that no quantitative cooling demands are present and it is simply assumed that the heat transfer on the chilled water side is set, so that all the heat given off by the water in the evaporator is permanently absorbed via the tube by the air conditioning. However, the water mass flow on the hot water side fluctuates strongly. This is mainly due to the fluctuating thermal load in the gascooler, which can be seen in red in figure 4.20. Since the mass flow of the hot water in simultaneous mode is controlled by the initial temperature of the water, and in cooling mode by the heat transfer in the evaporator, the mass flow reacts directly to changes in the thermal load in the gascooler. These changes are mainly caused by slight variations of the mass flow of the refrigerant, which depends on the effective flow area in the ejector. In order for the ejector to be able to control the high pressure to a smooth level without large fluctuations, this effective flow area

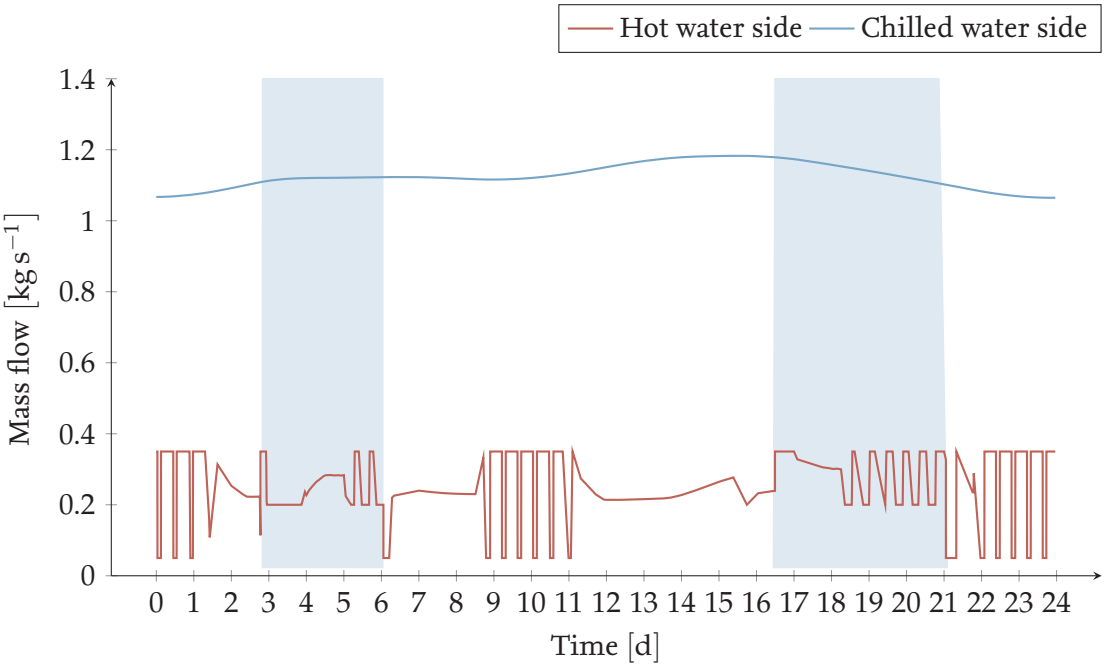

Figure 4.18: Mass flow of the hot and chilled water

and thus the CO_2 mass flow is permanently adjusted, which causes the fluctuations in the hot water mass flow.

The cooling tower is only active when the system is operated in cooling or heating mode. Since the heating mode cannot be active due to the permanent cooling demands, only the cooling mode is responsible for the activation of the cooling tower in this simulation. This can also be seen in figure 4.19. There the water inlet and outlet temperatures into the cooling tower and the ambient wet bulb temperature are shown. Since the cooling tower is only active during the cooling mode, the cooling tower specific temperatures are only shown for this range.

The graph shows that the water inlet temperature into the cooling tower fluctuates strongly. This seems counter intuitive at first, since the temperature of the water leaving the gascooler, which shall be cooled by the cooling tower, does not fluctuate as much. However, due to the risk of contamination, this water is not cooled directly in the cooling tower, but indirectly by transferring the heat via its own heat exchanger to another water circuit, which is cooled in the cooling tower. This heat transfer in the heat exchanger depends on the one hand on the respective inlet temperatures, but also on the mass flows. The mass flow of water heated in the gascooler is shown in red in figure 4.18. The mass flow of the water on the cooling tower side is controlled by the outlet temperature of the water, which is led to the gascooler. In this respect, the cooling tower water mass flow is dependent on the other and looks similar. It can be seen that the mass flow of the gascooler fluctuates at the same frequency as the inlet temperature to the cooling tower. When the mass flow increases, the inlet temperature also increases and vice versa. For areas where the mass flow is approximately

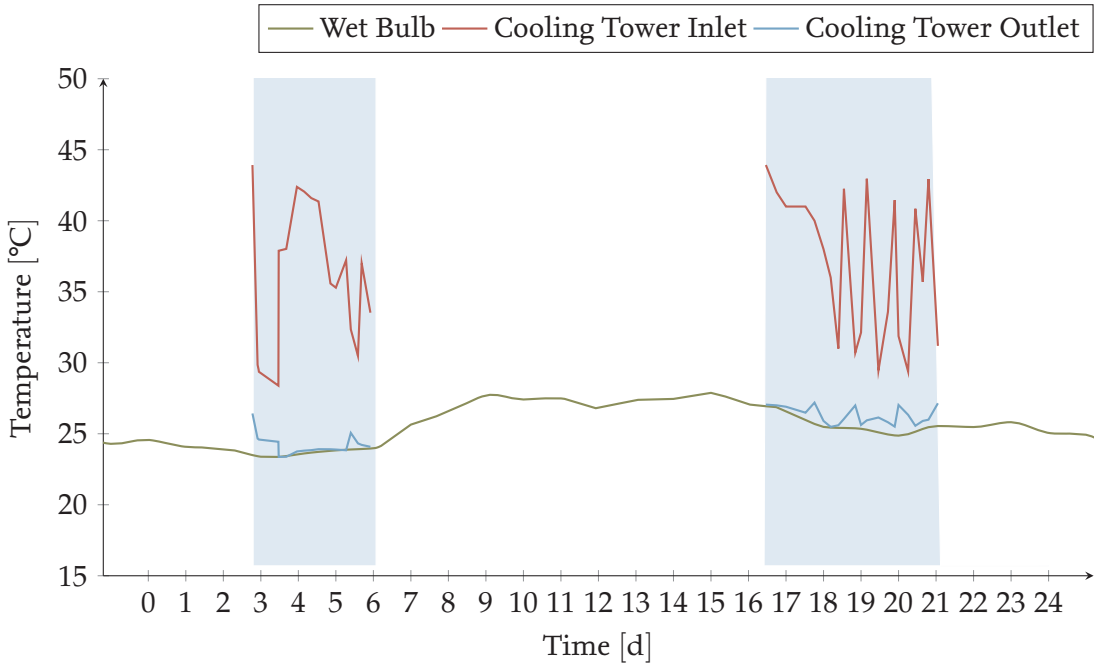

Figure 4.19: In- and outlet temperatures of the cooling tower

constant, the temperature does not fluctuate respectively.

Furthermore, it can be seen in figure 4.19 that the coolig tower outlet temperature is equal to or slightly above the ambient wet bulb temperature. This contradicts the statement made in chapter 2.3.3 that the cooling tower can cool the water only up to a difference of 2 K above the wet bulb temperature. However, for a more stable and faster simulation, the trade off was made that the temperature difference of 2 K applies to the outlet temperature of the water being directed to gascooler, not to the outlet of the cooling tower. In case of perfect heat transfer in the heat exchanger, these two temperatures would be identical, they differ due to inaccuracies of the control, so that the exit temperature from the cooling tower corresponds to the ambient wet bulb temperature instead of the outlet temperature of the water being led to the gascooler.

As mentioned before, the thermal loads in the gascooler and evaporator are shown in figure 4.20. These are shown with a heat flow absorbed by the evaporator in blue and a heat flow dissipated in the gascooler in red. The cooling load in the evaporator is at a relatively constant level, while the heating load in the gascooler shows slight differences between the cooling mode and the simultaneous mode. This is due to the lower CO_2 pressure on the high pressure side and the associated lower temperature in the cooling mode compared to the simultaneous mode. As a result, the temperature difference and the heating load are smaller in cooling mode. The small fluctuations are due to the fluctuating CO_2 mass flow, as already described, so that the high pressure can be kept smooth via the effective flow area of the ejector.

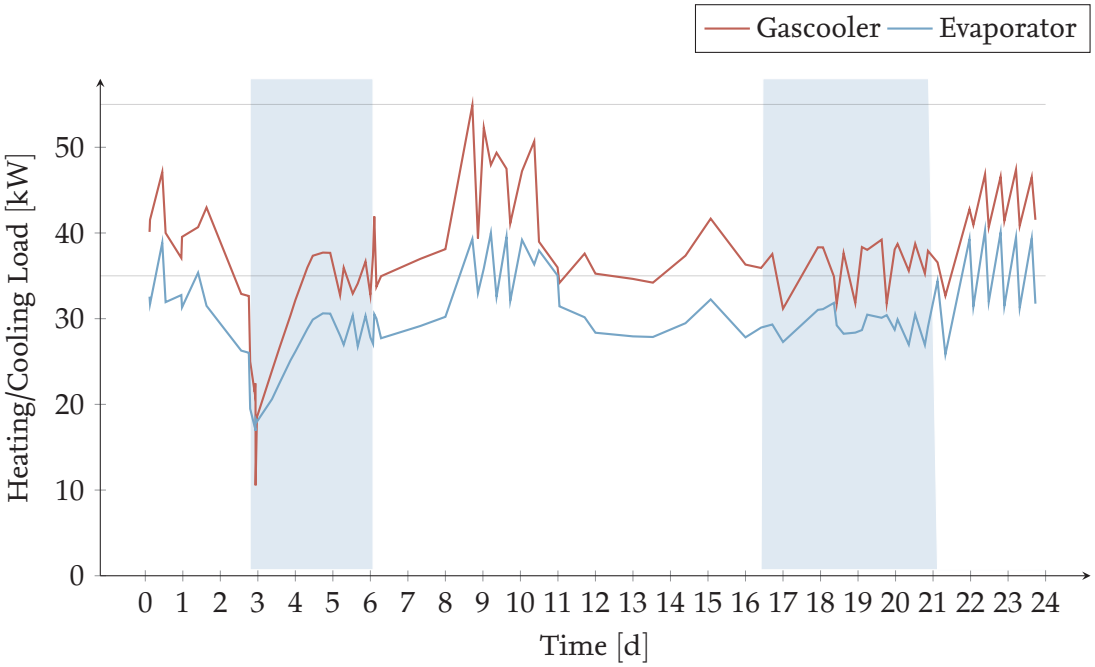

Figure 4.20: Heating and cooling load of the gascooler and evaporator

The maximum heating load in the gascooler is 54.9 kW, which reaches but does not exceed the maximum heating capacity of 55 kW. However, the maximum cooling load in the evaporator is 40.2 kW, exceeding the evaporator cooling capacity of 35 kW. The thermal capacities are also shown in figure 4.20 in gray. However, these overshoots are short-lived and can be attributed to fluctuations due to CO_2 mass flow changes. These are mainly numerical inaccuracies and should not occur in reality.

The electrical drive powers required to operate the system are shown in figure 4.21. These include the two compressors and the cooling tower with its fan. The pumps or the electric valves are not considered. Not surprisingly, the cooling tower only consumes electrical energy when cooling mode is active, otherwise it is off. The maximum power of the cooling tower is 4.8 kW by design and is reached only at the beginning of the first cooling mode period in the considered simulation period. Otherwise the power is only at part load.

The electrical powers of the two compressors depend on the shaft power and the compressor efficiency. Since the efficiency is assumed to be constant, the required compressor power can be used to determine the electrical drive power of the compressors. This is primarily dependent on the CO_2 mass flow and the respective compressor frequency. If one compares the curves of Com 1 and Com 2 in figure 4.15 and 4.21, one sees that they are very similar. If Com 2 has a speed of 0, then it is off and consuming no energy. The fluctuations and differences of the electrical powers to the speed can also be explained by the fluctuations of the CO_2 mass flow.

The maximum total power is 12 kW when both compressors are operated at maximum speed. The minimum power is 7.5 kW when between 6 h and 8.5 h only Com 1 is active while Com 2 and the cooling tower are off.

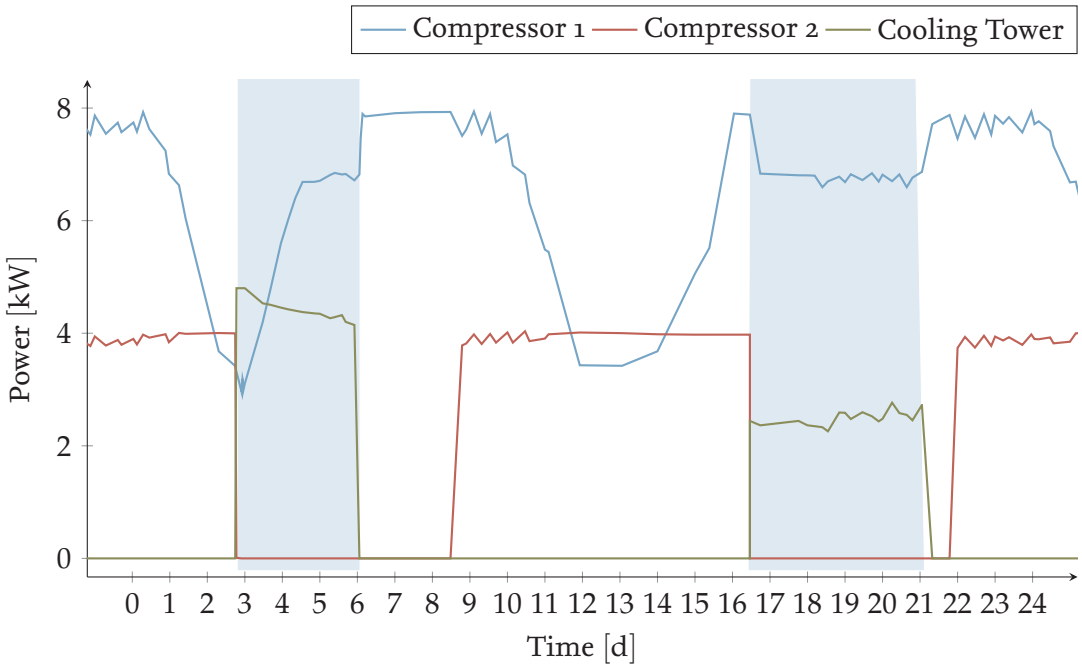

Figure 4.21: Electrical power consumption of the compressors and cooling tower

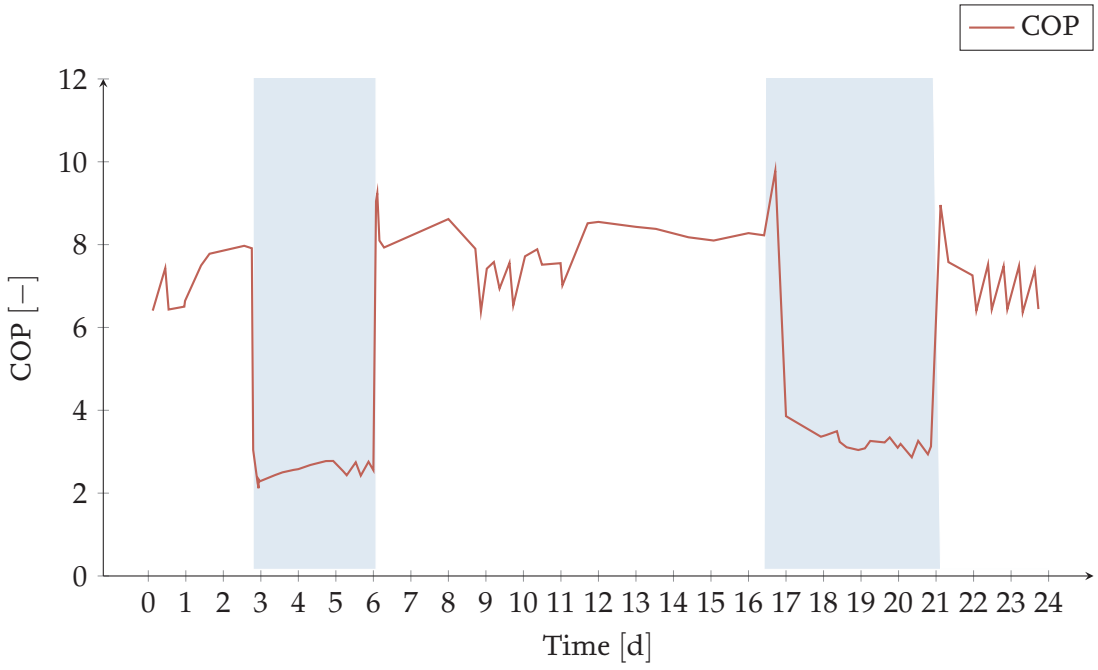

Figure 4.22: Coefficient of performance of the heat pump/chiller unit

From the heating and cooling loads from figure 4.20 and the electrical powers from figure 4.21, the COP of the heat pump/chiller unit can be determined according to equation 2.1. The cooling and heating loads are the usable heat $\dot{Q}_{use}$ and the sum of the electrical powers is the needed work $\dot{W}_t$. It is important to note that the COP of the heat pump/chiller unit is calculated as a whole, not differentiated in a heat pump and a chiller unit. While in simultaneous mode heating demands are present and the heat energy can be used to fill the TES, in cooling mode this heat is dissipated to the environment via the cooling tower and is not used. During the cooling mode the heating load is accordingly not counted to the usable heat. Accordingly, the COP and thus the efficiency of the heat pump/chiller unit drops significantly in cooling mode to values between 2 and 4. In simultaneous mode, COP values between 6 and 10 are achieved. The average COP over the day is 6, meaning the heating and cooling loads are on average 6 times higher than the electrical power. Comparing the average COP to Arpagaus et al [2], it achieves similar values to comparable heat pump/chiller units. Accordingly, it can be assumed that the system behavior is represented approximately correctly.

4.3.1 Economic Analysis

To make an economic analysis, several assumptions must be made. Accordingly, only an approximation of OpEx (operational expenditures) can be made, while no meaningful estimation of CapEx (capital expenditures) can be made. The goal is to determine the cost difference over a certain period of time, based on savings of OpEx compared to a reference system, and thus to determine a cost plan for the payback period of a possible investment.

In order to determine the savings of the OpEx, a reference system must first be determined. Since the hotel is newly built, there is no current energy system to work from. Accordingly, the energy system presented in this thesis will be compared to an industry standard system in India. Typically, the DHW is heated by a diesel boiler, which is assumed to have an efficiency of 1. Many industrial processes are build with boilers, even if with modern technologies and energy prices the usage of electricity would be more efficient. The air conditioning demands are satisfied by simple chiller units, with portable air conditioners having an average EER (Energy Efficiency Ratio) of 8.5 [27]. EER indicates the efficiency of an air conditioning chiller and, similar to the COP for heating processes, describes the ratio between the thermal cooling load and the electrical power to be applied.

For both systems, the one presented in this work without up-scaling as well as for the reference system, the work required to satisfy the heating and cooling demands of the simulation model has to be determined. These demands are shown for one day in figure 4.20 and are assumed to be periodic for the whole considered time span. When cooling mode is active, there are no heating demands. Therefore, those are not added to the total heating demands. In order to make statements about the cost savings, the costs for both systems have to be analyzed over the considered period. For this purpose, the electricity price in India is necessary, but also the energy density and the price of one liter of diesel.

As of April 2022, the diesel price per liter in India was \$1.168 [18]. With an energy density of diesel of 9.8 kW h L^{-1}, this translates to a price of \$0.2 per kW h. The cost of electricity in April 2022 per kWh was \$0.1087 [43].

The total heating demands for one day are calculated by integrating the heating loads. Those are 640 kW h for the observed day. The cooling demands are also integrated and are found to be 720 kW h. For this purpose, a total of 226 kW h electricity is consumed by the energy system observed in the model created in this work. This can also be determined with the average COP of 6. At an electricity price of \$0.1087 per kW h, this corresponds to daily OpEx of \$24.56.

The determination of OpEx for the reference model is split into satisfying heating demands and satisfying cooling demands. For the heating demands, 65.3 L of diesel must be burned, which leads to a cost of \$76.3.

The air conditioning chiller units with their EER of 8.5 are powered by electricity. In total, 724 kW h of cooling demand requires 85.2 kW h electricity. This results in a daily cost of \$9.22. The total cost per day is therefore equal to \$85.50.

Time	[year]	1	2	3	4	5	6	7	8	9	10
ΔCost	[\$1000]	22.3	44.5	66.8	89.1	111.3	133.6	155.9	178.1	200.4	222.7

Table 4.4: Cost savings of the heat pump/chiller unit compared to a reference system

The savings of the heat pump/chiller system per day compared to the reference system thus amounts to \$61.0. Table 4.4 lists the cost differences of the OpEx of the two systems for the first ten years. On the basis of these estimations, a decision can be made as to whether an investment should be made, and if so, how much, and how quickly it will pay off.

5 Discussion

In conclusion, the simulation model can represent the thermal and fluid dynamic properties of the energy system. However, for a better and more stable simulation, compromises had to be made that make the simulation model a little more unrealistic. A discussion of these compromises and possibilities for further work are done in this chapter. Additionally, an economic analysis is done based on these simplifications and assumptions.

5.1 Cooling Demands

The biggest compromise to ensure the stability of the simulation and to simplify the data collection is the simplification of the cooling demands. These were not considered quantitatively, but only in such a way that the heat pump/chiller unit can apply a sufficient cooling load to simulate stably. Accordingly, the climatic conditions, which are important for cooling or space heating demands, were considered mainly for the cooling tower. For the cooling demands it was simply assumed that these are always present due to the hot weather in Chennai, India. Comparing the cooling demands with a comparable hotel in Miami, Florida, resulted in instabilities in the simulation, since nights in Miami often cool down, resulting in extreme part load conditions. This reflects the reality in Chennai only to a limited extent, as the nights there are also very warm, requiring more air conditioning.

In order to obtain a representative data set on the cooling demands of the hotel in Chennai, elaborate calculations with further assumptions on e.g. insulation properties of the walls of the hotel, behavior of the guests, occupancy of the hotel, climatic conditions on site etc. have to be made. However, some of these assumptions are difficult to make, which would make the simulation only conditionally more realistic. It is also possible to implement the standardized method to calculate the cooling demands of a hotel dependent on the ambient temperature by the *Air-Conditioning and Refrigeration Institute* in the USA presented by Lemke [29].

Alternatively, when the hotel is fully built with the energy system, data of the consumption of cooling and heating loads can be collected over a reference period. This data can then either be added to the simulation model at a later stage, or the system can be optimized and fitted using machine learning.

When the collected cooling demands have been added to the simulation model, it can also be analyzed whether the part load conditions and the stability of the system allow the VFD compressor to be ramped up and down as well. This is not the case in the simulation model described in chapter 4, because due to the extreme part load conditions, when using the cooling demands of the hotel in Miami, the simulation becomes unstable after about one week. The resulting low heating loads, can no longer heat the TES sufficiently. As a result, the temperature in the TES continues to drop, which can no longer be counterbalanced by the control system.

If a realistic or empirical survey of the cooling loads has been made, the system can be adapted to these. If there are still extreme part load conditions, the control can also be adjusted. When implementing quantitative cooling demands, those have to be satisfied directly and are thereby controlling to a limited extend the possible heating load. Usually, this is no problem, because the DHW heating demands are only indirectly satisfied by the heat pump/chiller unit, since the TES serves as a kind of buffer storage. As long as the TES is charged, fluctuations of the heating load in the gascooler have no impact on the possibility to satisfy all DHW demands. For cooling demands, there is no buffer. However, if the TES can not satisfy the DHW demands, there might not be enough heating load to compensate. Then, another mechanism can be implemented into the control algorithm of the simulation model. If the control for part load cooling demands is adjusted, so that there is a sufficient heating load in the gascooler, it can exceed the needed cooling demands in the evaporator. Then, the excess cooling load in the chilled water, which is not needed for air conditioning, can be emitted via the cooling tower. Implementing this option enables the possibility, to operate part of the chilled water side similar to the cooling/simultaneous mode for air conditioning, and part of it similar to heating mode to remove excess cooling load.

However, these implications could not be taken into account due to delays in the construction of the heat pump/chiller unit in the hotel. This is where the greatest potential for further work exists.

5.2 Tank Type

Another assumption is the design of the TES tanks. In this work, five tanks in series were simulated, defined only by their volume and heat transfer properties, but not by their geometrical dimensions. The layering properties of a tall thin tank are different from those of a wide flat tank. Furthermore, the stratifications in five tanks connected in series are different from those of one large tank. Once the energy system is designed and implemented, the geometry of the tanks should be adjusted.

Furthermore, the way in which the tanks are layered is worth of consideration. In Europe and North America, overpressure tanks are standard. In these, there is an overpressure so that water from the tank can also be directed upwards via hydrostatics. As a result, the tank has a constant volume of water, which is replenished with cold water, when warm water is drawn from it. For the simulation, such a tank model was used based on existing Modelica libraries. However, in India, ambient pressure tanks are common [11]. If water has to overcome a geodetic head, it has to be pumped or placed above its sink. This also means that the volume of water in the tank does not have to be constant. Hot water, that is removed, is not compensated for by cold water, but the volume of water in the tank decreases until it is refilled. As a result, the temperature stratification in the tank is different from that in an overpressure tank. Since this type of tank is primarily used in India, it is worth analyzing and adapting the simulation model in this respect.

5.3 Up-scaling

The system studied in this work consists of the one heat pump/chiller unit and the associated chilled and hot water sites. However, this is only a part of the total system under construction. This will be larger by a factor of 4. Accordingly, a total of four heat pump/chiller units will be installed. The cooling tower and the TES will be shared by all subsystems. It is therefore necessary to check whether the system can be easily up scaled.

This can be better when the system operates on part load conditions, where whole subsystems are shut down and only part of the heat pump/chiller units are active. To achieve this, another layer must be added above the current top layer controller in the control algorithm. This will make the current top layer controller the first mid layer controller. If this is successfully implemented, the extreme part load conditions that have complicated the simulation analyzed in this work can be better and more accurately mapped.

5.4 Compressor Control

As already mentioned in chapter 5.1, the behavior of the VFD compressor can be further optimized. However, this does not only refer to the ramp-up and ramp-down, but also to the control described in chapter 4 and the resulting frequency curve. It can be seen that the frequency always moves between the minimum value of 30 Hz and the maximum value of 70 Hz. The rather long transition times do not come from the setpoints being reached, but because the PI-control parameters delay the response of the frequency to changes in the system. It is to be examined whether e.g., by adjustment of the displacement volume and the control, a usage of the VFD compressor is possible within the boundaries of the frequency, without always orienting at the extreme.

5.5 Losses

A further simplification of the system is the lack of consideration of multiple types of losses. For example, the pipes are considered ideal, without convection and pressure losses. These can be introduced and simulated in the simulation via *Tube*- elements from the TIL-library. For this purpose, corresponding heat transfer properties and pressure loss correlations must be selected and determined.

In addition, convection and heat conduction losses must be considered in the containers where fluids are present for extended periods of time. The TES has an insulation layer that inhibits heat transfer through the tank wall, but for a better approximation to reality, the heat loss should still not be set equal to 0 kW. The pressure losses in the heat exchangers could also be investigated in more detail.

Furthermore, the pumping drive powers for the water pumps can also be considered. These add up to the total electrical energy required by the system and consequently reduce the COP.

5.6 Two-stage Evaporation and Gascooling

As shown in figure 3.1, the energy system is planned to have a two-stage evaporator and a two-stage gascooler at the site. This will reduce the heat transfer losses in the heat exchangers. However, it is quite complicated to simulate this, so the simulation model created in this work focuses on other things, such as the TES. Nevertheless, it is worth analyzing the two-stage evaporator in particular. For this purpose, a new, more efficient type of two-stage evaporation can be used, where part of the compression work can be done by gravity. This type of evaporator is called *Gravity Fed Evaporator* and is explained in Hafner et al [21].

6 Summary

In this master thesis, a simulation model of a CO_2 heat pump/chiller unit and the associated energy system for a hotel in Chennai, India was created and analyzed. First an overview of state of the art heat pumps/chillers was given, with introduction to possible natural refrigerants, as well as thermodynamic description of the individual components. A more detailed description of CO_2 heat pump/chiller units with a description of a transcritical process and potential improvements like internal heat exchangers or ejectors gives a comprehensive overview of the system described in this thesis. Furthermore, possibilities for optimization of the secondary side, such as cooling towers or thermal energy storages are presented.

As a basis for the simulation model, the energy system of the hotel facility had to be analyzed first. This was under construction at the time of this thesis. Through the energy system, domestic heating water demands, air conditioning demands and, if necessary, space heating demands are to be satisfied. However, the latter are negligible due to the hot climatic conditions in Chennai. The system consists of a CO_2 heat pump/chiller unit with internal heat exchanger and ejector. Furthermore, a two-stage evaporator and a two-stage gascooler. However, these two were considered as single-stage in the simulation model. The secondary side of the energy system is divided into a hot water and a chilled water side. The hot water side has a buffer tank installed in the form of a TES. Furthermore, a cooling tower is implemented to dissipate excess heat. For a correct dimensioning, an estimation of the DHW demands and the air conditioning demands was made. Since these are not permanently available, different operational modes of the energy system had to be created. This includes a mode for simultaneous heating and cooling demands, a mode for cooling only and a mode for heating only. These differ in the water flows as well as the heat sinks and heat sources. For the cooling mode and the heating mode a cooling tower is integrated in the energy system.

The simulation model was created in Modelica, with using components of *Modelica Buildings Library*, *Modelica Standard Library* and *TIL Library*. Furthermore, some models were created specifically for this work. The difficulty was to create a control algorithm that can switch between the different operational modes, satisfy the heating and cooling demands and run the simulation in a stable way. Therefore a hierarchical control system was implemented, which controls the operational mode on the top layer and adjusts the control variables in the mid layer to reach the setpoints. To determine if the TES needs to be charged, the temperature at the center of the TES was taken. Once this falls below a threshold temperature of 65 °C, reheating is performed until the return temperature to the heat pump/chiller exceeds a temperature 35 °C, which would reduce the efficiency of the system. Cooling demands were not considered quantitatively to simplify the simulation, but only as permanently present to ensure a stable simulation. In order to simulate different load behaviors and thermal demands, a state chart control was implemented for a compressor group of two compressors, which allows for a better simulation of low thermal loads.

The analysis of the results has shown, that on the basis of simplifications, a stable and approximately thermo- and fluiddynamically correct simulation of the energy system of the hotel facility is possible. Furthermore, the operational expenditures resulting from the simulated energy consumption were compared with a reference system in order to make statements about the economic feasibility of the system. The economic savings of operational expenditures are up to $222.000 with an average COP of 6 for a planning horizon of ten years.

Finally,the simplifications and possible changes to the simulation model were discussed. Especially a quantitative consideration of the cooling demands would lead to a more realistic simulation model. However, this would require empirical data to be collected over a reference period as soon as the energy system of the hotel facility is completed. Furthermore, components such as a two-stage evaporator, two-stage gascooler or tube elements can be added to better represent heat transfer and losses.

Bibliography

[1] DIN EN 378-1:2018-04, Kälteanlagen und Wärmepumpen_- Sicherheitstechnische und umweltrelevante Anforderungen_- Teil_1: Grundlegende Anforderungen, Begriffe, Klassifikationen und Auswahlkriterien; Deutsche Fassung EN_378-1:2016. (2018). http://dx.doi.org/10.31030/2823383. – DOI 10.31030/2823383

[2] Arpagaus, C. ; Bless, F. ; Uhlmann, M. ; Schiffmann, J. ; Bertsch, S. S.: High temperature heat pumps: Market overview, state of the art, research status, refrigerants, and application potentials. In: *Energy* 152 (2018), S. 985–1010. http://dx.doi.org/10.1016/j.energy.2018.03.166. – DOI 10.1016/j.energy.2018.03.166. – ISSN 03605442

[3] Bansal, R. K.: *A textbook of fluid mechanics: [in S.I. units].* Bengaluru : Laxmi Publications (P) LTD, 2018. – ISBN 9788131802946

[4] Bergman, T. L. ; Lavine, A. S.: *Incropera's principles of heat and mass transfer.* 8th edition, global edition. Hoboken, NJ : Wiley, 2017. – ISBN 1119382912

[5] Byrne, P. ; Miriel, J. ; Lenat, Y. : Design and simulation of a heat pump for simultaneous heating and cooling using HFC or CO2 as a working fluid. In: *International Journal of Refrigeration* 32 (2009), Nr. 7, S. 1711–1723. http://dx.doi.org/10.1016/j.ijrefrig.2009.05.008. – DOI 10.1016/j.ijrefrig.2009.05.008. – ISSN 01407007

[6] Cao, F. ; Ye, Z. ; Wang, Y. : Experimental investigation on the influence of internal heat exchanger in a transcritical CO2 heat pump water heater. In: *Applied Thermal Engineering* 168 (2020), S. 114855. http://dx.doi.org/10.1016/j.applthermaleng.2019.114855. – DOI 10.1016/j.applthermaleng.2019.114855. – ISSN 13594311

[7] Cooling India: *Energy Saving In The HVAC Industry.* https://www.coolingindia.in/energy-saving-in-the-hvac-industry/. Version: 2016

[8] Delta Cooling Tower Inc.: *What is a Cooling Tower?* https://deltacooling.com/resources/faqs/what-is-a-cooling-tower. Version: 2021

[9] Eckert, M. (Hrsg.) ; Kauffeld, M. (Hrsg.) ; Siegismund, V. (Hrsg.): *Natürliche Kältemittel: Anwendungen und Praxiserfahrungen.* Berlin and Offenbach and Karlsruhe : VDE Verlag GmbH and cci Dialog GmbH, 2019 (cci Buch). – ISBN 9783800739363

[10] Elarga, H. ; Hafner, A. : Numerical investigation of a CO2 cooling system connected to SPAWN of EnergyPlus thermal zones. In: *Thermal Engineering Journal* (2022)

[11] ELARGA H. ; HAFNER A.: *CO2 heat pump/chiller system for a hotel in a tropical climate: a numerical investigation*

[12] Elbel, S. ; Hrnjak, P. : Experimental validation of a prototype ejector designed to reduce throttling losses encountered in transcritical R744 system operation. In: *International Journal of Refrigeration* 31 (2008), Nr. 3, S. 411–422. http://dx.doi.org/10.1016/j.ijrefrig.2007.07.013. – DOI 10.1016/j.ijrefrig.2007.07.013. – ISSN 01407007

[13] Elmegaard, B. ; Holm, F. ; Buehler, F. : *Potentials for the electrification of industrial processes in Denmark*. 2019

[14] Enerdata: *Total energy consumption*. https://yearbook.enerdata.net/total-energy/world-consumption-statistics.html. Version: 2022

[15] Energyworld: *India's cooling energy consumption to grow around 2.2 times by 2027: Report*. https://energy.economictimes.indiatimes.com/news/power/indias-cooling-energy-consumption-to-grow-around-2-2-times-by-2027-report/66094074?redirect=1. Version: 2018

[16] European Comission: *Heating and cooling: Heating and cooling constitutes around half of the EU energy consumption*. https://energy.ec.europa.eu/topics/energy-efficiency/heating-and-cooling_en. Version: 2020

[17] Försterling, S. : *Vergleichende Untersuchung von CO2-Verdichtern in Hinblick auf den Einsatz in mobilen Anwendungen: Zugl.: Braunschweig, Techn. Univ., Diss., 2003*. 1. Aufl. Göttingen : Cuvillier, 2004. – ISBN 3865370802

[18] GlobalPetrolPrices: *India Diesel prices, 05-Sep-2022*. https://www.globalpetrolprices.com/India/diesel_prices/. Version: 2022

[19] Gullo, P. ; Birkelund, M. ; Kriezi, E. ; Kearn, M. : *Summer performance comparison of transcritical R744 condensing units based on experimental data and several climates* (15th IIR-Gustav Lorentzen Conference on Natural Refrigerants)

[20] Gullo, P. ; Hafner, A. ; Banasiak, K. ; Minetto, S. ; Kriezi, E. : Multi-Ejector Concept: A Comprehensive Review on its Latest Technological Developments. In: *Energies* 12 (2019), Nr. 3, S. 406. http://dx.doi.org/10.3390/en12030406. – DOI 10.3390/en12030406

[21] Hafner, A. ; Hazarika, M. ; Lechi, F. ; Zorzin, A. ; Pardinas, A. ; Banasiak, K. : Experimental investigation on integrated two-stage evaporators for CO2 heat-pump chillers. 2022 (2022)

[22] Hebei Feiyu Cooling Equipment Co., Ltd.: *Cooling Towers*. Hengshui, Hebei Province, 2021

[23] India Brand Equity Foundation: *Renewable Energy Industry in India*. https://www.ibef.org/industry/renewable-energy. Version: 2022

[24] Jackman, J. ; TheEcoExperts (Hrsg.): *Which Countries Are Winning the European Heat Pump Race?* https://www.theecoexperts.co.uk/heat-pumps/top-countries. Version: 2022

[25] Jin, Y. ; Gao, N. ; Wang, T. : Influence of heat exchanger pinch point on the control strategy of Organic Rankine cycle (ORC). In: *Energy* 207 (2020), S. 118196. http://dx.doi.org/10.1016/j.energy.2020.118196. – DOI 10.1016/j.energy.2020.118196. – ISSN 03605442

[26] Jin, Z. ; Eikevik, T. M. ; Nekså, P. ; Hafner, A. ; Wang, R. : Annual energy performance of R744 and R410A heat pumping systems. In: *Applied Thermal Engineering* 117 (2017), S. 568–576. http://dx.doi.org/10.1016/j.applthermaleng.2017.02.072. – DOI 10.1016/j.applthermaleng.2017.02.072. – ISSN 13594311

[27] LearnMetrics: *Understanding EER: Energy Efficiency Rating For AC Explained*. https://learnmetrics.com/eer-rating/. Version: 2022

[28] Leeper, S. ; U.S. Department of Energy (Hrsg.): *WET COOLING TOWERS: 'RULE-OF-THUMB' DESIGN AND SIMULATION*. Idaho, 1981

[29] Lemke, N. : *Untersuchung zweistufiger Flüssigkeitskühler mit einem Kältemittel CO2*. Braunschweig, TU Braunschweig, Dissertation, 2004

[30] Lin, C. ; Xu, C. ; Yue, B. ; Jiang, C. ; Omori, H. ; Deng, J. : Experimental study on the separator in ejector-expansion refrigeration system. In: *International Journal of Refrigeration* 100 (2019), S. 307–314. http://dx.doi.org/10.1016/j.ijrefrig.2019.02.015. – DOI 10.1016/j.ijrefrig.2019.02.015. – ISSN 01407007

[31] Lorentzen, G. : Revival of carbon dioxide as a refrigerant. In: *International Journal of Refrigeration* 17 (1994), Nr. 5, S. 292–301. http://dx.doi.org/10.1016/0140-7007(94)90059-0. – DOI 10.1016/0140–7007(94)90059–0. – ISSN 01407007

[32] Milner, E. : *UPDATE: CO2 efficiency equator moves further south by grace of ejector technology*. https://r744.com/update-co2-efficiency-equator-moves-further-south-by-grace-of-ejector-technology/. Version: 2015

[33] NTNU: *Indee+ Objectives*. https://www.ntnu.edu/indee/about/objectives. Version: 2022

[34] Office of Energy Efficiency & Renewable Energy: *New Construction — Commercial Reference Buildings: Buildings*. https://www.energy.gov/eere/buildings/new-construction-commercial-reference-buildings. Version: 2012

[35] Picardo, J. R. ; Variyar, J. E.: The Merkel equation revisited: A novel method to compute the packed height of a cooling tower. In: *Energy Conversion and Management* 57 (2012), S. 167–172. http://dx.doi.org/10.1016/j.enconman.2011.12.016. – DOI 10.1016/j.enconman.2011.12.016. – ISSN 01968904

[36] Sarbu, I. ; Sebarchievici, C. : A Comprehensive Review of Thermal Energy Storage. In: *Sustainability* 10 (2018), Nr. 1, S. 191. http://dx.doi.org/10.3390/su10010191. – DOI 10.3390/su10010191

[37] Schulze, T. : *Gleichungsorientierte Modellierung der Wärme- und Stoffübertragungsprozesse in Verdunstungskühltürmen*. Dresden, Technische Universität Dresden, Dissertation, 04.12.2014

[38] Shublaq, M. ; Sleiti, A. K.: Experimental analysis of water evaporation losses in cooling towers using filters. In: *Applied Thermal Engineering* 175 (2020), S. 115418. http://dx.doi.org/10.1016/j.applthermaleng.2020.115418. – DOI 10.1016/j.applthermaleng.2020.115418. – ISSN 13594311

[39] Stephan, P. ; Schaber, K. ; Stephan, K. ; Mayinger, F. : *Thermodynamik*. Berlin, Heidelberg : Springer Berlin Heidelberg, 2009. http://dx.doi.org/10.1007/978-3-540-92895-9. http://dx.doi.org/10.1007/978-3-540-92895-9. – ISBN 978–3–540–92894–2

[40] Tafur-Escanta, P. ; Valencia-Chapi, R. ; López-Guillem, M. ; Fierros-Peraza, O. ; Muñoz-Antón, J. : Electrical energy storage using a supercritical CO2 heat pump. In: *Energy Reports* 8 (2022), S. 502–507. http://dx.doi.org/10.1016/j.egyr.2022.01.073. – DOI 10.1016/j.egyr.2022.01.073. – ISSN 23524847

[41] The Regents of the University of California: *Open source library for design and operation of building and district energy and control systems*. https://simulationresearch.lbl.gov/modelica/index.html. Version: 2022

[42] Tischendorf, C. : *Untersuchung eines Ejektors in einem R744-Kältekreislauf*, Universitätsbibliothek Braunschweig, Diss., 2013. http://dx.doi.org/10.24355/DBBS.084-201411071004-0. – DOI 10.24355/DBBS.084–201411071004–0

[43] Varadhan, S. ; Reuters (Hrsg.): *Average power price on Indian Energy Exchange hits 13-year high in March*. https://www.reuters.com/world/india/average-power-price-indian-energy-exchange-hits-13-year-high-march-2022-04-06/. Version: 2022

[44] Wang, Y. ; Ye, Z. ; Yin, X. ; Song, Y. ; Cao, F. : Energy, exergy and exergoeconomic evaluation of the air source transcritical CO2 heat pump with internal heat exchanger for space heating. In: *International Journal of Refrigeration* 130 (2021), S. 14–26. http://dx.doi.org/10.1016/j.ijrefrig.2021.06.028. – DOI 10.1016/j.ijrefrig.2021.06.028. – ISSN 01407007

[45] Weigand, B. ; Köhler, J. ; Wolfersdorf, J. von: *Thermodynamik kompakt*. 4., aktual. Aufl. 2016. Springer Berlin Heidelberg http://nbn-resolving.org/urn:nbn:de:bsz:31-epflicht-1578855. – ISBN 9783662497036

[46] Wilson, I. D.: Foundations of hierarchical control. In: *International Journal of Control* 29 (1979), Nr. 6, S. 899–933. http://dx.doi.org/10.1080/00207177908922740. – DOI 10.1080/00207177908922740. – ISSN 0020–7179

NTNU – Trondheim
Norwegian University of
Science and Technology